Multi-omics Assessment of Genomic Glucocorticoid Action in Murine Neural Stem and Progenitor Cells

by

Kimberly Jasmine Jeaneen Berry

Bachelor of Science, The Ohio State University, 2017

Submitted to the Graduate Faculty of the

Dietrich School of Arts and Sciences in partial fulfillment

of the requirements for the degree of

Doctor of Philosophy

University of Pittsburgh

2023

UNIVERSITY OF PITTSBURGH

DIETRICH SCHOOL OF ARTS AND SCIENCES

This dissertation was presented

By

Kimberly Jasmine Jeaneen Berry

It was defended on

February 27, 2023

and approved by

Committee Co-Chair: Shawn Sorrells, Ph.D., Assistant Professor, Department of Neuroscience

Laura E. Lillien, Ph.D., Professor, Department of Neurobiology

Mary M. Torregrossa, Ph.D., Associate Professor, Department of Psychiatry

Rebecca P. Seal, Ph.D., Associate Professor, Department of Neurobiology

Irtisha Singh, Ph.D., Assistant Professor, Molecular and Cellular Medicine with an affiliation with Biomedical Engineering, Texas A&M University [External Advisor]

Dissertation Director and Co-Chair: Donald B. DeFranco, Ph.D., Professor, Department of Pharmacology and Chemical Biology

Multi-omics Assessment of Genomic Glucocorticoid Action in Murine Neural Stem and Progenitor Cells

Kimberly Jasmine Jeaneen Berry, PhD

University of Pittsburgh, 2023

Prenatal exposure to synthetic glucocorticoids (sGCs) reprograms brain development and predisposes the developing fetus towards potential adverse neurodevelopmental outcomes. Using a mouse model of sGC administration, previous studies show that these changes are accompanied by sexually dimorphic alterations in the transcriptome of neural stem and progenitor cells (NSPCs) derived from the embryonic telencephalon. Because cell type-specific gene expression profiles tightly regulate cell fate decisions and are controlled by a flexible landscape of chromatin domains upon which transcription factors and enhancer elements act, we multiplexed data from four genome-wide assays: RNA-seq, ATAC-seq (assay for transposase accessible chromatin followed by genome wide sequencing), dual cross-linking ChIP-seq (chromatin immunoprecipitation followed by genome wide sequencing), and microarray gene expression to identify novel relationships between gene regulation, chromatin structure, and genomic glucocorticoid receptor (GR) action in NSPCs. These data reveal that GR binds preferentially to predetermined regions of accessible chromatin to influence gene programming and cell fate decisions. In addition, we identify SOX2 as a transcription factor that impacts the genomic response of select GR target genes to sGCs (i.e., dexamethasone) in NSPCs.

Table of Contents

List of Tables

List of Figures

Preface

This project was made possible by the services of University of Pittsburgh's Health Sciences Sequencing Core at UPMC Children's Hospital of Pittsburgh, the Department of Biomedical Informatics at the University of Pittsburgh, the Rogatsky lab at the Hospital for Special Surgery at Weill Cornell Medical, the Nicolis lab at University Milano-Bicocca**,** and the Monaghan-Nichols lab at UMKC School of Medicine.

A special thanks to Dr. Don DeFranco and the entire DeFranco lab for providing an encouraging environment for science exploration.

My academic successes are a manifestation of the dreams and sacrifices made by my parents and ancestors. I am proud to become the second 'Dr. Berry' in the family – thank you for lighting the path, Dad.

1.0 General Introduction

Antenatal administration of synthetic glucocorticoids (sGC) ameliorates infant complications of premature delivery by mimicking the endogenous surge of cortisol that peaks during late gestation[1,2]. However, potential adverse neurodevelopmental consequences of antenatal sGC exposure include short-term cortical architectural changes in mice, sheep, and non-human primates, and long-term behavioral or cognitive impairments in humans[3-9]. Mouse models of sGC administration revealed that a single dose of the synthetic glucocorticoid receptor (GR) agonist Dexamethasone (Dex) at embryonic day E14.5 altered neural stem and progenitor cell (NSPC) proliferation and differentiation *in vivo*, while *in-vitro* experiments with primary embryonic NSPCs demonstrated robust and sex-specific changes in gene expression following acute Dex treatment [7,10].

sGC drug exposure occurs during a fluid period of cerebral cortical development when dynamic chromatin remodeling, a flexible epigenetic process guided by specialized enzyme complexes and transcription factors (TF)[11-14], directs neurogenesis and other cell fate decisions. This is evidenced by the subpopulations of cells with neuronal or glial lineages expressing distinct global chromatin signatures[11,14]. Furthermore, gene-regulatory enhancer regions upon which TF act are often located far from their target promoters, highlighting the need for a genome wide assessment of chromatin architecture to fully understand how developmental programming of gene expression is established and/or maintained[15].

Transcriptional regulation by glucocorticoids is driven by GR, which associates directly or indirectly with DNA to activate or repress target genes[16]. Both chromatin accessibility and histone modifications play a major role in determining *de-novo* genomic GR occupancy[17-19]. However,

some GR binding sites occur in less permissive chromatin or genomic sites lacking distinct histone modifications[17,20,21]. Importantly, cell type-enriched co-factors or coregulators create unique GR occupancy patterns in different cell types by enhancing the receptor's ability to associate directly with specific DNA sequences (i.e., glucocorticoid response elements or GREs), or recruiting GR indirectly to genomic sites occupied by other TF[22,23]. While antenatal exposure to sGC reprograms the neurodevelopmental trajectories and cerebral architecture in the fetal forebrain, the molecular signatures that direct basal and hormone-induced genomic GR action in NSPCs have not previously been elucidated. In this study we characterized the chromatin landscape and GR cistrome of embryonic mouse NPSCs to determine whether robust acute sGC-induced alterations in gene expression are accompanied by changes in chromatin accessibility and GR distribution at regulatory genomic sites that control NSPC fate.

1.1 Glucocorticoids (GCs) and Glucocorticoid Receptor (GR) Biology

1.1.1 GC Synthesis, Regulation, and Function in the Human Body

Glucocorticoids (GCs) are steroid hormones that regulate various physiological processes in vertebrate animals. In primates, cortisol is the predominant endogenous GC while in other mammals including rodents, corticosterone is the major circulating GC. Under homeostatic or unstressed states, GC are released in a circadian and ultradian manner to control reproduction, skeletal growth, cardiovascular function, immune and anti-inflammatory responses, vascular tone, salt and water balance, and metabolism[24-27]. Within the central nervous system (CNS), receptors

for GC are widely expressed, and their actions influence behavioral outputs, learning and memory, emotional reactivity, and central control of autonomic function[28].

A major driver of GC release from the adrenals are physiologic and psychological stressors that regulate circulating levels of GC via the hypothalamic-pituitary-adrenal (HPA) axis, a neuroendocrine system connecting the hypothalamus and pituitary glands in the brain to the adrenal glands, resulting in the coordinated synthesis and release of GCs. In brief, stress causes the release of corticotropin releasing hormone (CRH) from specific neuroendocrine cells within the paraventricular nucleus (PVN) of the hypothalamus, which then stimulates the synthesis and release of adrenocorticotropic hormone (ACTH) from corticotrophs within the anterior pituitary. ACTH subsequently stimulates the synthesis and release of GCs, including cortisol in humans and corticosterone in rodents, from cells within the zona fasciculata of the adrenal cortex. GCs, in turn, provide negative feedback by acting on the glucocorticoid receptor (GR) at each level of the HPA axis, subsequently terminating its activation[29,30]. This neuroendocrine regulation is central for reestablishment of physiological homeostasis, since disruption of GC-regulated negative feedback is a major pathophysiological contributor to the development of stress-related diseases[31-33].

Further regulation of HPA axis activity is directly mediated by extrahypothalamic regions in the brain including the amygdala, as its activation can drive the HPA axis in response to a stressor[34]. Alternatively, GC-mediated feedback inhibition of HPA axis activity can be mediated by the hippocampus and the prefrontal cortex[35]. This feedback loop mechanism is impacted by inflammatory responses resulting from genetic factors (i.e., autoimmune disease, multiple sclerosis), stress-related diseases (i.e., psychiatric disorders), somatic fatigue and pain disorders (i.e., chronic fatigue syndrome, fibromyalgia), and environmental factors (i.e., allergic conditions). In turn, an exacerbated inflammatory response impacts extrahypothalamic inputs to any level of

the HPA axis, causing alterations in CRH, ACTH, or GC secretion, as well as inflammation-mediated impairments in GR responsiveness. Consequently, impaired HPA axis regulation promotes hypercortisolism or GC resistance by preventing a proper physiological response to GCs in populations of individuals with inflammatory susceptibility[36].

Lastly, while GR is occupied by endogenous GCs under conditions of stress to provide negative feedback to the HPA axis, the mineralocorticoid receptor (MR) has a 10-fold higher affinity for endogenous GCs compared to GR and is largely occupied under basal homeostatic conditions. Because of this, GR and MR exhibit distinct expression patterns and electrophysiological properties, and have distinct roles in modulating GC physiological responses, behavioral output, and learning[37].

1.1.2 Basic Physiological Role of GCs during Human Fetal Development

A developing human fetus is exposed to GC which are maternal-derived or fetal-derived depending on gestational age. A disruption in GC production from either source leads to abnormal fetal development[38]. The human maternal contribution to fetal GC content is negligible during most of pregnancy because of efficient cortisol metabolism by placental 11β-hydroxysteroid dehydrogenase 2 (11ß-HSD2), an enzyme with oxidase activity localized at the fetal-maternal interface that inactivates cortisol to cortisone. However, increased secretion of CRH by the placenta creates a surge in fetal GC content occurring during late gestation that is necessary for organ maturation and parturition[39-41]. As human gestation advances, cortisol suppresses CRH release from the hypothalamus but increases CRH release from the placenta, forming a positive feedback loop that persists until after birth[42,43]. However, under conditions of excess psychological or physiological stress, elevated maternal cortisol content can cross the placental barrier at earlier

gestational timepoints resulting in GR-dependent epigenetic programming, long-term changes in gene expression, and persistent HPA axis dysfunction in the offspring[44-47]. The human fetal adrenal (HFA) gland is another source of GCs that develops into a distinct morphological structure in the early gestational period (i.e. gestational week 7-8) to produce mainly dehydroepiandrosterone (DHEA) and its sulphate (DHEA-S) adrenal androgens, which act as substrates for placental estrogen production[48,49]. While cortisol synthesis by the HFA gland is transient early in gestation it is largely suppressed until late gestation, during which it is critical for fetal maturation and initiation of parturition. Cortisone located within the placental membranes may also be converted to cortisol by 11β-hydroxysteroid dehydrogenase 1 (11ß-HSD1), which exhibits increased expression and activity with advancing gestation[41].

1.1.3 Nuclear Receptor Structure and Function

The nuclear receptor superfamily are TF that interact with small lipophilic ligands including steroids (i.e. GC), retinoids, fatty acids and phospholipids, though 'orphan' nuclear receptors exist for which endogenous ligands are not yet known[50,51]. Nuclear receptors are divided into seven subfamilies based on their DNA-binding characteristics, and though they are structurally similar they generate diverse physiological responses. Overall, nuclear receptors are made of up a N-terminal domain (NTD), a well-conserved central DNA binding domain (DBD), a hinge region, and a ligand binding domain (LBD) with some shared structural features. The highly unstructured NTD contains the Activation Function 1 (AF-1) domain, which interacts with various co-regulator proteins and components of the basal transcriptional machinery. The DBD contains a zinc-finger structured subdomain that interacts with DNA in a nucleotide base-specific manner, while a second subdomain contains residues that enhance receptor dimerization for some

members of the family. The hinge region links the DBD to the LBD, which not only binds ligands in a hydrophobic binding pocket but also interacts with co-regulator proteins via the Activation Function 2 (AF-2) surface[51]. Ligand-bound nuclear receptors can act as monomers, but often form homodimers or heterodimers when DNA-bound to regulate major cellular processes via genomic and/or non-genomic mechanisms[52]. The classic genomic actions of steroid hormone receptors occur when the receptor, which normally predominantly resides in the cytoplasm bound to chaperone proteins, binds a ligand and undergoes conformational changes allowing disassociation from cytoplasmic-anchored chaperone proteins. This reconfiguration allows it to translocate to the nucleus through nuclear pores, accessing the genome leading to activation or repression of target genes.[22] For members of the nuclear receptor not associated with cytoplasmic chaperones when unliganded, conformational changes induced by ligand binding within the nucleus influence their DNA-binding properties, coregulator interactions and subsequently gene-specific changes in transcriptional output.

In addition to their well-established role as TF, nuclear receptors can trigger rapid activation of multiple cytoplasmic signaling cascades through non-classical pathways initiated by ligand binding to receptors in various cytoplasmic and membrane compartments[24,51,53]. The non-genomic actions of steroid hormone receptors are most well studied for androgen receptors (AR) and estrogen receptors (ER) in both physiological (i.e. cardiovascular and reproductive) and pathophysiological (i.e. disease) conditions using primary and secondary cell lines. These rapid non-genomic signaling capabilities involve a ligand-bound membrane-associated steroid hormone receptor initiating a cascade of activity by PI3K, MAPK and AKT kinases affecting intracellular signaling and cellular physiology in a transcription-independent manner[17,54,55]. This non-classical signaling can occur via alternate membrane G-protein coupled receptors (GPCRs) that are

associated with a steroid hormone receptor, or it can occur in conjunction with growth factor signaling. In addition, intricate crosstalk between genomic and nongenomic pathways controls transcriptional output and cell fate [56-59]. Relevant to this thesis, a more detailed overview of non-classical GR signaling specifically in NSPCs is provided (see the section titled 'Animal Research: Cellular Mechanisms of sGCs in NSPCs').

1.1.4 GR and Transcriptional Regulation

The transcriptional response to GCs is mediated by GR, which is encoded by the nuclear receptor subfamily 3 group C member 1 (*NR3C1*) gene, located on chromosome 5 (5q31)[16,60]. Its structure closely resembles those of other steroid hormone receptors such as MR (encoded by *NR3C2*), progesterone receptor (PR; encoded by *NR3C3*) and AR (encoded by *NR3C4*). Alternative splicing and/or translational start sides, as well as site-specific genetic polymorphisms yield diversified isoforms of NR3C family members with altered functional capacities[22]. The largely unstructured NTD of GR adopts a helical structure while bound by co-regulators, and this region is targeted heavily by post-translational modifications (PTMs) including phosphorylation, SUMOylation, ubiquitylation and acetylation [51,61]. PTMs provide regulatory potential beyond that imposed by binding of hormonal ligands and control allosteric states, protein interaction surfaces, protein localization of nearby transcription factors, stability, DNA binding, ligand response, and transcriptional regulatory activity. Of the most studied PTMs is direct Serine/Threonine (Ser/Thr) kinase-mediated phosphorylation of human GR, which occurs in a largely ligand-dependent manner at over 20 identified sites (5 of which are considered 'major' phosphorylation sites at amino acid positions of human GR 134, 203, 211, 226 and 404), and modulates selective GR action[62]. Aside from direct GR phosphorylation by Ser/Thr kinases (i.e., MAPKs, CDKs, AKT1,

glycogen synthase kinase 3β (GSK3β)), select kinases including Ser/Thr and others (i.e. PKC, mTOR) indirectly regulate GR action by phosphorylating other kinases and co-factors as well as signaling molecules within GR intracellular signaling pathways, ultimately impacting GR transcriptional outcome (reviewed by Kino et al)[63]. For a more detailed review on PTMs and GR activity, please see Weikum et al[16].

In the absence of a ligand, GR is sequestered within the cytoplasm via direct binding to chaperone proteins belonging to the heat shock family of proteins (HSP90; HSP70) and other co-chaperones such as FK506-binding protein 5 (FKBP51) that allow high-affinity ligand binding while simultaneously inactivating nuclear localization and DNA binding [64,65]. Classic GR-mediated signaling cascades occur when ligand-bound GR disassociates from its cytoplasmic-restricted chaperone proteins and undergoes conformational changes, unleashing nuclear localization sequences within the ligand binding region and hinge regions. Bi-directional nucleocytoplasmic shutting of GR occurs rapidly, as cytoplasmic-restricted FKBP51 is exchanged for nuclear-permissive FKBP52, both immunophilins associated with HSP90. FKBP52 favors the recruitment of dynein motors that facilitate nuclear accumulation of the receptor, ultimately regulating GC responsiveness[66]. Translocated nuclear GR interacts with specific DNA sequences termed GREs via the receptor's DBD. Classical GREs identified in the "pre-genomic era" are comprised of a motif containing an inverted palindromic sequence with two consensus 'AGAACA' motifs separated by 3 nucleotides[16,21,67,68].

The understanding of GR binding sequences became more complex with the discovery of the receptor's capacity to bind to half-site GRE motifs containing a single hexamer consensus sequence. Experiments performed *in-vitro* in which mutations interfere with one of GR's dimerization interfaces demonstrated that half-site GREs are likely bound by GR in a lower

oligomeric state and are associated with tissue-specific TFs, resulting in differential regulation of gene expression when compared to full-site GRE engagement[46,47,52]. Other *in-vivo* studies confirm GR dimerization is not required for transcriptional output and show that while GR-null mice die shortly after birth, mice with limited GR dimerization capacities are viable with normal adrenal medullary function[38,69,70]. In addition to GR binding patterns being dependent upon receptor oligomeric state and DNA motif structure, cell type-specific and sex-specific macromolecular complexes of co-regulator proteins (i.e., co-factors, TF) form GR-nucleated complexes and localize GR to genomic regions by acting as a 'tether', aiding GR in influencing transcriptional output independent of direct GR-DNA binding[22,71,72]. Tethering of GR to DNA, as well as direct GR binding to DNA, can occur at non-GRE motifs designed to interact with other cell type-specific TFs and because of this, the nucleotide sequences which proximally flank (+/- 2kb) GR binding sites may help explain unique GR occupancy in different cell types[68,73-76]. Tethering of GR to genomic regions may also occur at half-site GREs located nearby DNA binding sites for associated co-factor(s), providing a mechanistic role for half-site GREs in determining the cell type-specific GR cistrome[73,77,78].

Researchers have attempted to discern the regulatory elements at GR binding sites that discriminate gene repression from gene activation. Originally, gene regulatory profiling suggested the presence of 'negative GREs' (nGRE) that possess binding sites for GR and other associated TFs, and guide transcriptional downregulation following receptor activation. However, it seems the mode of GR-DNA interaction (i.e. direct GR-DNA binding vs. tethering), the DNA motif size (i.e. full-site GRE vs half-site GRE), and/or the receptor itself do not control the directionality of transcriptional output (i.e. activation vs repression) following hormone binding[73]. Rather, transcriptional outcome is likely established by cell type-specific epigenetic modifiers,

transcriptional machinery (i.e. RNA Polymerase II) targeted by GR, as well as understudied regulatory elements affecting GR structural conformation and oligomerization[79,80].

1.1.5 Genome Biology of GR

Recent advances in genome-wide technologies have allowed researchers to study the biological prerequisites for selective genomic GR action. Among these, the spatial organization of chromatin within the nuclear environment is a major determinant of *de-novo* genomic GR occupancy and a strict regulator of transcription[17]. Eukaryotic chromatin is a complex of nucleic acids and proteins that exist compacted inside the nucleus in a dynamic state, upon which TF act to influence DNA-templated processes (i.e., RNA transcription, DNA replication, repair, recombination). In this nuclear environment, 145-147 base pairs (bp) of DNA are wrapped around an octamer core comprised of two copies of each of the four core histone proteins (H3, H4, H2A, H2B), and together these make up a single nucleosome, whereas multiple nucleosomes strung together make up chromatin[81]. Nucleosomes are the functional units of chromatin that spatially restrict TF (i.e. GR) access to DNA with tighter or looser wrapping of DNA around histone core proteins[82]. The conformational dynamics of nucleosomes are modified by PTMs (i.e acetylation, methylation) of specific sites on core histone proteins (i.e. H3K27a) that influence chromatin compaction and confer regions of chromatin with increased or decreased accessibility to specific TFs[83]. Ultimately, because chromatin compaction restricts TF access to DNA, it controls transcriptional output.

Studies in primary and/or immortalized cell lines report that in response to ligand binding, *de novo* GR occupancy of DNA primarily occurs in pre-accessible chromatin, rather than GR altering chromatin structure to establish receptor-DNA contact. Furthermore, GR activity is biased

against binding to accessible chromatin located proximally to promoter regions[18,84,85]. Rather, GR binding occurs preferentially at distal noncoding regions, where chromatin is typically cell-type specific, to control transcriptional output via long-range enhancer-promoter interactions[18,86,87]. This genomic binding pattern is established by an increased presence of GREs at distal non-promoter regions, and cell type-enriched TFs, which guide GR to its genomic targets[88,89]. However, select chromatin sites are rendered more or less accessible to GR following receptor activation, probing an investigation of the importance of nucleosome remodeling in the GR transcriptional response and the nuclear conditions necessary for this to occur[90,91].

Selective GR binding to accessible chromatin is theorized to be mediated by co-factor proteins that act as transcriptional regulators by directly influencing key features of nuclear receptor activity. Experiments utilizing probes of chromatin accessibility (i.e. digestion with DNAse I) and TF/co-regulator immunoprecipitation with high-throughput sequencing reveal the colocalization of cell-type specific cofactors (e.g., AP-1 in 3134 mammary cells, FOXA1 in breast cancer cells) with steroid hormone receptors at genomic binding sites, which are required for the formation of accessible chromatin[92-94]. This recent model of nuclear receptor transcriptional regulation has challenged older theories that proposed a role for co-factors in modulating the recruitment and interaction capacities of the nuclear receptors and/or basal transcriptional machinery[71,95-100]. The fact that GR binds to pre-accessible chromatin suggests that prior to the introduction of a ligand, “pioneer” proteins prime chromatin for nuclear receptor binding by increasing accessibility of their DNA binding elements[20,88,101,102].

1.2 Clinical Use of Synthetic Glucocorticoids

1.2.1 Common Applications and CNS Side Effects

A pharmaceutical proxy of the endogenous steroid hormones that mediate cellular consequences of the stress response are sGCs, which include widely used medications such as prednisolone, dexamethasone, and betamethasone. Since their discovery in the 1940s as potent and effective anti-inflammatory and immunosuppressive agents, they have reliably been used to treat inflammatory diseases and autoimmune disorders including asthma, rheumatoid arthritis, inflammatory gastrointestinal disease, inflammatory joint and skin diseases, multiple sclerosis (MS), certain cancers, and are a part of immunosuppressive therapies following organ transplant[103]. sGCs have significant homology to endogenous GCs and their exposure leads to repression of pro-inflammatory cytokines and/or chemokines and key immunomodulatory factors, along with induction of anti-inflammatory protein synthesis[1,75-77]. These effects occur via direct or indirect activation of GR, with gene expression changes that are detectable within minutes of sGC exposure. Notably, the anti-inflammatory effects of GCs occur largely independent of MR activation[104-106].

Overuse of systemic sGC therapies, or GC imbalance resulting from stress, influences the magnitude and duration of GR responses in several bodily tissues and triggers an adaptive response involving several brain loci and brain mediators including monoamines, cytokines, glutamate and GABA, among others[107]. Though necessary for reestablishment of physiological homeostasis, dysregulation of this adaptive response often converges with genetic vulnerability and leads to cognitive and behavioral diseases, attention disorders, and unwanted side effects including immune suppression and metabolic irregularities[108-111]. For example, anxiety and depression are

the most common neurobehavioral manifestations of GC dysregulation, along with social withdrawal, dysphoria, altered pleasure and reward seeking, and aggressive behavior[107]. However, mild anxiety is often a 'normal' adaptive response to stress that is promoted by amygdala activation following downregulation of the subgenual prefrontal cortex's (PFC) inhibitory projections to this region. In turn, the activated amygdala's feedback projections inhibit the activity of the subgenual PFC in a cycle that can become dysregulated, resulting in 'abnormal' sustained amygdala activity and depressive symptomology[107]. Prefrontal cortical networks also control emotional memory and working memory, which are compromised during periods of prolonged GC exposure, accompanied by persistent changes in cortical architecture that precede lasting cognitive decline[112,113]. These sGC-induced cognitive and architectural alterations are associated with elevated risk of neuropsychiatric disorder or disease, though this may be reversed with moderations in sGC dosage or treatment cessation[114,115]

Another prevalent centrally-originating side effect is adrenal cortex atrophy and altered HPA regulation, contributing to adrenal insufficiency and Cushing's syndrome in humans, when the adrenal cortex does not respond effectively to stressors and release of endogenous GCs is suppressed[116,117]. Data from animal models corroborate this common side effect of chronic GC exposure, and reveal impairments in the natural circadian and ultradian rhythmicity of HPA-axis mediated GC release, accompanied by dose-dependent down-regulations of GR and MR activity in the brain[118]. Finally, though sGC therapy is a powerful tool used to reduce glioma-associated edema and risk of encephalopathy in patients who receive radiation therapy, steroid-associated neurotoxicity affecting any organ system is associated with negative survival outcomes in persons with brain oncogenic disease[119-121].

1.2.2 Antenatal Corticosteroids & Clinical Neurological Outcomes

Premature birth affects nearly 10% of all pregnancies in the United States and complications of prematurity are the second leading cause of infant mortality[122,123]. In 1972, Liggins and Howie published their seminal work demonstrating that antenatal administration of sGCs (e.g., betamethasone or dexamethasone) ameliorates multiple infant complications of premature delivery, including neonatal respiratory distress syndrome, necrotizing enterocolitis, cerebral intraventricular hemorrhage, and overall mortality[2]. This is because sGCs, which are 25 times more potent than cortisol and readily cross the placental barrier due to their resistance to 11ß-HSD2 metabolism, mimic the endogenous surge of cortisol that peaks during late gestation to promote rapid fetal organ maturation and parturition for premature birth[1,2,41,124]. Studies indicate that sGCs on average result in a 6% decrease in body length, a 9% decrease in head circumference, a 18% reduction in birth weight, and placental abnormalities when compared to untreated preterm-born or term-born infants[125]. However, they remain a life-saving treatment in the case of prenatal birth, and standard medical practices today recommend a course of antenatal corticosteroids (i.e. sGC) for pregnant women who are at imminent risk within 7 days for preterm delivery between the age of viability and gestational week 34 (GW34), a period in which endogenous fetal GC levels are very low[1,126].

Neurodevelopmental studies over the ensuing decades, however, have identified potential consequences of antenatal steroid exposure. sGCs tightly bind GR but have low affinity for MR[127,128]. GR is highly expressed in the fetal human brain throughout development in a region-specific manner and this shifts drastically with advancing gestation, suggesting that region-specific sGC sensitivity exists based upon the time of antenatal exposure[129]. Human and non-human primate postmortem neonatal brain tissue analyzed after antenatal sGC exposure have

demonstrated decreased hippocampal cell density[6,8]. Studies in children have also demonstrated long-term neuropsychiatric consequences, in particular increased rates of attention problems, lower cognitive scores, executive dysfunction, ADHD-analogous symptoms, and aggressive behavior following antenatal corticosteroid exposure[9,130]. In other words, rates of childhood diagnoses of mental and behavioral disorders is increased[131]. A separate study linked antenatal sGCs to proven or suspected neurocognitive disorders in children at age 5 based upon audiometry or visual testing, or physician service claims[132]. Conflicting data exists regarding sGCs and cerebral palsy outcomes, highlighting a need for larger cohorts and more detailed review criteria in order to discern neurodevelopmental risk[130,133]. A separate study reported sGC-exposed males, but not females, had increased risk of epilepsy in childhood[134]. However, standardized guidelines do not modify antenatal corticosteroid dosage, timing or type based upon birth weight, multiple gestation, maternal ethnicity, sex, or genetic polymorphisms even though significant differences have been observed in clinical outcomes, thus complicating the interpretation of sGC risk when using data from large cohorts[43,124,135-140].

Certain studies have evaluated children who were exposed to sGCs *in-utero* given the concern for premature delivery, but then were carried to term (occurring in increasing frequency at approximately 25-40% of sGC-exposed pregnancies)[4,141-145]. In these cases, early-term sGC administration (≥14 days before birth) was associated with increased fetal morbidity compared to sGCs given <7 days before birth[146]. Elevated risk for placental dysfunction contributing to fetal growth restrictions was also reported[125]. This population of term-born infants were not immune to adverse neurologic consequences of sGC exposure, as they displayed a decreased cortical surface area, decreased complexity of cortical folding, as well as increased risk of neurocognitive and/or psychological impairment[147,148]. A separate study of sGC-exposed term-born babies found

evidence of cortical thinning on brain MRI scans of the subjects aged 6-10 years, particularly affecting the anterior cingulate gyrus[24,149]. Furthermore, these children displayed more behavioral affective problems[149]. However, other investigations found no neurodevelopmental deficits in sGC-exposed term born children, highlighting the need for standardized neurofunctional and neuroanatomical measurements across studies[150,151]. Another clinical concern exists because treatment frequency is not standardized, though evidence exists against multiple courses of antenatal corticosteroids. For example, a comprehensive study of 5 year old children (MACS-5 study) argued that repeated courses of antenatal sGCs triggered higher risk for neuropsychiatric and neurodevelopmental conditions compared term-born children who received a single course of sGCs[152,153].

Clinical studies observe associations of antenatal sGCs with HPA axis dysfunction across the lifespan of the offspring, as well as an increased risk for metabolic, reproductive, and cardiovascular abnormalities[44,47,154]. Amniotic fluid and cord blood assessments of antenatal sGC-exposed fetuses indicate an acute suppression of GC production in the immediate postnatal period which returns to normal in the first 1-2 weeks of life, but the effects on HPA axis reactivity and GC sensitivity persist[155-157]. For example, sGC-exposed infants had a suppressed cortisol response to stressful medically-necessary stimuli in comparison to non-sGC exposed infants to 6 weeks after birth[158-160]. This cortisol response is further dampened by multiple courses of antenatal sGCs[161]. In contrast to sGC-exposed premature-born infants, term-born infants display elevated cortisol responses to stressful stimuli, but no change in basal GC production, further suggesting that programming of HPA axis function by sGCs is dependent upon gestational age[162]. However, premature birth or painful medical procedures can hinder HPA axis development independent of sGC exposure, potentially confounding these interpretations[163,164]. Evidence of altered HPA axis

reactivity exists in children, with sGC-exposed females exhibiting elevated stress-induced cortisol compared to unexposed female controls or sGC-treated males. This sex-specific effect occurred independent of maternal stress, suggesting the programming mechanisms of sGCs differ from cortisol[165]. However, some clinical studies associate maternal stress with fetal outcomes in sGC-exposed children, suggesting the fetal HPA axis is susceptible to elevated endogenous GCs secondary to sGCs during development[165,166]. Finally, the circadian regulation of cortisol production is blunted in sGC-exposed term-born children, suggesting that basal HPA axis activity is affected[143,167]. Outcomes in adulthood are not well studied in humans, often because they are beyond the scope of most clinical trials, but animal studies support a biological basis for sGC-induced long-term programming of HPA axis function (see next section titled Animal Research: Excess GC during Neurodevelopment)[168]. This often manifests as an increased or decreased sensitivity to endogenous GCs and interferes with the body's ability to maintain or reestablish proper homeostatic conditions following stressful stimuli. In turn, sustained hormonal imbalance has potential for adverse neurodevelopmental effects, as GCs are critical regulators of early brain development and behavior[44,47,169].

1.3 Animal Research: Antenatal sGCs Influence HPA Axis Development & Behavior

Despite the widespread use of antenatal corticosteroids, clinical data examining the adverse long-term outcomes associated with this treatment remain inconclusive. Therefore, it is reasonable to rely on animal models of antenatal sGC exposure to probe the cellular and molecular mechanisms that reprogram HPA axis function, stress responses, and behavior. Antenatal sGCs impact learning and memory in rodents, while non-human primates display hyperactivity, reduced

concentration, and dampened motivation[170,171]. A separate study found reduced long-term synaptic depression in the CA1 hippocampal field contributing to impaired spatial learning in nonhuman primates exposed to a single course of Dex *in-utero*[172]. Behavioral studies performed in the DeFranco laboratory showed that in an elevated plus maze test, adult mice exposed to a single dose of Dexamethasone (Dex) *in-utero* had a significantly increased presence in the center and open arms of the open field and decreased time in the closed arms. In addition, during a forced swim test they spent less time floating compared to controls[7,173]. The results of these two behavioral tests suggest a blunted HPA stress response compared to controls resulting from antenatal Dex. Alterations in HPA axis function and reactivity are a consistently reported outcome of antenatal sGC exposure in animals. Studies in adolescent non-human primates, sheep, and rats exposed to Dex *in-utero* report elevated plasma cortisol both basally and/or in response to a stressor, compared to untreated controls[174-178]. The directionality of this significant disruption in cortisol production may change with age, and is often dependent upon the developmental stage at birth[47,175,179,180].

A cellular etiology of HPA axis dysregulation is reported in several species following antenatal sGC exposure. In nonhuman primates, antenatal sGCs are associated with smaller brain and cerebellum weight, with attenuations in the dentate gyrus and Cornu Ammon (CA) hippocampal regions. These changes may be due to decreased amounts of presynaptic protein synaptophysin and/or microtubule associated proteins in the frontal region, or elevated cortisol causing neurotoxicity[174,181]. Rodents and non-human primates show reductions in hippocampal GR protein expression and decreased hippocampal cell density, particularly affecting pyramidal and dentate granular neurons[5,177]. Meanwhile, studies of the offspring of Dex-treated pregnant guinea pigs report elevated GR mRNA levels in the anterior pituitary and increased GR protein

expression in the hippocampus of males and females, respectively, indicating heterogeneity in GR responses that are likely region, sex, and dose-specific[182,183]. These alterations of GR in HPA axis regions, as well as in upstream extrahypothalamic regions, have potential to impact GC responsiveness and therefore alter negative feedback inhibition of HPA axis activity, leading to imbalances in GC production and regulation. This HPA axis dysregulation directly alters the serotonergic and dopaminergic systems in term-born mice exposed to antenatal sGCs, resulting in drug seeking behavior, stress-related behavior, and impairments in social interaction[173,184-186]. In particular, antenatal sGCs decrease dopaminergic cell count in several brain regions including the hypothalamus and amygdala, likely impacting the meso-cortico-limbic system which controls reward processing, coordination of autonomic activity, endocrine systems, cognition, memory and behavior[185,187-189]. This is supported by reports of impaired motor functioning, sexual performance, and spatial memory in mice or rats expressed to antenatal sGC[186,190-192]. sGC also target the serotonergic system, causing reduced neuronal expression in the hypothalamus, hippocampus, and frontal cortex with possible implications for stress regulation and affective disorders[184,187,193]. Attenuations in the size of the medial, orbital, and dorsal cortices is also reported[194,174,177,194].

1.4 Animal Research: Cellular Mechanisms of GC Action in Early Neurodevelopment

Classical genomic GR signaling regulates genes responsible for cell survival, terminal maturation, and axonal and dendrite remodeling during early brain development[184]. Importantly, GC-mediated signaling tightly controls proliferation, differentiation, and survival of neural stem and progenitor cells (NSPCs), the lineage precursors which have capacity to self-renew or differentiate into the committed cell types which populate the brain during rapid periods of cerebral

cortical expansion[195]. Non-classical (i.e., nongenomic) GR signaling cascades also converge to influence synaptic plasticity, neurogenesis, and glial plasticity[24,53]. Evidence from human and preclinical models suggest sGCs alter the transcriptional output of GR, causing altered NSPC fates and leading to size reductions in various brain regions. In the DeFranco lab, we have used a mouse model of antenatal Dex administration to confirm certain adverse neurodevelopmental effects in agreement with the idea that Dex alters NSPC fate. A single dose of Dex *in vivo* at embryonic day (E)14.5 leads to decreased brain-to-body weight ratio, cortical thickness, and cortical surface area of the brain at E17.5.[7] However, despite the smaller cortical surface area and thickness, the cellular structure of the cortex was found to be more densely packed, particularly in cortical layer V, suggesting a Dex effect on NSPC proliferation and/or cell fate[7,24]. Studies of embryonic rats exposed to multiple antenatal Dex treatments *in-vivo* beginning at embryonic day 14.5 (E14.5), or E15, exhibit decreased NSPC proliferation in the hippocampus, striatum, and dentate gyrus[196]. Similar antiproliferative and apoptotic effects occur in Dex-treated newborn rats, specifically in the subgranular zone of the dentate gyrus[197,198]. These antiproliferative effects may trigger developmental deficits that manifest as cognitive or behavioral impairments in animals and humans exposed to sGCs *in-utero*[44,47].

Studies conducted *in-vitro* revealed that Dex had antiproliferative effects on NSPCs via multiple mechanisms. Experiments using neurospheres formed in culture from fetal mouse NSPCs demonstrate that Dex decreased NSPC proliferation by altering the expression of genes controlling cell senescence and cell cycle, without impacting cell death or differentiation[199]. Other studies report Dex-dependent transcription downregulated the expression of apoptosis protein inhibitors (i.e. BRUCE/Apollon) which may contribute to overall reductions in cell number[200]. Studies in other cell lines report GC repression of cyclin-dependent kinases (CDK4, CDK6) or activation of

cyclin-dependent kinase inhibitors (CDIs; p27, p21), two families of factors that control cell cycle advancement[201]. In some cases, sGCs had a dose-dependent pro-proliferative effect in human induced pluripotent stem cell-derived NSPCs, in comparison to anti-proliferative effects in primary embryonic NSPCs, demonstrating that the sensitive response to sGCs is largely cell-type-specific[202].

Rapid transcription-independent GR signaling mechanisms also control proliferation in NSPCs. In particular, studies in the DeFranco lab and others showed that a membrane-associated GR is localized to caveolin-1-enriched lipid rafts near the cell membrane [203]. When the receptor is ligand-bound, GR-activated intracellular MAPK signaling controls the activity of connexin-43-containing gap junctions, intracellular channels made up of connexin proteins that allow the passage of ions (i.e. Ca^{2+}) and small molecules (<1kD) from cell-to-cell[55]. MAPK-dependent site-specific phosphorylation of connexin 43 promotes attenuations in gap junction intercellular communication (GJIC) and disruptions in spontaneous Ca^{2+} waves, leading to decreases in S-phase progression and enhanced cell cycle exit[204-206]. The importance of intracellular Ca^{2+} in NSPC proliferation is confirmed in other studies[55,207,208]. Interestingly, pharmacological inhibition of GJIC reduces S-phase progression but unlike GCs it does not alter cell cycle exit, suggesting GCs decrease GJIC through cooperativity of both nongenomic and genomic pathways[55]. These experiments in embryonic mouse NSPCs shed light on the vast variety of intracellular mechanisms controlling the GC transcriptome and NSPC cell fate.

This cooperativity of signaling pathways is characterized in studies utilizing NSPCs derived from caveolin-1 knock-out (KO) mice to demonstrate that interference with the nongenomic GR signaling pathway (i.e., via caveolin-1 ablation) impacts genomic GR action and transcriptional output, due to a loss of caveolin-1-dependent phosphorylation of GR at serine 220

(serine 211 in humans). This important PTM controls the proliferative response to sGC, because the anti-proliferative response to Dex does not occur in caveolin-1 KO NSPCs, possibly due to the loss of hormone induction of *Sgk-1*, a gene shown to mediate antiproliferative responses of GCs in human hippocampal progenitor cells[209,210]. In a follow-up study conducted by the labs of Dr. Don DeFranco and Dr. Paula Monaghan-Nichols, mutant mice with a serine-to-alanine replacement at serine 220 (GR^{S220A}) exhibit robust differences in both basal and Dex-induced transcriptomes, providing further evidence of the importance of PTMs in regulating genomic GR action (unpublished). Lastly, a valuable resource published by Frahm et al. provides genome-wide RNA-seq gene expression data profiling over 1,000 genes that are induced or repressed by Dex at 4h in male and female mouse cerebral cortical and hypothalamic embryonic NSPCs *in-vitro*, providing unique insight on the sex and region-specific robust responses that reprogram fetal brain development following sGC exposure[10]. Gene ontology analyses of these data reveal cell proliferation as a functional network highly regulated by Dex[10]. However, less is known about GR's interactions with DNA, chromatin, and other factors inside the nucleus that fine-tune transcriptional outputs specifically in NSPCs.

1.5 Using a Mouse Neurosphere Model

We use a mouse model of embryonic cortical-derived NSPCs (E14.5) grown as three dimensional neurospheres to study fetal neurodevelopment. The animal dissection and preparation of the neurosphere assay, originally developed in 1992 by Reynolds and Weiss, is described in detail by Azari et, al.[211,212]. In brief, embryonic-derived cortical NSPCs (collected at E14.5) are grown as neurospheres in ultra-low adherence cell culture plates to maintain their undifferentiated

state, in NeuroCult™ media supplemented with NeuroCult™ Proliferation Supplement (Stem Cell Technologies). This is a standardized, serum-free supplement for the culture of mouse and rat neural stem and progenitor cells. It is optimized to maintain mouse and rat neural stem cells in culture for extended periods of time without the loss of their self-renewal, proliferation, or differentiation potential. Media was also supplemented with epidermal growth factor (EGF) and fibroblast growth factor-1 (FGF-1) to maintain self-renewal, neurosphere expansion, and inhibit differentiation. Penicillin streptomycin is included in cell culture media for sterility[203].

GR is expressed throughout gestation[44,47,213]. Although organ system development is not synchronously timed in humans and mice, the environment in the E14.5 mouse brain resembles the earliest ages that human fetuses are exposed to antenatal sGCs with respect to robust gliogenesis and ongoing neurogenesis[214]. Importantly, E14.5 is a period during which fetal glucocorticoid levels are relatively low, at least 2 days before endogenous fetal glucocorticoid production begins and three days before the maternal corticosterone production increases by >2-fold to stimulate parturition in mice, mimicking the environment of most developing human fetuses exposed to sGC (up to ~30 gestational weeks[215]) [216,217]. Like mid-gestational periods in humans, placental expression of 11ß-HSD2, the enzyme that catalyzes inactivation of corticosterone to 11-dehydrocorticosterone in rodents, is highly expressed in mice at E14.5 and limits fetal exposure to endogenous GCs. It is important to note that sGC are 25 times more potent than endogenous GC, and readily cross the placental barrier due to their resistance to 11ß-HSD2 metabolism[1,2,41,124]. sGC (i.e. Dex) exposure at E14.5 in mice is also relevant to humans as evidenced by published findings of reduced cortical size and cortical surface area immediately prior to birth resulting from E14.5 Dex exposure, a brain phenotype that has also observed in newborn term infants exposed to antenatal sGCs[7,142,149]. In addition, published data demonstrates

cortical-derived embryonic NSPCs are more sensitive to Dex-induced changes in gene expression (n=1000 genes significantly changed) compared to NSPCs derived from the embryonic hypothalamus at the same timepoint (n=14 genes) , highlighting E14.5 as a temporal window that is especially sensitive to sGC-triggered perturbations in cortical-derived NSPC fate decisions[10].

While previous studies in the DeFranco lab model prenatal administration of sGC *in-vivo*, these studies were conducted *in-vitro* to study effects of Dex on an enriched NSPC population, which requires isolating the cells in culture at E14.5 (passage zero, P0) and sub-culturing for 3 passages (P2-P3) prior to an acute 4-hour Dex treatment[204,218]. This approach allows us to avoid cell-sorting and additional sample manipulation that compromises cell viability prior to sequencing, which would be required to measure the acute effects of Dex on NSPCs *in-vivo.* In culture, 100nM (1.0×10^{-7}M) Dex is a saturating concentration for GR binding and has been used extensively by our group to characterize genome-wide responses in NSPCs[7,10,209,219]. Detailed rationale for the choice of Dex concentration (1.0×10^{-7}M) used in these *in-vitro* studies is provided in a prior publication. In brief, this previous study demonstrates a pro-proliferative NSPC response to Dex at lower concentrations (1.0×10^{-9}M), similar to the NSPC response seen following Dex *in-vivo* (0.4 mg/kg; approximates the minimal dose used clinically in humans), and an anti-proliferative response at higher concentrations (1.0×10^{-7}M)[7]. NSPCs derived from the E14.5 brain allow detailed *in-vitro* analyses of the dose-dependent response to Dex, as GR is expressed in NSPCs in the embryonic cerebral cortex at this timepoint *in-vivo* [7,213,220]. The neurosphere culture model system is also advantageous because it recapitulates the NSPC self-renewal, neuronal and glial differentiation, and cell-cell coupling properties of NSPCs that occur *in-vivo*[221,222].

1.6 Goals of Dissertation

This study sought to identify novel relationships between chromatin structure, genomic GR binding, and cell-type-specific TF which guide transcriptional responses to the sGC Dexamethasone (Dex) in embryonic cortical-derived NSPCs. This was accomplished with three aims:

Aim 1: Characterize the chromatin landscape of vehicle- and Dex-treated NSPCs. An assay for transposase accessible chromatin followed by whole genome sequencing (ATAC-seq) was performed to characterize the chromatin landscape of NSPCs to explore the impact of Dex on chromatin accessibility at GR target genes, with the following hypothesized outcomes: **(Outcome 1.1)** The chromatin landscape displayed some differential accessibility at GR target genes following exposure to Dex. These targeted changes in chromatin accessibility may represent regulatory regions that guide the transcriptional response of NSPCs to GCs. **(Outcome 1.2)** The chromatin landscape predominantly did not display differential accessibility following exposure to Dex, suggesting that the transcriptomic response to GCs is mediated primarily by genomic GR binding to pre-determined accessible sites within chromatin.

Aim 2: Characterize the role of chromatin accessibility in determining genomic GR binding patterns in vehicle- and Dex-treated NSPCs. Dual crosslinking chromatin immunoprecipitation followed by whole genome sequencing (ChIP-seq) was performed to characterize genomic GR binding in NSPCs and predict co-factors and pioneer factors which guide GR to specific genomic regulatory regions involved in NSPC maintenance and fate. These data are combined with data collected in Aim 1 to explore the following hypothesized outcomes: **(Outcome 2.1)** Genome-wide

GR binding occurs in regions of the NSPC genome with predetermined chromatin accessibility. **(Outcome 2.2)** Genome-wide GR binding triggers increased accessibility of regions of the chromatin previously closed within NSPCs. **(Outcome 2.3)** Specific transcriptional regulatory proteins occupy regions of the genome that are near GR binding sites in NSPCs.

Aim 3: Characterize genomic interaction(s) between GR and SOX2 to determine if SOX2 is required for the effects of Dex on the NSPC transcriptome. A proximity ligation assay (PLA) was performed in vehicle and Dex-treated NSPCs to characterize nuclear localization and protein-protein proximity of GR and SOX2 *in-vitro*. In addition, a *Nestin-CRE* transgenic mouse line was crossed with $Sox2^{flox/flox}$ mice allowing for ablation of *Sox2* in cultured primary NSPCs. Microarray gene expression profiling was performed to determine if SOX2 is required for the response of established GR target genes *in-vitro*. **(Outcome 3.1)** SOX2-GR nuclear proximity suggests that interactions between these two proteins coordinate gene responses to Dex. **(Outcome 3.2)** Ablation of *Sox2* significantly alters the profile of GR target genes, implicating SOX2 as a GR-interacting factor directing the transcriptional response to pathways responsible for regulating cell fate and/or proliferative responses in NSPCs.

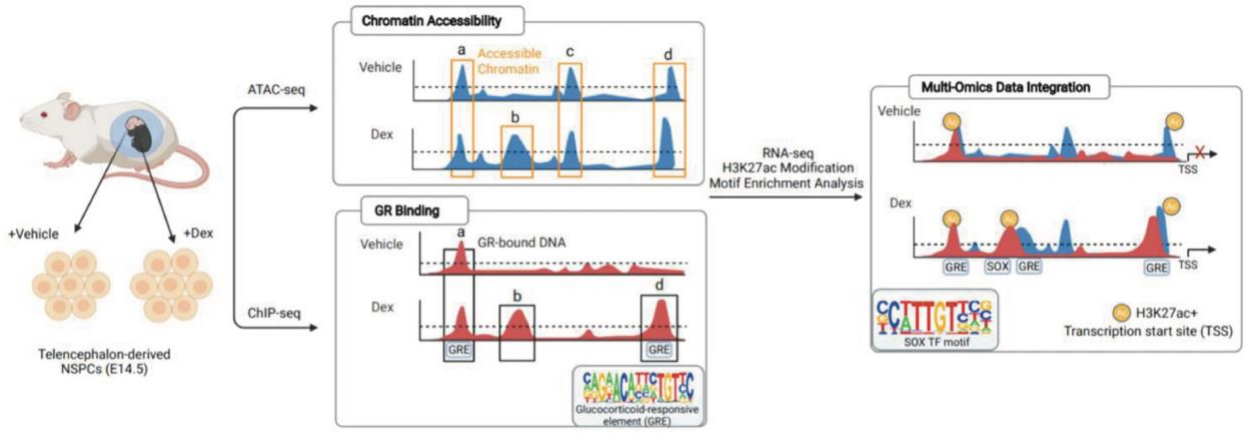

Figure 1 Overview of Aims 1&2

Figure 1. Schematic overview of bioinformatic processing of vehicle-treated or Dex-treated NSPCs (E14.5) in Aims 1&2. The black dotted line represents the cut-off threshold ($p<0.05$) for called ATAC-seq peaks (top) or ChIP-seq peaks (bottom) (boxed in). Genomic regions are categorized as a) constitutively accessible and GR-bound in both treatment conditions, b) differentially accessible and GR-bound in Dex-treated NSPCs only, c) constitutively accessible but not GR-bound in either condition, or d) constitutively accessible in both treatment conditions but GR-bound only in the presence of Dex. Multi-Omics Data Integration (right) allows visualization of (i) peaks proximal to the TSS of a Dex-regulated gene, (ii) peaks enriched for a glucocorticoid responsive element (GRE) or SOX TF motif, and (iii) peaks with a H3K27ac histone modification.

2.0 Aim 1: Genome-wide Accessible Chromatin Profiling of Mouse Embryonic Cortical NSPCs

2.1 Introduction

2.1.1 NSPCs in Fetal Cerebral Cortical Development

Primary neural stem and progenitor cells (NSPCs) are the apical progenitors (AP) that make up the neuroepithelium, the specialized epithelium which lines the lumen of the lateral ventricle. All neurons in the mammalian neocortex arise directly or indirectly from these AP cells, which exhibit apical-basal polarity with the apical process at the surface of the ventricular zone (VZ) and undergo symmetric cell divisions via mitosis to span the cortical wall. At the onset of neurogenesis, neuroepithelial cells express glial markers and are then termed radial glial cells (RGCs). RGCs undergo symmetric divisions to self-renew the RGC pool, as well as asymmetric stem cell-like divisions to generate a predetermined number of neurons or a secondary group of NSPCs termed basal or intermediate progenitors (BP; IPC)[223]. BP are biologically distinct from AP due to their localization to the basal region of the VZ to form the subventricular zone (SVZ), the second germinal later of the neocortex. BP are transit amplifying cells that undergo predominantly symmetric divisions away from the lateral ventricle, producing two neurons. Importantly, the laminar fate of neural progenies changes over time, with early born neurons migrating to deep cortical layers (LVI-LV) and late-born neurons migrating to upper cortical layers (LIV-II)[223]. At a later stage of neurogenesis, gliogenesis begins[224]. The architectural features of AP and BP determine the asymmetric vs symmetric cell divisions which populate the developing

mammalian cortex. This processes is believed to be in part autonomously controlled by a cell-intrinsic biological clock of NSPCs, but it is also tightly regulated in a temporal manner by specific growth factors and TFs[223,224] (reviewed by Kageyama et al. [225] and Tamura et al. [226]).

With respect to **Aims 1&2**, the environment in the E14.5 mouse brain resembles the earliest ages that human fetuses are exposed to antenatal GCs with respect to robust gliogenesis, ongoing neurogenesis and a period of limited endogenous GC exposure. sGC (e.g., Dex) exposure at E14.5 in mice is also relevant to humans as evidenced by our published findings of reduced cortical size and cortical surface area immediately prior to birth resulting from E14.5 Dex exposure, a brain phenotype that has also observed in newborn term infants exposed to antenatal sGCs[7,142,149]. In addition, Dex exposure at E14.5 results in increased supernumerary neuron production by E17.5 in mice, an effect which occurred in all layers of the cortical plate with a maximal effect in LV[7]. These data suggest Dex alters the cell intrinsic or extrinsic programming controlling cell divisions in the developing neocortex.

2.1.2 Chromatin Organization of Mammalian NSPCs

Chromatin landscapes are measured with elegant bulk or single-cell assays that perform whole genome sequencing (ATAC-seq; scATAC-seq) to identify transposase accessible chromatin. These approaches allow the identification of DNA regions deemed less compacted and more accessible to TFs and/or transcriptional machinery in one experimental group compared to another[227]. As discussed in Section 5 of the Introduction titled ‘Genome Biology of GR’, the chromatin landscape undergoes dynamic changes in structural organization and exerts precise control of transcriptional output and, ultimately, mammalian cell fate transitions. This is evidenced in neurodevelopmental scATAC-seq studies in human and chimpanzee stem cell-derived brain

organoids which revealed that cortical neural progenitors exhibit differentially accessible chromatin regions compared to neurons across the psuedotime of development *in-vitro,* with some regions being enriched for distinct biological processes[228]. Single nuclei ATAC-seq (snATAC-seq) profiling of AP or BP neural progenitors and postmitotic neurons derived from the E12.5 mouse brain shows distinct region-specific chromatin landscape profiles associated with differences in neurogenic potential and lineage commitment[229]. In addition, studies in blastocyst-derived stem cells describe chromatin accessibility-mediated changes required for neuronal and glial differentiation *in-vitro*[230]. Other developmental time course ATAC-seq studies in mice report Hopx-expressing neural progenitors have similar chromatin landscapes at embryonic, early postnatal, and adult stages, while mature dentate gyrus samples exhibit a drastically altered landscape, suggesting that the chromatin architecture of progenitors are stable across the lifespan until it receives intrinsic or extrinsic biochemical cues initiating a transition in cell state[231]. Integrative analysis of these data and with global gene expression results associate chromatin accessibility with transcriptional regulation across neocortical development.

A re-occurring theme of ATAC-seq studies is the existence of accessible chromatin regions located predominantly in distal noncoding genomic regions[85,228,231]. This is an important observation because accessible chromatin often overlaps with identified enhancer regions, DNA regulatory elements which are accessible to TFs and typically located in distal noncoding regions[87]. This overlapping of accessible chromatin with distal enhancer regions occurs in part because enhancers are often depleted of nucleosomes and thus are sensitive to chromatin measurement assays (i.e. DNase I digestion, ATAC-seq)[232,233]. Aim 1 of this study places emphasis on overlap of accessible chromatin with enhancer regions enriched for the histone 3 lysine 27 acetylation (H3K27ac) histone modification marker in NSPCs (E14.5), a reliable predictor of

enhancer elements that actively influence NSPC self-renewal and neuronal differentiation in humans and mice[19,234-238]. Experimental models of *Drosophila melanogaster* embryonic development also identify H3K27ac as a reliable predictor of *de novo* enhancer activity, along with RNA polymerase II (RNA Pol II) occupancy[239]. Importantly, these 'active' enhancer regions, enriched with both H3K27ac and H3K4me1, are distinguishable from 'poised' enhancer regions marked only by H3K4me1, which are not yet transcriptionally active[236].

Active enhancers influence transcriptional outcome directly through chromatin looping, a biological process which brings distal enhancers within close physical proximity of their target gene promoters, or indirectly by destabilizing nucleosomes and recruiting H3K27ac-binding proteins[240,241]. A vast array of 3-dimensional chromatin loops exist in the nuclear space that hosts the human genome[242]. Additionally, active enhancers recruit RNA Pol II transcriptional machinery and produce noncoding enhancer RNAs (eRNAs) that aid in their function to regulate transcription[243,244]. Recent technologies have allowed the visualization of RNA Pol II in enhancer transcriptional complexes and suggest that it stabilizes the interacting chromatin networks by restricting the fluidity of chromatin[82]. Recent advances in next-generation sequencing have also allowed the discovery of 'super enhancers', defined as a cluster of enhancers heavily occupied by TFs that positively regulate spatiotemporal gene expression in a highly cell-type specific and TF-dependent manner, and are capable of regulating cell identity[245].

To characterize gene promoter-proximal and distal genomic regions with high potential for transcriptional regulation**, Aim 1** maps accessible chromatin in NSPCs derived from the fetal (E14.5) mouse telencephalon.

2.1.3 Chromatin Remodeling by GR

The remodeling of nucleosomes is a fundamental feature of steroid hormone receptor-regulated transcription. The conformational state(s) of chromatin are changed by a broad range of molecular and physical factors including TFs (i.e. GR), covalent modification of histones, DNA methylation, ATP-dependent remodeling complexes, and liquid-liquid phase separation (LLPS)[246,247]. Studies of GR in acute lymphoblastic leukemia cell lines have demonstrated various modes of nucleosome remodeling that occur following GR-DNA binding resulting in (i) enhancer activation and induction of gene expression, (ii) creation of *de-novo* enhancer regions, and/or (iii) nucleosome eviction allowing GR or co-factors to bind to target genomic regions[248]. Another impressive study by McDowell et al. measured GR binding in Dex-treated A549 cells (a human lung epithelial cell line) over a 12-hour time course and found that GR binds to pre-established enhancer regions within minutes, followed by coordinated switches in TF occupancy and histone modifications, leading to alterations in chromatin accessibility and gene expression output[18]. Additional studies in A549 and adipocyte cell lines report similar conclusions in which GR activation triggers nucleosome remodeling[249,250]. A landmark study in the field of GR by Fletcher et al. proposed a 'hit and run' model, developed using chromatin reconstitution techniques in HeLa cells, which suggested that ligand-bound GR that is bound to chromatin recruits cell-type specific co-regulators and ATP-dependent chromatin remodeling complexes (i.e. BRG1 complex SWI/SNF), then becomes disassociated from chromatin due to chromatin remodeling activity that destabilizes GR-DNA binding with concurrent recruitment of the transcriptional preinitiation complex and RNA Pol II[251,252]. Together, these studies illustrate a dynamic series of events for GR-regulated gene expression to occur, all dependent upon nucleosome remodeling by distinct biologically functional complexes.

In recent years, the intranuclear organization of steroid hormone action was further compartmentalized by the discovery of nuclear GR in membrane-less compartments termed liquid condensates, as opposed to a homogenous distribution of GR in nuclear space[253]. GR liquid condensates, created by phase separation, share biochemical similarities with so-called 'transcription-related liquid condensates' containing transcriptional machinery and other key TFs, and both use chromatin as a scaffold. The co-localization of GR condensates and transcription-related condensates at chromatin increases the likelihood of transcription[254]. Currently, however, the role of GR liquid condensates in determining the chromatin landscape is unclear.

Chromatin remodeling caused by antenatal GC exposure is less studied. One study reports the late cortisol surge during gestation causes global changes in DNA promoter methylation and acetylation in the hippocampus of guinea pig offspring, providing a potential epigenetic mechanism by which GCs alter chromatin landscape *in-vivo*[255]. Similarly, decreases in DNA methylation and DNA methyltransferases, accompanied by gene expression changes and attenuated proliferation, suggest GR-induces epigenetic changes in Dex-treated rat NSPCs *in-vitro* which may affect chromatin structure[256]. **To directly address this topic, Aim 1 presents first published data examining if Dex alters the chromatin landscape in embryonic (E14.5) mouse NSPCs.**

2.1.4 Rationale and Summary

Dex is a clinically relevant sGC that results in altered cell fate outcomes in primary embryonic NSPC cultures and in the developing mouse brain[7,10]. A comprehensive characterization of the epigenetic mechanisms guiding the acute transcriptomic response to Dex will enhance our understanding of sGC's effects on the developing telencephalon and provide

insight into the genomic programming mechanisms contributing to neurodevelopmental deficits triggered by antenatal sGCs. We modeled single-dose sGC administration during mid-gestation by treating primary embryonic NSPCs with 100nM Dex or an ethanol vehicle for 4h and probed the global chromatin landscape by ATAC-seq.

2.2 Materials and Methods

We began by measuring these parameters in only female-derived NSPCs to conserve resources and establish a pipeline for bioinformatic processing. An important question to investigate in future studies is whether the sexually dimorphic effects of sGCs on gene expression is controlled by sexually dimorphic changes in the chromatin landscape and/or the GR cistrome.

2.2.1 Animals and Cell Culture

Cortical NSPC cultures derived from the C57BL/6 mouse embryonic telencephalon (E14.5) were generated in Neurocult media supplemented with epidermal growth factor (EGF), fibroblast growth factor-1 (FGF-1), penicillin streptomycin, and proliferation growth supplement (StemCell Technologies), in accordance with the technical manual provided by StemCell Technologies and the ethical and Environmental Health & Safety practices required by the University of Pittsburgh IACUC and the National Institutes of Health[10,204,209]. Cultures from each embryo were kept separate, and fetal sex was determined by digesting tail tissue overnight in 200µl of nonionic detergent buffer with 1.2µl of proteinase K at 56°C. Afterwards, samples were heat

inactivated at 95°C for 10 minutes and isolated DNA subjected to PCR analysis to detect the Y chromosome *Sry* gene[10].

For drug treatment after the third passage (P3), 100nM Dexamethasone (Dex), a saturating concentration for GR binding that has been used extensively to characterize genome-wide responses in NSPCs, or an ethanol vehicle, was added directly to the culture media for 4h[7,10,209]. Cells were removed from the culture media and collected immediately afterwards for analyses. ATAC-seq samples were technical replicates (n=3) derived from one female embryo.

2.2.2 Omni ATAC-seq

A detailed protocol and library assessment for Omni ATAC-seq is described by Corces et al. and is outlined by **Berry et al.** (see Supplementary Table 1)[257]. In brief, 100,000 cells with >90% viability were lysed in ice-cold buffer (10mM Tris-HCl pH 7.4, 10mM NaCl, 3mM MgCl2, 0.015% NP-40). Nuclei isolated by centrifugation were resuspended in transposase reaction mix containing a 1:20 dilution of Transposase (TDE1) in 1X TD buffer (Illumina) and incubated at 37oC for 30 minutes with mixing. Fragmented product was purified using a DNA Clean and Concentrator-5 kit (Zymo Research) according to the manufacturer's instructions. DNA fragments underwent 3-5 cycles of preamplification to incorporate Illumina adapter sequences. qPCR was carried out on 10% of the pre-amplified product to determine if further amplification cycles were required. The amplified library was purified using Ampure beads (Beckman Coulter). Following quality and quantity assessment with Qubit (Invitrogen) and HSD1000 Tape Station assay (Agilent), libraries were diluted to 10pM, pooled, and sequenced with NextSeq 500 (Illumina).

Flowcells for the NextSeq 500 were seeded with 1.8pM denatured library for automated cluster formation and 2 x 75 paired end sequencing, approximately 50 million reads per sample.

2.2.3 Data Analyses

2.2.3.1 Quality Check (Pre-Analysis)

Quality control of raw sequenced reads, which determines total number of reads, read length, and GC content among other measures, was performed using FASTQC. Sequencing quality control was performed using FASTQC. After sequencing, adaptors were removed using Trim Galore! with --paired –nextera parameters. Paired-end reads without adapter sequences were aligned against the mm10 reference genome using bwa mem with default parameters. Mitochondrial reads were removed using a python script removeChrom. PCR artifacts and duplicates were removed using MarkDuplicates, available in the Picard toolkit. A python script, SAMtoBED, was used to convert the read alignments (BAMs) into paired-end BED format (BEDPE) for downstream peak calling. ATAC-Seq peak regions of each sample were called using MACS2 with parameters -f BEDPE -g mm. ATAC-seq specific quality metrics were evaluated with ATACseqQC R package 28. An average of ~56 million paired-end sequencing reads per sample were procured, after removal of mitochondrial reads and mark duplicates, and the average fraction of reads in peaks (FRiP) was 0.06 (see Berry et al., Supplementary Table 2). The insert size analysis revealed that approximately 50% of all sequenced reads map the content of <1 nucleosome (<150bp) (**Figure 2A-F**). This agrees with the expected results as described by Buenstoro et al., though we did not observe an abundance of nucleosome multimer-sized fragments beyond a dimer[227]. ATAC-seq peaks were called in each of three technical replicates using MACS2 ($n=3$, $p<0.05$) (see **Berry et al.,** Supplementary Table 3), and consensus peaks occurring in at least

2 replicates were used in all successive analyses (see **Berry et al.,** Supplementary Tables 4-5). A heat map of read densities shows a symmetric distribution of mapped reads relative to transcriptional start sites (TSSs) (**Figure 3**).

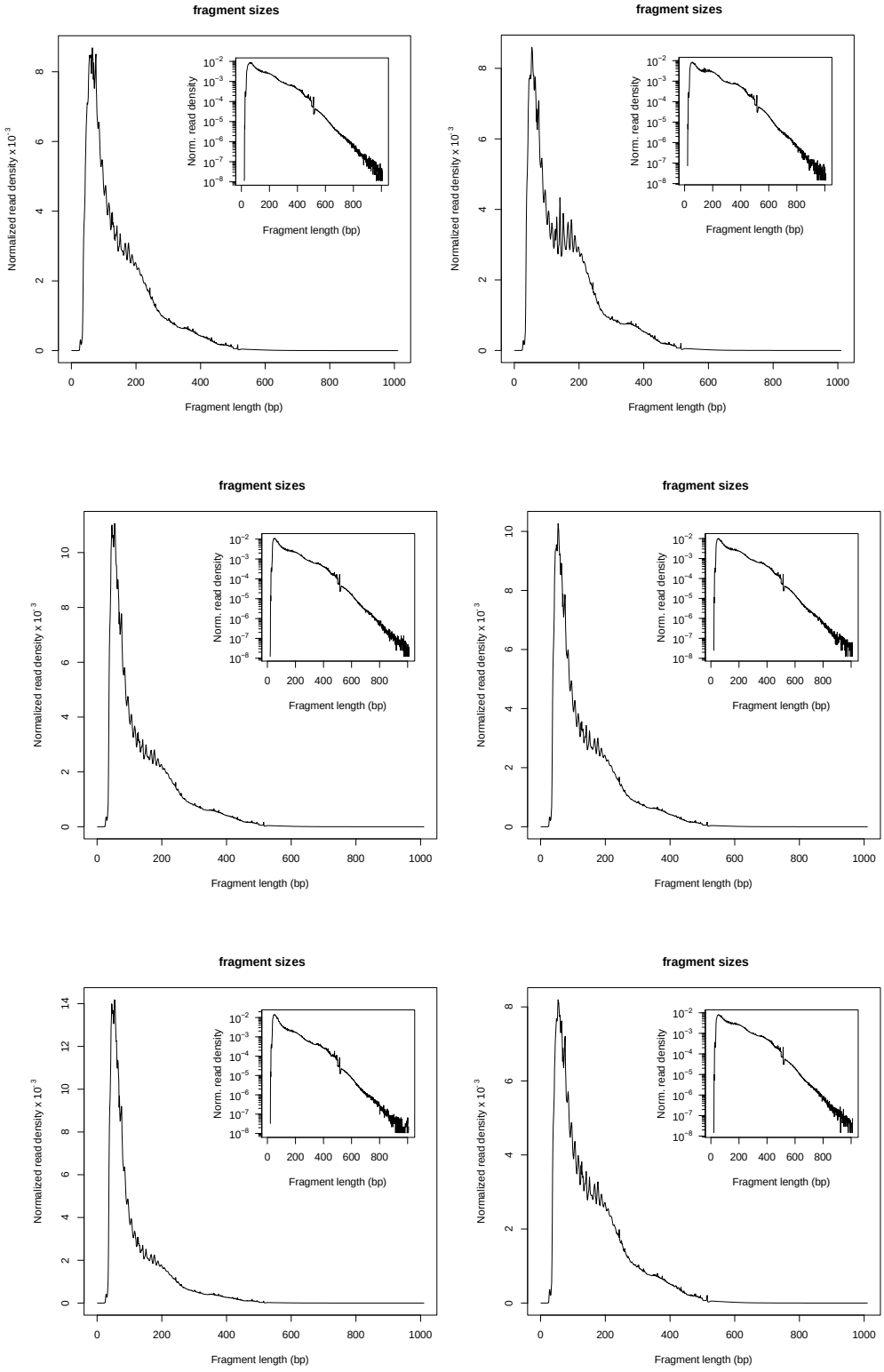

Figure 2 Insert sizes of ATAC-seq sequenced reads

F2 Legend: Insert sizes of vehicle-treated (1-3) or Dex-treated (4-6) NSPC replicates map the content of ~1 nucleosome (<150bp), determined by high throughput sequencing. DNA helical pitch ~10bp. Inset; histogram shows log-transformed periodicity does not clearly persist after 1 nucleosome.

2.2.3.2 Peak Calling (Core Analysis)

The DiffBind (DBA) R package was used for identifying differential sites between two experimental groups[258]. An experimental design sample table, which includes a set of peaks and associated metadata, was generated as described in the DiffBind manual. The experiment DBA object is constructed through dba() using this sample table. Deseq2 results were extracted from DiffBind, with default normalization of full library sizes of the samples. Reads are modeled in a generalized linear model framework of a two-group comparison. We identified significantly different peaks with FDR<0.05 in two comparison groups (see **Berry et al.,** Supplementary Table 6). A merging function was used to find all overlapping peaks from our GR ATAC-seq data and published H3K27ac ChIP-seq data (GEO104686) and derive a single set of unique genomic intervals covering all the supplied peaks (see **Berry et al.,** Supplementary Tables 7-9)[235]. dba.count() with option minOverlap=0.5, summits=200, was then used to take the alignment files and compute count information for each of the peaks/regions in the consensus set. To determine whether open chromatin regions from the ATAC-seq analysis correlated with transcription, overlap between ATAC-seq peaks with -5kb/+3kb from the TSS of significantly Dex-upregulated genes (log FC>0.8, p<0.05; n=300) was computed by bedtools intersect (see **Berry et al.,** Supplementary Tables 10-11; **Table 2).** These genes were previously identified using RNASeq data[10].

2.2.3.3 Data and Code Availability

ATAC-seq and GR ChIP-seq, as well as microarray data are openly available via the Gene Expression Omnibus resource (GEO: GSE175850 and GSE222392).

2.3 Main Results

2.3.1 Accessible regions of chromatin were highly correlated between vehicle-treated and Dex-treated NSPCs

A Pearson's correlation analysis reveals ATAC-seq peaks are highly correlated (**Table 1**; mean r=0.97) between vehicle and Dex-treated NSPCs indicating that overall, the global chromatin landscape is not significantly changed by Dex at 4h.

Table 1 Pearsons correlation coefficients of veh- and Dex-treated NSPCs

	1	2	3	4	5	6
1	1	0.97	0.97	0.97	0.97	0.97
2	0.97	1	0.98	0.97	0.97	0.97
3	0.97	0.98	1	0.97	0.97	0.97
4	0.97	0.97	0.97	1	0.97	0.97
5	0.97	0.97	0.97	0.97	1	0.98
6	0.97	0.97	0.97	0.97	0.98	1

T1 Legend: ATAC-seq identified n=26,326 regions of accessible chromatin in vehicle-treated NSPCs and n=28,798 regions in Dex-treated NSPCs. A Pearson's correlation coefficient for reads in peaks for vehicle-

treated (1-3, red text) and Dex-treated (4-6, blue text) NSPCs was calculated based on the Log10 RPM matrix of consensus ATAC-seq peaks, with a value of 1 representing perfect correlation.

2.3.2 Accessible chromatin densely surrounded transcriptional start sites

Accessible chromatin was distributed densely nearby the TSS (±2kb) (**Figure 3**), and may have gene regulatory potential as they are physically permissive to sequence-specific transcription factors and protein complexes necessary for the initiation of transcription[227,259].

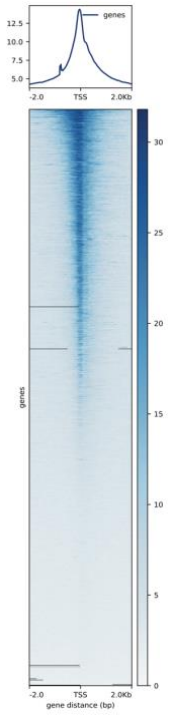

Figure 3. Heatmap of the ATAC-seq read intensities surrounding gene TSS

F3 Legend: The calculated read intensity of ATAC-seq peaks (Dex-treated NSPCs, n=28,798) surrounding a random selection of Ref-seq genes (n=106,155) is shown as a heat map. The color scale represents ATAC-seq read intensity. The top inset is a plot of the overall read density surrounding the TSS of core promoters (+/-2kb).

2.3.3 Accessible chromatin predominantly occurs in genomic noncoding regions

The majority of ATAC-seq peaks were detected within intronic or intergenic regions of the genome (**Figure 4**). These may represent enhancer, promoter, or insulator regions that are physically permissive to interactions with gene regulatory chromatin-binding factors in NSPCs [227,259]. Similar findings are reported in models of human forebrain development [14,228,259].

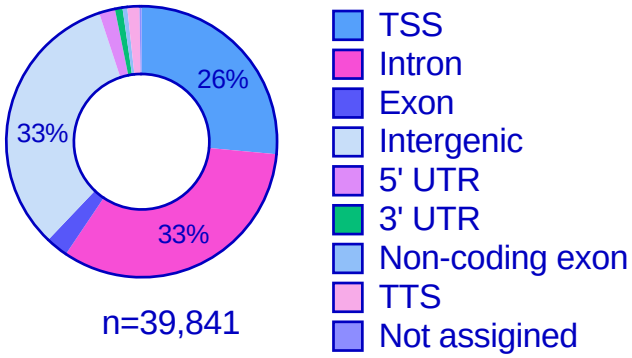

Figure 4. Genome annotation of all ATAC-seq consensus peaks

F4 Legend: The genomic location annotation of total ATAC-seq consensus peaks in vehicle- and Dex-treated NSCPs (n=39,841 peaks, mitochondrial reads removed) shown as parts of a whole. TSS; Transcriptional start site. UTR; untranslated region. TTS; Triplex target DNA site.

2.3.4 Accessible chromatin overlaps with putative enhancer regions

To predict which ATAC-seq peaks occur at active transcriptional enhancers, defined as distal genomic regions denoted by distinct histone modifications associated with an active role in transcriptional regulation, we utilized publicly available H3K27ac ChIP-seq data obtained in untreated E14.5 mouse NSPC cultures (Gene Expression Omnibus accession no. 104686)[19,235-238] **(Figure 5)**. The isolation of cortical NSPCs, culture preparation, and culture maintenance used for

this data set closely resembled ours, and based upon studies conducted in MM.1S, T47D and A1-2 cells, acute Dex exposure does not change the vast majority of the H3K27ac cistrome, though it may create some hormone-dependent regions with increased transcriptional regulation capability [260,261]. Studies in A549 cells also report ligand-bound GR binds to pre-established enhancers within minutes, but it rarely binds to regions lacking key histone modifications[18].

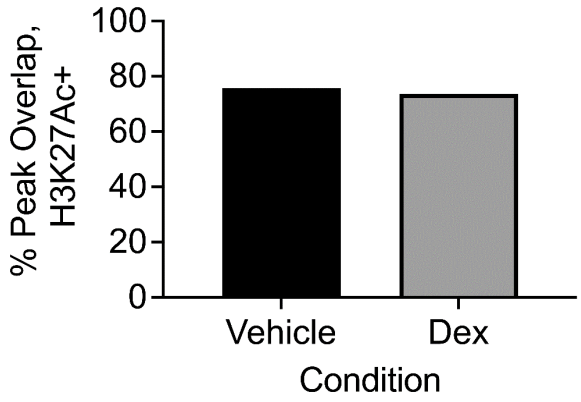

Figure 5. Predictions of H3K27ac+ accessible chromatin

F5 Legend: ~75.7% (n=19,919) and ~78.7% (n=22,673) of ATAC-seq peaks in vehicle-treated or Dex-treated NSPCs, respectively, overlap with H3K27ac ChIP-seq peaks and thus, likely correspond to active promoter or enhancer regions.

2.3.5 Accessible chromatin is located proximal to Dex-responsive genes

We utilized published gene expression data collected in NSPCs to assess the chromatin landscape surrounding Dex-regulated genes, focusing on ATAC-seq peaks located proximal (-5kb/+3kb) to the TSS of Dex-induced genes (log FC>0.8, n=300)[10]. This -5kb/+3kb TSS-proximal range was chosen because it includes promoter and surrounding non-promoter regions bound by RNA Pol-II in the mouse brain genome[262]. Thus, this range spans the region of Dex-regulated

genes that are likely to be closely associated with actively transcribing RNA Pol-II. In both vehicle and Dex treatment groups, a vast majority (274 and 278, respectively) of the 300 highly Dex-induced genes had one or more regions of proximally located accessible chromatin (**Figure 6**)(see Berry et al., Supplementary Tables 10-11).

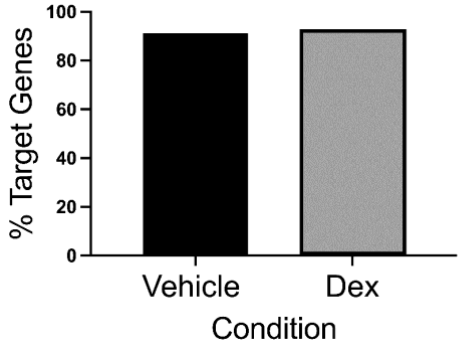

Figure 6. Dex-repsonsive genes with accessible chromatin located proximally

F6 Legend: Percentage of Dex-induced target genes, identified by RNA-seq (log FC>0.8, n=300), with at least one consensus TSS-proximal (-5 kb/+3kb) ATAC-seq peak in vehicle- or Dex-treated cortical NSPCs (E14.5) (Vehicle, 91.33%, n=274) (Dex 92.7%, n=278).

A small subset of these genes underwent a change in chromatin structure surrounding their TSS in response to Dex (4 hour), with 11 proximally located accessible regions appearing only in Dex-treated NSPCs and 1 appearing only in vehicle-treated NSPCs (ATAC Peak ID #8) **(Table 2).**

Table 2. Diffential chromatin responses located proximal to Dex-responsive gene(s)

ATAC Peak ID	Annotation	Dex-increased Accessibility	Dex-decreased Accessibility
32291	intron (NM_001162950, intron 1 of 14)	yes	no
26038	intron (NM_183024, intron 4 of 11)	yes	no
17689	intron (NM_022021, intron 3 of 8)	yes	no
15128	intron (NM_178665, intron 10 of 12)	yes	no
8	intron (NM_001177795, intron 2 of 5)	no	yes
22271	intron (NM_009743, intron 2 of 2)	yes	no
12504	intron (NM_001162366, intron 2 of 30)	yes	no
37046	intron (NM_001029838, intron 2 of 12)	yes	no
21980	intron (NM_001177840, intron 1 of 3)	yes	no
37047	intron (NM_001029838, intron 2 of 12)	yes	no
24377	intron (NM_145542, intron 1 of 16)	yes	no
20478	promoter-TSS (NM_001252568)	yes	no

T2 Legend: Genomic location and associated information for differentially expressed (p<0.05) ATAC-seq peaks in vehicle-treated vs. Dex-treated NSPCs located proximal (-5kb/+3kb) to the TSS of a Dex-upregulated gene.

These results suggest that for the vast majority of GR-inducible genes in mouse NSPCs, the chromatin landscape surrounding their TSS is not significantly changed within 4h of Dex treatment. Furthermore, promoters of most Dex-inducible genes are already in an accessible chromatin state prior to Dex exposure.

2.3.6 Differential chromatin accessibility in Dex-treated NSPCs

Only 95 ATAC-seq peaks (~0.24% of total peaks) were uniquely present in Dex-treated NSPCs ($p<0.05$). We characterized the directionality of each structural alteration to further understand the role of GR binding in chromatin landscape remodeling. 85 ATAC-seq peaks were identified that are more accessible after exposure to Dex, whereas 10 are rendered less accessible by Dex ($p<0.05$). These data suggest that within the Dex-responsive chromatin of NSPCs, GR binding results primarily in increases, but not decreases, in chromatin accessibility (**Figure 7**).

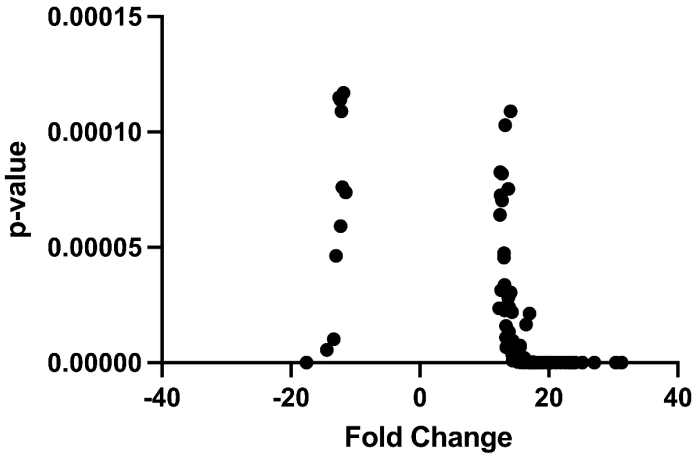

Figure 7. Differentially accessible chromatin in vehicle-treated vs. Dex-treated NSPCs

F7 Legend: Points representing an ATAC-seq differential peaks between vehicle- vs. Dex-treated samples (n=95). Fold change of normalized average ATAC-seq peak read intensity (Dex-Veh) (x-axis); p-value ($p<0.05$) (y-axis).

2.3.7 Chromatin remodeling by Dex (4h) occurs primarily in noncoding regions

Approximately 95% (n=90) of the Dex-responsive dynamic chromatin occurred in intronic or intergenic genomic regions (**Figure 8**), with the majority located outside of the -5kb/+3kb TSS-proximal range surrounding Dex-regulated genes (n=79).

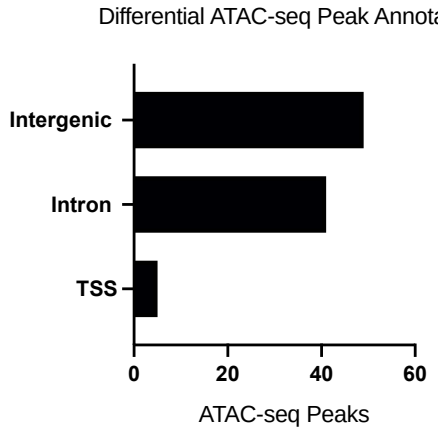

Figure 8. Genone annotation of differentially expressed chromatin

F8 Legend: Genome annotation of differential ATAC-seq peaks in vehicle- and Dex-treated NSPCs (n=95 total). TSS; Transcriptional start site.

2.3.8 Differential chromatin near Dex-responsive genes in NSPCs

To determine if Dex preferentially alters the chromatin structure of genomic regions with a particular functional role in gene regulation, we grouped each of the 95 differential ATAC-seq peaks according to their genomic location. 12 of them were located intergenically within -5kb/+3kb of the TSS for a Dex-regulated gene (log FC>0.8, p<0.05; n=300), and the majority (n=10) had increased accessibility in response to Dex. An additional five differential regions were mapped directly to a TSS. At three of these TSS locations, the TSS belongs to a GR-occupied, Dex-regulated gene (i.e., *Fam107a, Hsd17b4, Phyhd1*) (**Table 3**). These data suggest that although most ATAC-seq peaks occur far away from a gene body, Dex can also regulate the glucocorticoid transcriptome by altering the chromatin landscape surrounding TSS-proximal regions. For example, *Hif3a* is a significantly and robustly Dex-upregulated gene with a Dex-inducible accessible region of chromatin located -5kb/+3kb from the TSS (i.e., within its first intron; **Figure**

9, blue bracket) in addition to a constitutively open chromatin region within the same intron (**Figure 9**, red bracket).

Table 3. Differential ATAC-seq peaks located proximal to Dex-regulated gene(s)

Peak ID	Gene	Peak Proximity to Gene	RNA-seq log FC	RNA-seq p-value
32291	Hif3a	-5kb/+3kb	6.50	5.87E-60
26038	Raver2	-5kb/+3kb	1.09	1.64E-08
17689	Cables1	-5kb/+3kb	1.87	1.10E-27
15128	Lpp	-5kb/+3kb	0.79	7.04E-06
8*	Rgs20	-5kb/+3kb	-0.68	6.74E-07
22271	Bcl2l11	-5kb/+3kb	-1.50	2.00E-11
12504	Ptk2b	-5kb/+3kb	5.29	1.48E-26
37046	Pknox2	-5kb/+3kb	1.49	2.57E-19
21980	Smox	-5kb/+3kb	1.88	1.27E-15
20478	Phyhd1	-5kb/+3kb	2.53	4.40E-16
37047	Pknox2	-5kb/+3kb	1.49	2.57E-19
24377	Ahcyl1	-5kb/+3kb	0.84	2.11E-10
11540	Fam107a	TSS	8.72	6.63E-125
12169	Ndrg2	TSS	1.11	0.07
18206	Hsd17b4	TSS	0.67	6.27E-08
20478	Phyhd1	TSS	2.53	4.40E-16
33880*	Sox6	TSS	0.55	0.01

*decreased chromatin accessibility post-Dex

T3 Legend: Peak ID of differential ATAC-seq peaks (p<0.05), which occur within the -5kb/+3kb region of a Dex-regulated gene, or at a Dex-regulated gene TSS. Asterisks indicate ATAC-seq peaks with a Dex-induced decrease in chromatin accessibility. RNA-seq data previously published by Frahm et al., 2018[10]. RNAseq log Veh/Dex fold change.

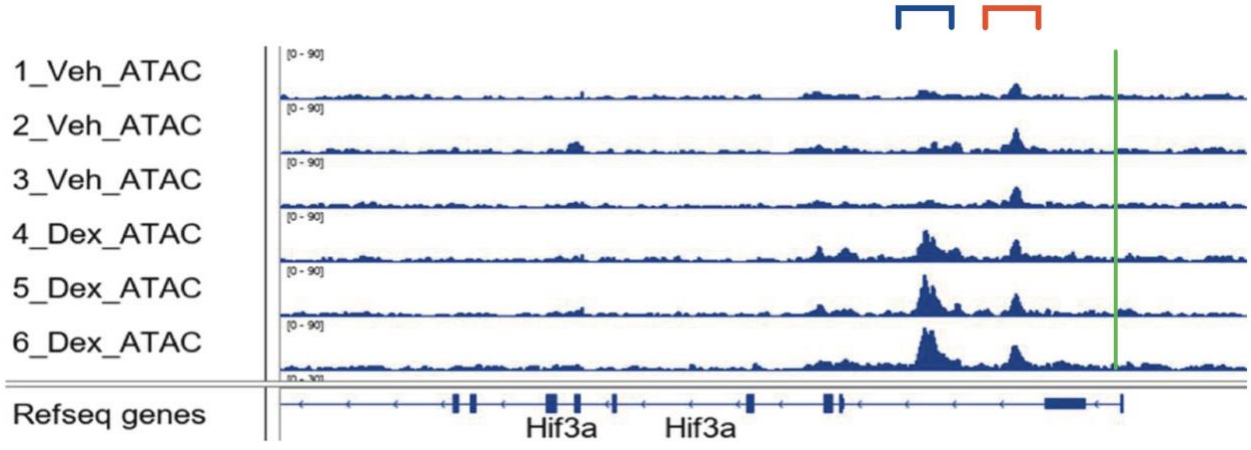

Figure 9. Visual example of ATAC-seq called peaks near Hif3a, a highly Dex-regulated gene.

F9 Legend: Constitutive and Dex-induced ATAC-seq peaks in the proximal (-5kb/+3kb) regulatory region of the Dex-induced *Hif3a* gene. TSS is marked by a green line. The red and blue brackets indicate constitutive and induced peaks, respectively.

2.4 Discussion

Defining the structure and dynamics of the chromatin landscape of embryonic-derived telencephalon-derived NSPCs will further an understanding of how functional coding and noncoding genomic sequences shape early neuronal development in fetuses exposed to sGCs *in utero* [263,264]. Our study revealed that most genomic regions that are accessible to TF occur in H3K27ac+ noncoding genomic regions, a property that highlights distal enhancer regions are critical influencers of transcriptional output during neurodevelopment [11,234,265,266]. However, we recognize histone modification markers are not perfectly predictive, and we cannot directly interpret the functionality of these distal enhancer regions in regulating gene expression. Recently developed chromatin conformation capture technologies (i.e. Hi-C[267]) profile long range enhancer-promoter chromatin connectivity in mouse and human NSPCs, and multiplexing these data with ours would allow stronger predictions of the functional relevance of distal accessible chromatin regions harboring an enrichment of histone modifications, at least in vehicle-treated NSPCs[268,269].

Of the n=95 differentially expressed chromatin regions, we found most Dex-inducible accessible chromatin sites (n=85, **Figure 7**) also occur in noncoding regions far removed from promoters (**Figure 8**), preventing us from examining how Dex-induced chromatin remodeling directly impacts transcription or cell fate outcomes. Future endeavors which profile chromatin connectivity changes in response to Dex would provide valuable insight as to why chromatin

remodeling occurs at these unique sites to facilitate GR TF activity. An interesting question is whether these unique differentially accessible sites are connected to homologs of genes identified as being involved with pathological disease processes in humans[270]. This would strengthen the concept of GR programming contributing to neurodevelopmental deficits, which is observed clinically in humans exposed to sGCs *in-utero*, discussed in the 'Introduction' (See: 'Antenatal Corticosteroids and Clinical Outcomes').

Nonetheless, the 17 the differential ATAC-seq peaks which are located proximally to the TSS of Dex-regulated genes are likely to be functionally relevant, because these proximal regions often host pioneer factors, co-activators, and sequence-specific TFs that recruit clusters or condensates of RNA Pol II machinery necessary for transcriptional activation[271]. We also infer functional relevance by examining the identity and role of the genes near Dex-inducible chromatin remodeling. For example, Dex treatment increased chromatin accessibility near 3/10 of the most highly Dex-regulated genes (*Fam107a, Hif3a, Ptk2b*)[257], but decreased accessibility near genes which control lineage specification of NSPCs in the developing telencephalon (Sox6, *Rgs20)* [272-275]. A limitation of our study is the measurement of chromatin accessibility at a single time point. Thus, some early subset of remodeled chromatin near Dex-responsive genes may have returned to pre-Dex conditions by 4h. Nonetheless, our characterization of the chromatin landscape of embryonic NSPCs with 4h Dex exposure reveals unique features of the chromatin landscape in NSPCs that could impact cell maturation trajectories[276-278].

2.5 Aim 1 Summary

(i) The majority of accessible chromatin occurs in distal noncoding regions, preventing direct predictions of their functional relevance in the gene response to Dex.

(ii) (ii) Most accessible chromatin regions have an enrichment of H3K27ac histone modification markers and are putative enhancers, guiding transcription in NSPCs.

(iii) (iii) Overall, most of the global chromatin landscape was not altered by Dex, indicating that chromatin landscape is accessible and ready for GR to bind, even in the absence of exogenously added GC.

3.0 Aim 2: The GR Cistrome in Mouse Embryonic Cortical NSPCs

3.1 Introduction

3.1.1 *De novo* GR Binding Patterns are Context and Cell-type Specific

The General Introduction sections titled 'GR and Transcriptional Regulation' and 'Genome Biology of GR' describe how studies conducted in primary and immortalized cell lines discovered consensus nucleotide sequences termed 'classic GREs'. GREs guide *de novo* DNA occupancy by ligand-bound GR, and this GR-DNA binding is the driving force of robust gene responses. With the advent of ChIP sequencing technologies it became apparent that *de novo* genomic sites occupied by ligand-bound GR outnumbers GR-regulated genes, indicating that direct GR binding is required but not always sufficient for a significant gene response[52]. This prompted investigations that revealed *de novo* GR binding patterns are determined by a host of cell-type specific factors including nucleotide motif composition (i.e. classic GRE vs half-site GRE), PTMs, histone modification markers (i.e. H3K27ac), chromatin compaction, transcriptional co-regulators, and pioneer factors (also discussed in detail in the General Introduction). These concepts are largely confirmed in peripheral tissues yet understudied in neuronal contexts or models of mammalian neurodevelopment, hence the gap in scientific knowledge that we begin to address in **Aim 2**.

The first report of genome-wide *de novo* GR binding in a neural subtype was published in 2012. Experiments in Dex-stimulated PC12 cells, which are derived from a transplantable pheochromocytoma of the rat adrenal medulla with an embryonic origin, found a majority of *de novo* GR binding occurs at GREs near (+/- 100kb) genes associated with general cell functions

(i.e. apoptosis, cell motion), while *de novo* GR binding at non-GREs occurs near genes responsible for neuronal functions (i.e. synaptic transmission, neurotransmitter synthesis)[279]. Strikingly, the non-GRE motifs identified under GR binding sites belong to TFs that are highly cell-type specific (i.e. Gabpa, Prrx2, Zfp281, Gata1, Zbtb3), and the neural-specific *de novo* GR binding patterns are not observed in GR studies of non-neuronal cell types. These results demonstrate that the signatures of *de novo* GR binding are neural-specific perhaps because GR is guided by neural-specific TFs[279].

A separate study of nuclear extracts from Dex-stimulated rat hypothalamic cells reported nuclear proteins recognize half-site GREs in addition to full-site GRE consensus motifs. These data suggest that GR binds DNA as a monomer and a dimer following Dex stimulation. However, it is unclear if different oligomeric GR structures engaged in *de novo* binding confer diverse gene responses in centrally-originating tissues, as has been suggested in non-neuronal cell types (i.e. U-2 OS epithelial cell line, mouse bone marrow-derived macrophages, mouse mammary adenocarcinoma cells, etc.)[77,78,280,281].

Lastly, a study conducted by the DeFranco lab in mouse cortical NSPCs (E14.5) reported that the recruitment of total GR to the promoter regions of Dex target genes (i.e. *Sgk-1, Fkbp5)* is dependent upon Caveolin-1-mediated phosphorylation of GR at S220. These data suggest that different GR phosphoisoforms yield diverse *de novo* GR binding and transcriptional outputs[209]. Collectively, these studies highlight the importance of probing additional biological factors (i.e. nucleotide motif composition, PTMs) to discern the cell-type specific mechanisms driving transcriptional regulation by *de novo* GR binding. **To study this in the neurodevelopmental context of sGC exposure, Aim 2 measures genome-wide *de novo* GR binding in vehicle vs.**

Dex-treated cortical NSPCs (E14.5). Aims 2 also quantifies GR binding at consensus GREs, half-site GREs, and non-GRE genomic loci.

3.1.2 GR Transcriptional Coregulators: Tethers and Pioneer Factors

GR interacts with transcriptional coregulators at nearly all gene regulatory sites. The concept of 'tethering', first described in the General Introduction section titled 'GR and Transcriptional Regulation', refers to cell type-specific and sex-specific macromolecular complexes of transcriptional coregulator proteins (i.e., co-factors, TFs) that form GR-nucleated complexes and localize GR to GRE, half-site GRE, or non-GRE genomic region by acting as a 'tether'. This is one mode by which transcriptional coregulators influence GR transcriptional output independent of direct GR-DNA binding[22,71,72,66,72-75,73,77,78]. Current opinion leaders in the steroid hormone signaling field argue that if tethering occurs in close proximity to a GRE, a consensus binding motif for another cell-specific TF may be located adjacent to the GRE[52]. This is best confirmed in liver and primary macrophages by the ChIP-exo technique, a modified ChIP-seq protocol which maps locations surrounding TF binding sites at a near single-nucleotide base pair resolution[77]. Alternatively, bioinformatic methodology can be applied to ChIP-seq or ChIP-exo data to confidently predict transcription factor binding[279,282]. Though tethering likely occurs to a smaller degree than direct GR-DNA binding, it is a mechanism by which GR activation elicits cell-type specific gene responses and stokes curiosity regarding the NSPC-specific TFs that guide the Dex transcriptome in the developing brain. Indeed, discovering the transcriptional coregulators that aid GR in Dex action in NSPCs will provide detailed insight into the etiology of observed neurodevelopmental abnormalities associated with sGC exposure *in-utero*.

Aside from tethering, some TFs can act as 'pioneer factors' by priming chromatin for nuclear receptor binding, a concept first mentioned in the 'Genome Biology of GR' section of the Introduction[20,88,101,102]. This 'primed' chromatin state was originally measured by the presence of cell type-specific TFs at promoter-proximal or distal regions, which marked developmental genes which were not yet active but become activated once several additional TFs were bound. Pioneers increase direct accessibility of their DNA binding elements by stabilizing factor complexes, recruiting enhancer elements, or by other understudied mechanisms[283]. They also mediate transient gene derepression via direct DNA demethylation, by recruiting demethylating enzymatic activities, or by decreasing the number of additional factors needed for DNA binding[284,285].

In mouse NSPCs, clusters of specific TFs are associated with distinct chromatin states (i.e. primed vs active) and predetermine *de novo* TF binding[286]. Redistributions of these factors reprograms the epigenetic and transcriptional profiles towards neurogenic cell fates[287,288]. Specifically in mouse NSPCs (E14.1), the SOX family of TFs (i.e. SOX2, SOX2, SOX11) function as pioneer factors by binding to preselected, silenced neural-specific genes in a sequential manner and keeping them in a poised state (H3K4me3+, H3K27me3+) for gene activation to occur as the cell state transitions towards a neuronal identity[289]. It is tempting to ponder if the Dex-induced changes in gene expression and the enhanced cerebral cortical proliferation observed *in-vivo* are accompanied by a redistribution of such pioneer factors. However, prior to this study the transcriptional coregulators of GR in mouse cortical NSPCs (E14.5) were unknown[7]. To explore this, Aim 2 utilizes ChIP-seq data in combination with bioinformatic methodologies to predict GR cofactors mobilized by Dex in NSPCs.

3.2 Rationale and Summary

Pre-accessible or primed chromatin, established by histone modifications and the association of clusters of transcriptional coregulators, is a prerequisite for most GR binding to the genome[17]. Based on this prominent observation, we predict that GR binds to a subset of accessible chromatin in telencephalon-derived NSPCs (E14.5), mapped by ATAC-seq in **Aim 1**. We performed GR ChIP-seq in vehicle-treated and Dex-treated cortical NSPCs (E14.5) and integrated these results with chromatin accessibility information obtained in Aim 1 to test this prediction and:

(i) map NSPC-specific *de novo* GR binding patterns that could drive Dex regulated transcription.

(ii) determine if *de novo* GR binding triggers chromatin remodeling at specific sites of the genome.

(iii) identify transcriptional cofactors and/or coregulators closely associated with GR binding sites in the genome that could influence GC regulated transcriptional responses.

3.3 Materials and Methods

3.3.1 Animals and Cell Culture

Embryonic (E14.5) telencephalon-derived mouse NSPCs were prepared as described in **Aim 1**. Biological replicates (n=3) combining neurospheres from multiple female embryos per replicate were used for GR ChIP-seq analysis.

3.3.2 Dual Cross-Linking Chromatin Immunoprecipitation for Next Generation Sequencing (ChIP-seq)

A detailed protocol is described by Rollins and Rogatsky et al.,[290]. In summary, Dynabeads (ThermoFisher) were washed three times with 1% BSA in PBS on ice and resuspended with 1-10ug of antibody against GR (ThermoFisher PA1-511A) overnight at 4°C. Approximately 5 x 10^6 cells, as a single cell suspension, were incubated in 0.2 mM DSG-PBS (ProteoChem #c1104) for 30 minutes at room temperature (RT) prior to a 10-minute incubation at RT in a 1:16 diluted solution of 16% methanol-free formaldehyde and fixing buffer (10X prepared at 500mM HEPES-KOH, pH7.5, 1M NaCl, 10mM EDTA, pH 8.0, 5 mM EGTA, pH 8.0). Cross-linking was terminated by addition of 2.5M glycine for 5 minutes at RT, and following multiple washes in PBS, cell pellets were flash frozen in liquid nitrogen and stored at -80°C until further processing. Fixed cells were incubated in lysis buffer (50 mM HEPES-KOH, pH 7.5,140 mM NaCl, 1mM EDTA, pH 8.0, 10% glycerol, 1% NP-40, 0.25% Triton X-100 containing protease and phosphatase inhibitors) for 10 minutes at 4°C and spun down at 600g for 10 minutes at 4°C to isolate cell nuclei. Following several washes (10mM Tris-HCl, pH 8.0, 0.2 mM NaCl, 1 mM EDTA, pH 8.0, 0.5 mM EGTA, pH 8.0), nuclei were resuspended in shearing buffer (0.1% sodium dodecyl sulfate (SDS), 10mM EDTA, pH 8.0, 50 mM Tris, pH 8.0), incubated for 15 minutes on ice, and sonicated using a Diagenode Bioruptor Pico water bath sonicator. Following sonication, nuclear lysates were cleared by centrifugation at 14,000 g x 20 minutes at 4°C and transferred to a DNA LoBind (Sigma) 1.5mL tube. Nuclear lysates were incubated with the antibody-conjugated Dynabeads overnight at 4°C. The next day, the Dynabeads antibody-conjugated complexes were washed eight times with modified RIPA buffer containing protease and phosphatase inhibitors, and finally washed once with TE (10mM Tris, pH 8.0 and 1 mM EDTA, pH 8.0) containing 50mM

NaCl. DNA was eluted into TE containing 0.5% SDS with Proteinase K at 55ºC for 1.5h. Cross linking was reversed by incubation at 65ºC for a minimum of 6h. Purified DNA was purified using the QIAquick PCR Purification Kit (Qiagen) according to manufacturer's directions. 2uL of eluted DNA was set aside for qPCR analysis, and 2uL was used for quality analysis using a Qubit fluorometer and Agilent Bioanalyzer. Remaining eluted DNA was stored at -20ºC until NextGen sequencing using an Illumina HiSeq 2500 system.

3.3.3 Data Analyses

Quality control of raw sequenced reads, which determines total number of reads, read length, and GC content among other measures, was performed using FASTQC. Adaptors were removed from the sequenced reads using Trim Galore! with *-q 20 --stringency 2* parameters. Single-end reads were then aligned against the mm10 reference genome using *bowtie2* with default parameters. ChIP-seq peaks were called using MACS2 with parameters *-B --SPMR --qvalue .05 --gsize mm --nomodel --extsize 200*. An An input sample of DNA, which was cross-linked and sonicated but not immunoprecipitated with the GR antibody, was used as background for MACS2. Strand cross correlation metrics show significant clustering of enriched DNA sequence tags at the locations bound by the protein of interest (see **Berry et al.,** Supplementary Figure 8). A standard peak list was established by merging the union of all peaks which occur in any replicates within a treatment condition. Using the same parameters described for ATAC-seq, the DiffBind (DBA) R package was used for identifying differential sites between two groups[258]**.** Hypergeometric Optimization of Motif Enrichment (HOMER v4.10.3) package *annotatePeaks.pl* was used for performing peak annotation. Known motif enrichment analysis was carried out by *findMotifsGenome.pl* (HOMER), searching for motifs of 8, 10, and 12 bp in length within the

± 200 bp flanking regions of the peak summits. *p* values were calculated by comparing the enrichments within the target regions and those of a random set of regions (background) generated by HOMER. Overlap between two feature files was determined with the *intersect -wa -wb* function in bedtools v.2.27.1. For example, the overlap between ATACseq differential peaks with H3K27ac consensus peaks are determined by *bedtools intersect -wa -wb -filenames -a atacseq.peaks -b H3K27ac.consensus.peaks*.

3.4 Results

3.4.1 GR binding sites are distributed across functional genomic regions

ChIP-seq was performed to identify GR-bound regions of DNA in NSPCs treated with 100nM Dex or vehicle for 4h. The genomic distribution of all GR ChIP-seq peaks (n=3162) is similar to that of the ATAC-seq peaks (n=39,841), with over ~70% of GR binding occurring in intronic or intergenic regions in Dex-treated NSPCs (**Figure 10**).

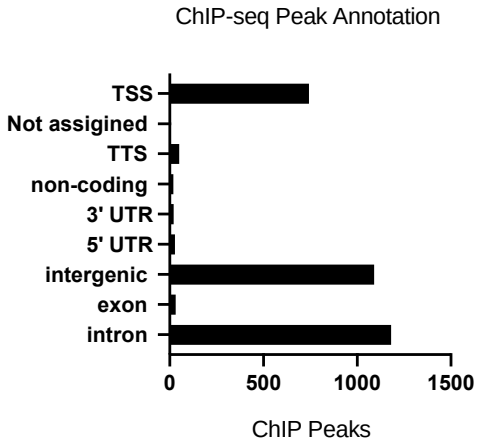

Figure 10. Distribution of GR cistrome across functional and noncoding gene regions

F10 Legend: Genome annotation of ChIP-seq peaks in Dex-treated NSPCs (n=3,162 total). TSS; Transcriptional start site. UTR; Untranslated region. TTS; Triplex target DNA site. x-axis shows the number of GR ChIP-seq peaks per annotated group.

3.4.2 Dex increases GR binding, mostly at accessible chromatin, in NSPCs

In line with this, ChIP-seq reveals 941 genomics sites are bound by GR in vehicle-treated NSPCs, whereas Dex addition resulted in a ~236.0% increase in GR binding sites (n=3162) (**Figure 11,** pre-Dex vs. post-Dex). To relate GR binding pattern to chromatin accessibility, we overlayed the ATAC-seq and GR ChIP-seq profiles which revealed that ~92.2% (n=2915) and ~79.6% (n=2519) of GR binding occurred in constitutively accessible (i.e., pre-accessible) chromatin in vehicle- or Dex-treated NSPCs, respectively, as opposed to a minority of GR binding which occurred at inaccessible chromatin (**Figure 11).** Our results agree with findings in other cell types which show open chromatin in distal genomic regions as a biological prerequisite for the majority of GR binding[17,18,85].

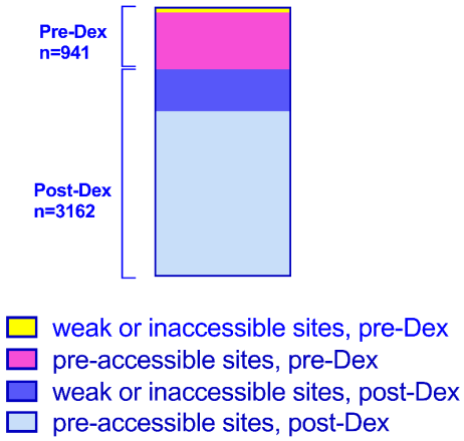

Figure 11. GR Cistrome determined by ChIP-seq

F11 Legend: Quantification of GR ChIP-seq peaks that occur in vehicle- (Pre-Dex, n=941) or in Dex-treated NSPCs (Post-Dex, n=3162). Within these groups, ChIP-seq peaks occurred at (i) weak or inaccessible regions of chromatin, or (ii) pre-accessible sites of chromatin.

3.4.3 GR binds preferentially to constitutively accessible chromatin

Because open chromatin in distal genomic regions appears to be a biological prerequisite for the majority of GR binding in NSPCs, we investigated whether GR binding occurs preferentially in regions marked by the presence of histone H3K27ac, a marker of active enhancers[19]. We utilized our chromatin accessibility data, along with publicly available H3K27ac ChIP-seq data preciously described in Aim 1, to characterize GR binding in (i) H3K27ac-positive accessible regions (H3K27ac+), (ii) H3K27ac-negative accessible regions (H3K27ac-), or (iii) inaccessible regions of chromatin (**Figure 12**) [235]. A Fisher's test of independence revealed that GR binding in vehicle vs. Dex-treated NSPCs is associated with H3K27ac presence (***$p<0.01$). Due to reports of GR binding primarily increasing H3K27ac ChIP-seq signals in other cell types, it is possible our use of a non Dex-treated NSPC dataset may underestimate the number of Dex-

stimulated GR binding events at putative enhancers[291]. A DNA site-specific example of GR binding at H3K27ac+ accessible chromatin is depicted on the next page (**Figure 13**).

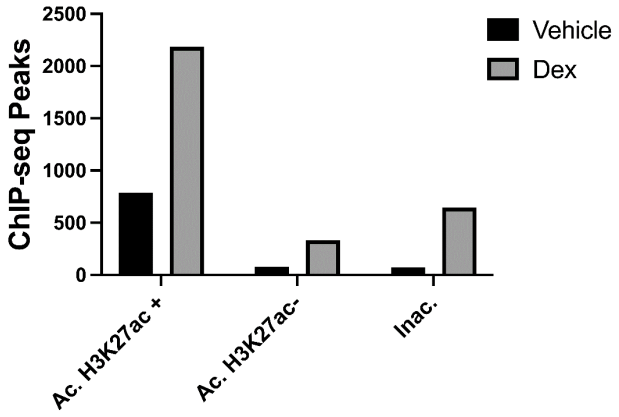

Figure 12. Overlap of GR ChIP-seq, H3K27ac ChIP-seq, and ATAC-seq peaks

F12 Legend: Quantification of GR ChIP-seq peaks (y-axis) that occur in (i) accessible regions of chromatin, which have an H3K27Ac mark (Ac. H3K27ac+), (ii) accessible regions of chromatin that lack an H3K27ac mark (Ac. H3K27ac-), or (iii) inaccessible regions of chromatin (x-axis) in vehicle- or Dex-treated NSC. Genomic localization of H3K27ac was delineated in cortical NSPCs (E14.5) from an independent study (Gene Expression Omnibus accession no. 104686). Fisher's exact test of independence between category (i) and (ii) (*p<0.01).**

3.4.4 Integrative genomics view of GR binding at a putative transcriptional enhancer

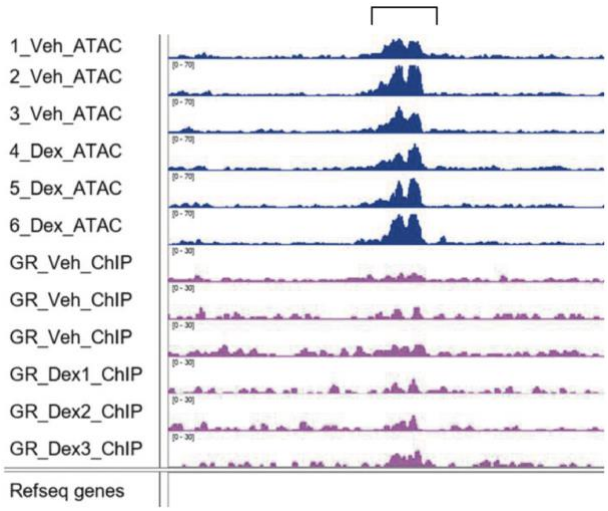

Figure 13. An example of GR binding at H3K27ac+ accessible chromatin

F13 Legend: ATAC-seq and GR ChIP-seq peaks located in a H3K27ac+ distal enhancer region of DNA (frame view chr18:16,552,637-63,558,00). Horizontal rows from top to bottom: ATAC-seq peaks in triplicate of vehicle- or Dex-treated NSPCs (blue), ChIP-seq peaks in triplicate of vehicle- or Dex-treated NSPCs (pink). Genomic regions with a ChIP-seq peak for the H3K27ac promoter/enhancer mark detected in cortical NSPCs (E14.5) from an independent study (GEO104686) are indicated by the black bracket (top). The RefSeq horizontal row indicates location of any protein coding regions in the murine (mm10) reference genome (bottom). The nearest gene to this position is ~100 kb away (out of frame).

3.4.5 Motif enrichment analyses predict with confidence the major TFs involved in GR transcriptional responses

Next, we aimed to identify TF binding motifs that underlie each GR ChIP-seq peak to delineate genomic regions that are (i) bound by GR, or (ii) occupied by potential GR pioneering factors or cofactors. The HOMER motif discovery algorithm was used to determine enrichment of non-random consensus TF binding motifs in our ChIP-seq reads relative to random background

(**Figure 14**). The Homer algorithm classified GR ChIP-seq peaks as occurring at a canonical GRE if they were enriched (p<1E-10) for a motif containing an inverted palindromic sequence with two consensus 'AGAACA' motifs separated by 3 nucleotides [16,21,67,68]. The extremely high enrichment of GREs under GR ChIP-seq peaks indicates the high quality of GR ChIP-seq technical processing. The nucleotide compositions of AREs and PGR elements are near identical to GREs, meaning the enrichment of these motifs under our GR ChIP-seq peaks also indicate direct GR-DNA binding. While, NF-1 is an identified GR co-factor in rat hippocampal cells[292] and a GR pioneering factor in *Xenopus* oocytes[293], we did not pursue further validation of this in NSPCs.

Rank	Motif	Name	P-value	Log P-value
1		GRE	1 e-344	-7.924e+02
3		ARE	1e-290	-6.678e+02
4		PGR	1e-258	-5.956e+02
6		NF-1	1e-56	-1.306e+02
7		AR-half site	1e-52	-1.219e+02
9		SOX10	1e-46	-1.066e+02
10		SOX3	1e-43	-1.013e+02
11		SOX4	1e-38	-8.960e+01
12		SOX9	1e-38	-8.888e+01
13		SOX2	1e-38	-8.850e+01

Figure 14. Enrichment of TF motifs at GR binding sites

F14 Legend: Enrichment of non-random consensus TF binding motifs in our ChIP-seq reads relative to random background, determined by the HOMER motif algorithm. Glucocorticoid responsive element; GRE. Androgen responsive element; ARE. Progesterone receptor; PGR. Nuclear factor-1; NF-1. Androgen receptor; AR.

3.4.6 Dex increases GR occupancy at glucocorticoid-responsive elements (GRE)

Motif enrichment analyses showed that although a significant fraction of GR binding events occurred even in the absence of added Dex (**Figure 11**), only ~4% (n=41) of GR ChIP-seq peaks contain a canonical GRE in vehicle-treated NSPCs (**Figure 15**, top). These data suggest that in the absence of added GCs, GRs in primary NSPC cultures may have the capacity to occupy genomic regions that do not contain the classic palindromic sequence of a GRE. Possible rationale for these instances is provided in the discussion. In contrast, with the addition of Dex, there is a ~20-fold increase in the total number of GR ChIP-seq peaks enriched for a GRE (n=823, 26% of total) (**Figure 15**, bottom). Since the Homer algorithm only predicts canonical GREs, the percentage of GR-ChIP peaks directly occupying DNA in Dex-treated NSPCs (i.e. 26%) may be an underestimate since GR binding sites with minor variations in the canonical GRE sequence will not be detected [294,295]. Nonetheless, these data suggest that Dex-induced GR binding to the genome is facilitated through direct GRE binding in NSPCs.

To our surprise, the second-most significantly enriched motif within the GR ChIP-seq peaks belonged to the SOX family of transcription factors (TFs). We combined GR ChIP-seq peaks enriched (($p<1E-10$)) for any SOX TF motif expressed in E14.5 cortical NSPCs (SOX2, SOX3, SOX4, SOX6, SOX9, SOX10, SOX15) because their consensus binding motifs are similar in sequence and position weight matrix (Figure 13)[10,296,297]. We observed enrichment of SOX TF binding motifs in ~33% (n=308) of GR ChIP-seq peaks in vehicle-treated samples (**Figure 15**, top). In contrast, with the addition of Dex, there is a ~4-fold increase in the number of GR ChIP-seq peaks enriched for a SOX motif (n= 1319, 41% of total). (**Figure 15**, bottom).

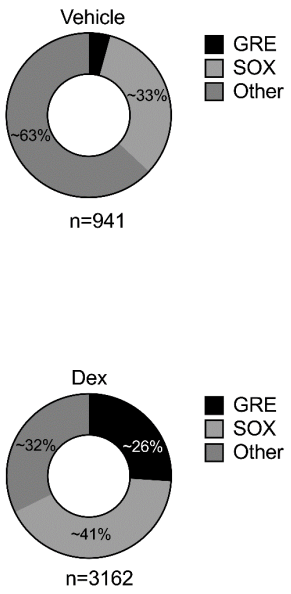

Figure 15. GR binding at cannonical GREs and/or SOX motifs

F15 Legend: Percentage of ChIP-seq peaks enriched for GR or SOX TF motifs in cortical NSPCs exposed to vehicle or Dex *in-vitro*. The number of ChIP-seq peaks are indicated at the bottom of each chart. GRE; glucocorticoid responsive element.

3.4.7 GR occupancy preferentially occurs at regions co-occupied by SOX TFs

The results of the motif enrichment analyses were unexpected and novel because, to our knowledge, SOX TF are not reported as transcriptional coregulators of GR action in other cell types. We interrogated these data and found approximately 10% of total GR ChIP-seq peaks (n=308 of 3162) were enriched for both a GRE and a SOX motif. In most instances, a peak was enriched for multiple GRE or SOX motifs, resulting in over 2,000 GRE or SOX motifs identified under 308 GR ChIP peaks. To speculate on the possibility of SOX acting as a co-factor for GR, we determined the exact nucleotide positioning of the motifs and calculated the number of nucleotide base pairs separating a GRE and SOX motif at each GR binding site. This revealed that, in 88% of instances where a ChIP-seq peak was enriched for both a GRE and SOX motif in Dex-

treated NSPCs, the motifs were located less than 100 nucleotide bases apart and may exist in the same nucleated complexes (**Figure 16**). These data suggest that in addition to direct GRE binding, Dex-induced genomic GR activity preferentially occurs at sites that are co-occupied or closely associated with the binding of SOX TFs.

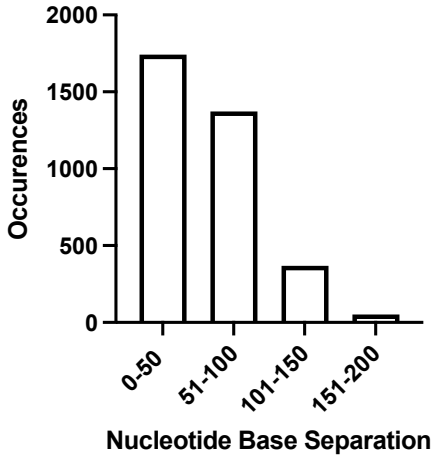

Figure 16. GRE-SOX motif proximity

F16 Legend: Nucleotides separating a GRE and SOX TF binding motif under individual GR ChIP-seq peaks. Number of GRE and SOX co-occurrences under a ChIP-seq peak (y-axis) is grouped by intervals of base pair separation (x-axis) between a GRE and SOX TF binding motif.

3.4.8 Published SOX2 ChIP-seq in mouse NSPCs validates bioinformatic predictions of SOX2-bound DNA

Though our bioinformatic approach is shown to predict TF-DNA occupancy with confidence, further validation is needed. Ideally, the same biological samples used to measure the GR cistrome would have been probed to measure the SOX TF occupancy as well (i.e. SOX2 ChIP-seq). However, we could not have predicted this need and did not collect enough material to perform these experiments. As an alternative, we utilized published SOX2 ChIP-seq data collected

in wild-type mouse NSPCs derived from the fetal telencephalon at postnatal day 0 (P0). We chose this dataset because the establishment, maintenance, and expansion protocols of neurospheres resembles ours. Although the SOX2 cistrome at P0 may vary from the E14.5 developmental timepoint, SOX2 binding patterns seem to change more with cell fate transitions (i.e. neural progenitor cell to maturing neuron)[298]. Thus, our comparison of cortical-derived NSPCs (E14.5) to cortical-derived NSPCs (P0) is made with these caveats. We determined that in vehicle- and Dex-treated NSPCs (E.145), 86% and 83% of the genomic sites, respectively, predicted to host a close association of GR and SOX (**Figures 14-16**) are bona-fide SOX2 binding sites at P0 (**Figure 17**).

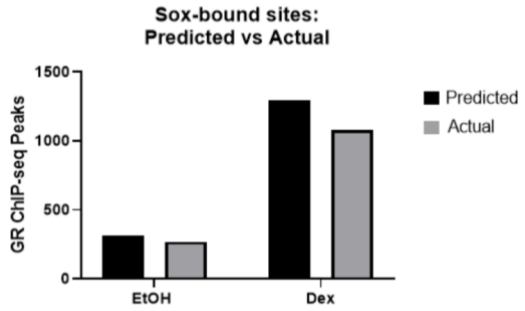

Figure 17. SOX-bound genomic sites: predicted (E14.5) vs bona-fide (P0)

F17 Legend: In vehicle-or Dex-treated NSPCs, a quantification of the number of GR ChIP-seq peaks enriched for a SOX family binding motif (predicted) (E14.5), or GR ChIP-seq peaks which overlap with a bona-fide SOX2 ChIP-seq peak from Bertolini et al., 2019 (actual) (P0).

Interestingly, the Bertolini et al. reports over 90% of SOX2-bound sites occur in H3K27ac+ nucleosomes, with an enrichment ($p<0.001$) of SOX2 binding in distal H3K27ac-positive sites when compared to 1,000 random sets of H3K27ac+ genomic loci[269]. Together, these data suggest

the HOMER motif enrichment algorithms successfully identified real SOX TF binding sites in close association with GR binding sites in NSPCs (E14.5), and that the majority of these sites are likely H3K27ac+ active enhancer regions.

3.4.9 Higher oligomeric states drive GR transcriptional activation in NSPCs

GR studies in non-neuronal live cells (i.e. mouse embryonic fibroblast, mouse mammary cell line) show higher oligomeric states drive stronger gene regulatory responses to GR activation compared to lower oligomeric states[281]. To gain a deeper mechanistic understanding of the GR-DNA interactome in NSPCs, we utilized HOMER to measure enrichment of half-site GRE motifs sites containing a single hexamer consensus sequence within GR ChIP-seq peaks, thought to be bound by GR in a lower oligomeric state (i.e. monomer GR)[46,47]. This revealed that in the absence of Dex, genomic GR binding occurs at half-site GREs, with ~36.9% of GR ChIP-seq peaks enriched for at least one half-site GRE in NSPCs (**Figure 18**). Interestingly, the addition of Dex did not drastically change the overall percentage of GR ChIP-seq peaks enriched for a half-site GRE, but it did cause a ~20-fold increase in the overall number of full-site GREs bound at 4h (**Figure 18**). In addition, a Fisher's Exact test of independence reveals that there is a significant relationship between the size of the enriched motif (i.e. half-site vs. full-site) and treatment group (***$p<0.001$).

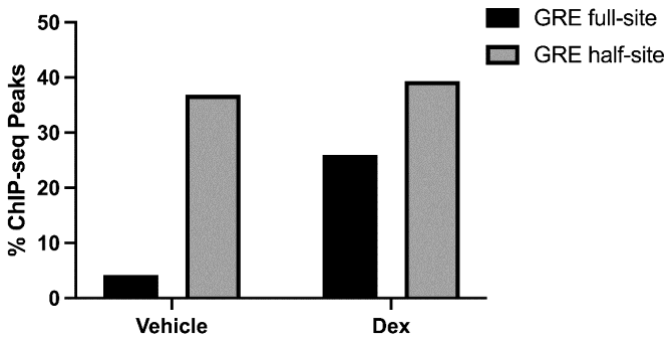

Figure 18. GR binding at full-site (i.e. canonical) vs half-site GREs

F18 Legend: Percentage of ChIP-seq peaks enriched for a GRE full-site or GRE half-site using the HOMER motif enrichment algorithm. Fisher's Exact test (*p<0.0001).**

3.4.10 Motif enrichment analyses predicts GR cofactors involved in chromatin remodeling

Because SOX TFs are identified as putative transcriptional coregulators of GR action in NSPCs, we asked whether they also play a role in Dex-induced chromatin remodeling of the 95 unique sites identified in Aim 1 (**Figure 7**). We ran the motif enrichment analyses to search for TF motifs at the 95 regions of chromatin that exhibited remodeling by Dex at 4h. This revealed ~84% (n=71) and ~46% (n=39) of differential peaks with Dex-increased accessibility were enriched for at least one GRE, or a GRE and a SOX TF binding motif, respectively, relative to random background sequences ($p<1e-38$). In contrast, differential peaks with decreased accessibility lacked both GR binding and GRE enrichment, but 5 are enriched for a SOX TF binding motif (**Figure 19**) ($p<0.05$). Thus, Dex-dependent increases in chromatin accessibility may be facilitated by genomic GR binding at GREs with a close association to SOX TFs, whereas decreases in chromatin accessibility occur at sites not bound by GR and, perhaps, are SOX TF-affiliated genomic regions (example schematic depicted in **Figure 20**).

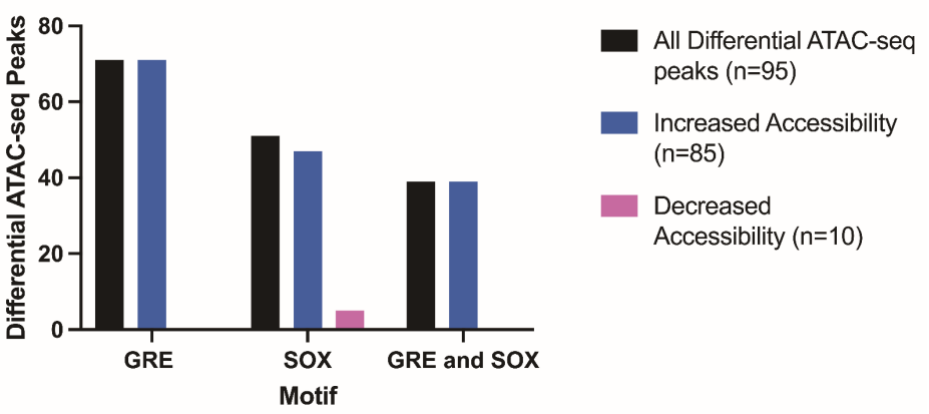

Figure 19. Putative TF motifs within Dex-remodeled chromatin

F19 Legend: HOMER motif analyses predict enrichment of GRE and/or SOX TF motifs (x-axis) under (i) all differential ATAC-seq peaks (black), differential ATAC-seq peaks induced by Dex (blue), or differential ATAC-seq peaks attenuated by Dex (pink). HOMER motif predictions were called using a ($p<0.05$) cut-off for significance.

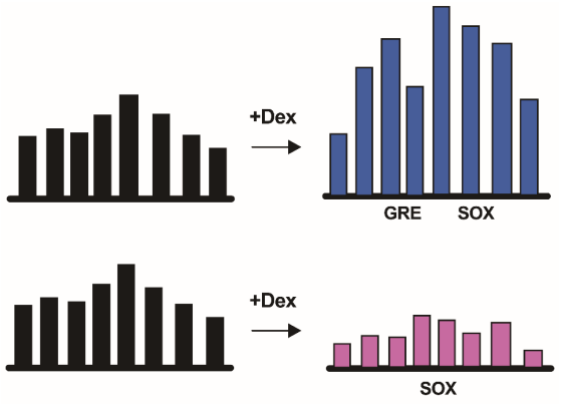

Figure 20. Schematic depiction of the TF motifs guiding chromatin remodeling by Dex

F20 Legend: A model of TSS-proximal TF motifs with facilitate the dynamic chromatin response to Dex in embryonic cortical NSPCs. Each vertical bar represents a cluster of ATAC-seq reads, with a set of bars representing a single ATAC-seq peak. The vertical height of each bar represents intensity of ATAC-seq reads at a single genomic location.

3.4.11 Chromatin remodeling occurs at GR-bound active enhancer regions

To test for a potential association between chromatin remodeling and functional noncoding genomic variants specific to GCs, we quantified the number of differential ATAC-seq peaks which overlapped with previously described H3K27ac+ ChIP-seq peaks [235]. 64 (~67%) of differential ATAC-seq peaks overlapped with a H3K27ac+ ChIP-seq peak, indicating that most Dex-induced changes in the chromatin landscape occur within active enhancer regions. These changes in chromatin accessibility strongly correlated with direct genomic GR binding, evidenced by the enrichment of 51 H3K27ac+ differential ATAC-seq peaks for the GRE motif, and an overlap with a GR ChIP-seq peak. However, some chromatin dynamics occurred independent of genomic GR binding because 13 H3K27ac+ differential ATAC-seq peaks lacked GR ChIP-seq peaks (**Figure 21**). Thus, Dex-activated GR alters the chromatin landscape of enhancer regions predominantly via direct DNA binding but can exert some effects on chromatin structure via other TFs secondary to or independent of direct association with DNA.

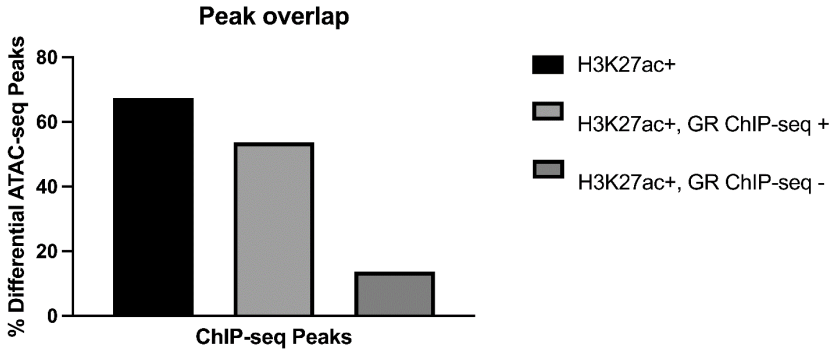

Figure 21. Quantification of GR binding in H3K27ac+, Dex-remodeled chromatin

F21 Legend: Percentage of differential ATAC-seq peaks (x-axis) that overlap with a ChIP-seq peak for H3K27ac and/or GR. Genomic localization of H3K27ac was delineated in cortical NSPCs (E14.5) from an independent study (Gene Expression Omnibus accession no. 104686).

3.5 Discussion

We explored chromatin accessibility as a molecular determinant of genomic GR action in fetal mouse telencephalon-derived NSPCs (E14.5) and identified 3162 genomic GR binding sites, mostly in noncoding regions and at accessible chromatin, that facilitate the robust primary gene response following 4h of Dex stimulation (**Figure 10-11**)[10]. Similar sizes of the GR cistrome are reported in neural cell lines (i.e. 1183 GR ChIP-seq peaks following 90min Dex (100nM) stimulation in neuronal PC12 cells), in comparison to non-neuronal or cell lines overexpressing GR, which report tens of thousands of ChIP-GR seq-peaks[18,279]. While it is logical to conclude the GR cistrome is unique to our cell type, a reliable comparison of GR binding sites between different tissues is prevented by the lack of a standard acceptable cut-off values for positive GR binding used in different ChIP-seq studies.

We studied the effects of Dex on primary cultures of embryonic NSPCs instead of native NSPCs treated with Dex *in-vivo* to avoid cell-sorting and additional sample manipulation that compromises cell viability prior to sequencing. Thus, our understanding of GR action in NSPCs *in-vitro* is limited by a single acute timepoint (E14.5), which in human fetuses resembles the earliest ages of antenatal GC exposure with respect to robust gliogenesis, ongoing neurogenesis, and a period of limited endogenous GC exposure. In addition, a single Dex exposure in mice *in-vivo* (E14.5) is relevant to humans as causes similar brain phenotypes, such as reduced cortical size and cortical surface area, observed in newborn infants exposed to sGCs[7,142,149]. Our data indicate the number of GR binding sites outnumber Dex-regulated genes measured by RNA-seq at 4h by roughly 3-fold[10], an observation that is commonly reported in GR ChIP-seq studies[17,279,299,300]. These data indicate that a single GR binding site alone is not always a direct predictor of nearby gene responses. Thus, clusters of GR binding events may be necessary to evoke

a transcriptional response either from a nearby promoter or distant promoters brought into proximity to DNA-bound GR complexes by chromatin loops.

We recognize that a number of molecular events regulate the intensity and duration of a cellular response to GR stimulation. Patterns of GR-responsive gene expression change over time and vary based upon pulsatile (i.e. circadian, ultradian), constant, or transient hormone stimulation, which each produce biological variabilities in the transiency of GR action, cofactor interactions, and chromatin remodeling in cell culture and animal models[301-303]. Thus we cannot exclude the possibility that the actual number of GR-bound genomic regions in NSPCs is higher than what we report[304]. Our cell culture system can be used to capture the expression of GC-responsive 'secondary response' genes that are preceded by a time lag of over 12h, require protein synthesis, and are associated with so-called 'secondary GREs' that are uniquely bound by GR in a delayed manner[18,305]. Ultimately, an understanding of GR actions on a temporal scale will contribute to our understanding of how dynasticity in GR binding and chromatin remodeling directs sexually dimorphic gene expression patterns[18]. This will inform the pathology driving altered NSPC fate decisions following Dex exposure *in-vitro*[196], or during critical periods of cortical expansion *in-utero* in fetuses exposed to a single course of sGCs[7]. With respect to pulsatile GC action, studies in humans suggest either multiple course administrations of sGCs or episodes of high maternal stress trigger a higher risk for neuropsychiatric and neurodevelopmental conditions in the offspring[44,47,152,153]. Animal studies which administer fluctuating patterns of GCs will inform our understanding of how GCs program fetal neurodevelopment *in-vivo*, though they must consider the accumulation of endogenous GCs in the fetal brain is controlled by placental metabolism by 11ß-HSD2, while sGCs are mostly unaffected by 11ß-HSD2 and thus will have longer occupancy of GR and will be metabolized at a slower rate compared to endogenous GCs[1,2,41,124].

We were interested in determining whether *de novo* GR binding triggers chromatin remodeling in NSPCs, as is reported in non-neuronal cell lines [248,18,249,250]. A minority subset (~20%; n=644 of 3,162) of Dex-induced GR binding occurred in inaccessible regions of chromatin, pointing to GR's potential to function as a pioneer factor or nucleosome remodeling protein at a limited number of sites (**Figure 11**)[21,248]. In addition, chromatin remodeling strongly correlated with direct genomic GR binding (**Figure 21)**, though this relationship is not bidirectional and only occurred in ~0.24% (n=95) of total accessible chromatin. Nonetheless, because GR primarily binds to accessible chromatin, many have aimed to understand what additional factors guide GR to specific genomic regions. Possible explanations include the addition of epigenetic modifications of histone H3, which yields a more permissive environment for GR to bind, or the presence of cell type-enriched TFs that define basal chromatin state and facilitate GR occupancy or activity [18,92]. These additional factors may impact unliganded vs. ligand-bound GR differently given our observed predominance of GR binding to GRE half-sites in vehicle-treated cells relative to GR enrichment at palindromic (i.e. full-site) GRE sequences in NSPCs treated with Dex (**Figure 18**). Similar Dex-responsive binding patterns are observed in the liver, implicating half-site GREs as suboptimal for protein binding compared to palindromic GREs[306]. GR binding to palindromic GREs may occur as dimeric or quaternary oligomeric structures, the latter of which elicits the greatest changes in genomic occupancy and transcription[21,77,281,307,308].

Our data suggest that the culture conditions used to maintain NSPCs, in the absence of added GCs, do not promote GR dimerization and engagement of canonical GREs, but rather, allow a low level of monomeric GR to occupy GRE half-sites. This could be in part due to supplementation of the culture media with growth factors (i.e. EGF and FGF-1) that impact GR-based mechanisms via altered phosphorylation states, and regulate GR co-factors (i.e. AP-1, SGK-

1) in some cell types[309-312]. In this case, the assumption is made that half-site GREs correspond to monomeric GR binding. However, the physiological role(s) for genomic binding of GR monomers remains controversial. Specifically, some studies show GR cannot bind DNA if the dimerization function is impaired[21,70,313], while others argue that GR monomers can function as a tether or cofactor for other TFs[314]. Lastly, aside from GR binding frequency or differences in subcellular signaling pathways upstream of GR, the discrepancy in transcriptional response that results from basal vs hormone-induced GR binding in NSPCs may be explained by differences in the nucleotide sequences flanking the core GRE that modulate activity downstream of GR binding[315]. Collectively, these data indicate GR may play unique roles during distinct stages of neurodevelopment depending upon the levels of endogenous fetal GCs, which rise in late gestation, or in response to therapeutic antenatal sGCs.

The strength and temporal nature of GR binding is dictated by the density of enhancer modification markers, as well as a ligand-specific rate of receptor-DNA interaction[18,316]. Our study uncovered several established and unique features of the GR cistrome in NSPCs. Genomic GR binding preferentially occurred at distal H3K27ac+ sites (**Figure 12**), which are associated with transcriptionally 'active' enhancers, but not 'poised' enhancers that have potential to be active in transcription, leading us to conclude that GR binds preferentially to active enhancer regions in NSPCs [236,237]. Like the global chromatin landscape, most enhancers seem to be established prior to GC ligand binding, aside from some hormone-independent regions with increased transcriptional regulation capability. Although the recruitment of GR to enhancers is dynamic, these data suggest that transcriptional responses to GCs could be modulated by the duration and efficacy of GR-DNA binding [260,261,18].

In addition to enhancer modification marker density, GR genomic binding patterns are established by an increased presence of GREs at distal non-promoter regions, and cell type-enriched TFs, which guide GR to its genomic targets[88,89]. These data corroborate the notion that the GC transcriptome is controlled not only by promoters and cis-regulatory elements, but also through GR-responsive distal regulatory elements. The advent of chromatin conformation technologies has enabled the profiling of over 40,000 enhancer-promoter interactions in mouse NSPCs[317]. However, the precise mechanisms underlying remote regulation by GR have not been fully elucidated in primary cell cultures, as they have been in cell lines[85,318,319].

Our studies identified SOX TF recognition motifs as significantly enriched in GR ChIP-seq peaks (**Figure 14-16**). This is compelling due to the extremely high confidence value ($p<1E-10$) needed to consider predictions using the Homer motif enrichment software, though this also presents a limitation of the approach in that it may underestimate motifs in comparison to other computational algorithms (i.e. MEME suite software)[286]. SOX TFs are of relevance to transcriptional regulation in NSPCs because SOX2, SOX3 and SOX11 exhibit developmental stage-specific binding to DNA in embryonic stem cells, neural progenitor cells, and differentiating neurons, respectively[298]. Identification of the specific SOX protein(s) that influence GR action may allow mechanistic insight into the Dex-regulated cell fate decisions that occur *in-vivo*[213]. A separate landmark study by Bertolini et al. demonstrates SOX2 is critically involved in the maintenance of up to ~50% of all enhancer-promoter interactions in NSPCs *in vitro*[269]. SOX2 also shares hundreds of target genes with GR in NSPCs[10,269]. Despite the lack of direct evidence of GR controlling transcriptional output via long-range chromatin connectivity in our cell type, these observations suggest SOX2 may control long range genomic interactions that enable or facilitate

GR action at regulated enhancers[269,296,320]. **In Aim 3, we pursue this possibility by investigating SOX2 as a transcriptional coregulator of GR.**

3.6 Aim 2 Summary

(i) GR binding sites outnumber Dex-regulated genes, indicating that a single genomic GR binding event alone is not always a direct predictor of nearby gene response.

(ii) Genomic GR binding preferentially occurs at distal H3K27ac+ enhancer regions, corroborating the notion that the GC transcriptome is controlled not only by promoters and cis-regulatory elements, but also through GR-responsive distal regulatory elements.

(iii) In some cases, genomic GR binding triggers chromatin remodeling.

(iv) SOX2 is a putative cell-type specific transcriptional cofactor for GR in NSPCs.

4.0 Aim 3: The Role of SOX2 in the Transcriptomic Response to Dexamethasone in Mouse Embryonic NSPCs

4.1 Introduction

4.1.1 SOX2 is a critical determinant of healthy brain development and function.

SOX2 is a primary marker of the embryonic neuroepithelium in the CNS and is expressed in undifferentiated NSPCs, as well as some neurons and glia in the developing hippocampus and dentate gyrus[321]. A large body of research confirms SOX2's role in maintaining pluripotency in the developing CNS, and designate it as one of four main TFs that reliably reprograms differentiated cells into induced pluripotent stem cells (iPSCs)[322,323]. This is accomplished in part via SOX2-dependent programming of sonic hedgehog (*Shh*) and Wnt/β-catenin signaling[324-327]. SOX2's role in maintaining pluripotency is confirmed by a reduction in proliferation measured in cultured SOX2 knock-down NSPCs(E14.5 or P0-derived), though they continue to proliferate for several passages before cell numbers markedly decrease[269,325]. SOX2 is also required for proper establishment of thalamocortical projections[328], visual system development, hippocampal development[329], and cortical patterning[328]. Meanwhile, SOX2 deficiencies result in a host of CNS developmental defects including intellectual disability, motor control insufficiency, epilepsy[330], microcephaly[325,331], and severe vision impairments[328,332] in animal models[319,322,333]. Lastly, the roles for SOX factors are not limited to CNS development. SOX2 expression in the adult SVZ of the lateral ventricle and dentate gyrus subgranular zone (SGZ) of the hippocampus maintains neurogenesis throughout adulthood[334,335]. It also influences cell death, survival, tissue

regeneration[336], and homeostatic processes in various adult tissues[337]. These topics, along with SOX2-expressing cells in the thalamus, hypothalamus, medial ganglion eminence, and cerebellum are reviewed in detail by Mercurio et al.[321,333] and Ribiero et al.[335].

4.1.2 SOX2 is a Core Transcriptional Regulator of NSPC Gene Expression Programs

All members of the SOX TF family harbor two nuclear localization signals that are activated by an association with the calcium-binding protein calmodulin (CaM) at their N-termini and/or importin alpha (IMPα) at the C-termini of the DNA binding domains[338]. SOX2 nuclear import is tightly regulated by isoform specific IMPα expression, which differentially influences cell fate outcomes[339,340]. Once inside the nucleus, SOX2 exerts precise control of progenitor-to-neuron cell fate transitions by directly associating with cell-type specific TFs and various components of basal transcriptional machinery[341]. Combined proteomics, transcriptomics, and chromatin landscape profiling reveals the genomic distribution of SOX2 drastically shifts from pluripotency enhancers to neuronal promoters during differentiation, driven by switches in pro-pluripotent TFs (e.g., OCT4, Nanog[337,342]) and proneuronal TFs (e.g., ATRX) that colocalize with SOX2. This does not occur at astrocytic or quiescence-associated genes, and is accompanied by increased proneuronal gene expression[343,344]. Other models propose that SOX2 binding only represses proneuronal genes in embryonic stem cells, while other SOX family members (i.e. SOX3, SOX9, SOX10, SOX11) specify neuronal and/or glial differentiation[337]. Considering these alternative interpretations, it is unclear whether the shift of SOX2 to neuronal-associated genes directly activates proneuronal gene expression. It is perhaps more likely that SOX2 functions as a pioneer factor or chromatin remodeling protein to prime proneuronal genes for activation[298,345-349]. SOX2-binding also enables recruitment of additional pioneer factors (i.e. TFAP2, ATRX) or

chromatin remodelers that increase DNA accessibility and/or enhancer activity[344,350,351]. However, priming of chromatin accessibility alone is necessary but not sufficient for gene activation[344]. Together, these data highlight the need to study the entire SOX2 interactome in addition to the NSPC proteome at temporal intervals to fully understand how coordinated changes in TF occupancy drive cell fate transitions.

Chromatin connectivity mapping provides mechanistic insight regarding the gene regulatory potential of SOX2 occupancy at distal genomic regions. In mouse NSPCs (P0), SOX2 directly mediates thousands (<~18,000; 35-46% of total) of promoter-promoter and promoter-nonpromoter (i.e. enhancer-promoter) chromatin contacts. SOX2 loss attenuates or completely ablates a large subset of these 3-dimensional contacts along with the expression of a subset of genes (n= ~700) influenced by SOX2-bound chromatin interactions. Importantly, these studies stress the importance of SOX2-bound enhancer-promoter interactions, which increase gene transcription and have more frequent chromatin contacts when compared to SOX2-bound promoter-promoter interactions[269,352]. Because distal SOX2 binding is associated with active enhancer regions[286,343], and SOX2 is a predicted transcriptional coregulator of GR at distal genomic sites (see **Aim 2**), it is tempting to theorize that SOX2 facilitates GR transcriptional activity by maintaining enhancer activity and chromatin connectivity to target GR gene promoters in a cell-type specific manner.

4.1.3 Rationale and Summary

In the developing ventral and dorsal telencephalon, all multipotent NSPCs express SOX2[353]. SOX2 mediates thousands of enhancer-promoter contacts in NSPCs, with a direct effect on transcriptional output[269]. Since SOX2 is a predicted cofactor of GR at distal enhancer regions,

we first performed a proximity ligation assay to determine the nuclear protein-protein proximity of GR and SOX2 in vehicle and Dex-treated NSPCs (E14.5). We then performed microarray gene expression analyses of wild-type vs. SOX2 knock-out NSPCs (P0) to determine if SOX2 ablation significantly alters the Dex-responsive transcriptome.

4.2 Materials and Methods

4.2.1 Animals and Cell Culture

E14.5 wild-type NSPCs were prepared as described in Aim 1.

Mice with *Sox2*^{loxP} and *Sox2*$^{loxP\Delta neo}$ alleles, together a *nestin-cre* transgene[354], were generated as described by Favaro et al., 2009[325]. Cre activity is driven by the neural *nestin* enhancer and begins at E10.5, causing complete SOX2 KO in the CNS by E12.5[325]. Neurosphere cultures of SOX2 knockout (KO) NSPCs and control non-deleted wild-type NSPCs (C57BL/6) derived from the fetal telencephalon were established at postnatal day (P0) as previously described [325,355,356]. At P0, neurogenesis is not significantly altered, though limited abnormalities are observed in SOX2 KO mice. These include a slight reduction of hippocampal volume and posterior ventrolateral cortex size, and a moderate enlargement of the lateral ventricle[325]. The establishment, maintenance, and expansion of SOX2 ablated neurospheres has been found to be optimal with cerebral cortical tissue derived from P0 mice[269,325]. It is important to note that SOX2 KO NSPC cultures retain their self-renewal potential for up to 7-10 passages (~30 days), followed by a decline in proliferation capacity[325]. This study collected cultured cells after the third passage. Biologically

distinct replicates of both sexes were treated *in-vitro* with 100nM Dex for 4h and processed for microarray gene expression analysis (n=6 wild-type; n=7 SOX2 KO males and females combined).

4.2.2 Proximity Ligation Assay

A detailed protocol for the Duolink® proximity ligation assay (PLA) (Sigma Cat no. DUO92102) is described by Alam[357]. After the third passage, wild-type NSPCs derived from the embryonic telencephalon (E14.5) were plated in 24-well cell culture plates (Falcon) containing glass coverslips coated with Poly-D-Lysine (Sigma P1524) and Laminin (Corning™ via Fisher CB-40232, Mouse). 24h after plating, cells were treated with vehicle or Dex for 4h as previously described, then fixed in a 10% neutral buffered formalin solution (ThermoScientific REF9990244) for 30 minutes at 4°C [10]. The Duolink® PLA protocol was followed, using 80ul reaction volumes. In brief, cells on coverslips were incubated with Duolink® blocking solution for 1 hour in a heated humidity chamber at 37°C with gentle shaking, then overnight with a SOX2 anti-rabbit antibody (1:500) (Abcam ab97959) and a GR anti-mouse antibody (1:500) (Invitrogen MA1-510) at 4°C with gentle shaking. To control for non-specific PLA-probe activity, the GR anti-mouse antibody ($Control^{GR}$) or the SOX2 anti-rabbit antibody ($Control^{SOX2}$) were omitted from the overnight incubation, followed by the complete experimental protocol. The next day, cells were washed 2 x 5 minutes in Wash Buffer A and incubated with mouse MINUS and rabbit PLUS PLA probes at a 1:5 dilution in Duolink® antibody diluent for 1 hour in a preheated humidity chamber at 37°C. Coverslips were washed in Wash Buffer A as previously described and incubated with ligase, at a 1:40 dilution in 1X ligation buffer, for 30 minutes in a preheated humidity chamber at 37°C. Coverslips were washed again and incubated with polymerase at a 1:80 dilution in 1X amplification buffer for 100 minutes in a preheated humidity chamber at 37°C. Coverslips were

washed 2 x 10 minutes in Wash Buffer B. Nuclei were stained with Dapi in PBS (1:10,000) for 1 minute, washed a final time with PBS, then mounted on glass coverslips and stored at 4°C protected from light.

4.2.3 Confocal Microscopy and Image Quantification

For PLA assay quantification, each experimental group of cells was plated on 4 coverslips of a 24-well plate, and 6 images were taken per slide per embryo for a total of 24 images per embryo per treatment group (for n=3, 72 images per treatment group). Using an FV1000 Olympus confocal microscope, PLA probes were visualized at 60X magnification in the Alexa Fluor 594 channel (excitation wavelength 543nm, emission wavelength 618nm), with variable voltage detector levels (<650), minimal gain (<2) and no photobleaching (offset <12) (lens parameters: sampling speed 2.0 us/Pixel, 12bits/pixel, 640 pixels total). Nuclei were visualized with the same parameters in the DAPI channel. To quantify PLA probe photoactivation, each nucleus was outlined and defined as an individual region of interest (ROI), and the average intensity profile was determined for the ROIs. Overall average intensity is defined as the average ROI per cell per image per embryo. For downstream analyses, probe-positive cells are defined as a ROI with an average intensity profile >100, due to baseline levels of background photoexcitation in the Alexa Fluor 594 channel present in the negative control samples (average background intensity profile ~59). To compare the average abundance of PLA probe photoactivation between all four experimental groups, One-way ANOVA test was performed to quantify significant differences among group means. Multiple comparisons were performed when necessary. For comparisons between two experimental groups, an unpaired two-tailed t-test was used.

4.2.4 Microarray Gene Expression Array

The RNeasy micro kit (Qiagen) was used to extract total RNA. RNA integrity was determined by both the absorption ratio (260/280) of ≥1.8, as well as the RNA integrity value of ≥8.0 measured by a Bioanalyzer 2100. 100ng of purified total RNA underwent transcription *in-vitro* via the MessageAmp Premier Enhanced assay protocol (Thermo Fisher Scientific). The diversity of cRNA was confirmed by Nanodrop, which generates one electrophoretogram per reaction with sample integrity, yield, and size diversity against a Universal Human Reference RNA. Following purification and amplification, 15 μg of biotin-labeled cRNA was fragmented and hybridized to the Affymetrix Mouse Clariom S^{TM} array in accordance with the manufacturers protocol (ThermoFisher Scientific). After 18h, the arrays were washed and stained on an Affymetrix Fluidics Station, then immediately scanned using a Scanner 3000 after hybridization.

4.2.5 Microarray Gene Analysis

Of the 22,206 genes measured, transcriptome analysis software identified those with a p-value <0.05, considered as having a significant change in expression in Dex-treated groups compared to vehicle controls. Significant ($p<0.05$) and robust fold changes ($-1.5 \leq FC$; $1.5 \geq FC$) induced by Dex within WT or SOX2 KO groups were compared to reveal how SOX2 ablation alters the direction and intensity of gene response. All microarray gene expression data was uploaded to IPA (QIAGEN Inc., https://www.qiagenbio- informatics.com/products/ingenuity-pathway-analysis), containing the gene identifiers and their corresponding expression, fold-change, and p-value, among other common metrics. Using the “build” and “overlay” pathway functions, the gene identifiers were then sorted by fold change and mapped to the corresponding

gene object in the “glucocorticoid receptor signaling” and “FGF signaling” canonical signaling pathways, determined in the Ingenuity Pathway Knowledge Base (IPKB).

4.3 Results

4.3.1 GR and SOX2 nuclear proteins are in close proximity (<40nm) in primary NSPC cultures

To validate our bioinformatics-informed prediction of a close association between GR and a SOX factor, we performed a PLA to identify proximity (<40nm) between GR and SOX2 in vehicle- or Dex-treated NSPCs (Dex; 100nM)(E14.5) (**Figure 25A**). SOX2 was chosen because is a predicted GR cofactor, and it shares many target genes with GR in NSPCs, with over 145 genes significantly altered by both SOX2 ablation or Dex exposure *in vitro* [10,269]. The overall average PLA probe intensities indicating instances of GR-SOX2 proximity (<40nm) in vehicle-treated NSPCs and Dex-treated NSPCs were similar (overall average intensity = 123.5 and 124.4, respectively), while negative control groups for antibody-specific PLA-probe activity had significantly reduced amounts of PLA probe photoactivation ($Control^{GR}$ and $Control^{SOX2}$; overall average intensity = 56.9 and 60.8, respectively) ($p<0.001$) (**Figure 25B**). Because PLA probes were detected above baseline intensity values (>100) in 62.8% and 40.4% of vehicle or Dex-treated NSPCs (i.e., probe-positive cells), respectively (**Figure 25C**), we determined whether the abundance of PLA probes was changed by Dex in this probe-positive cell population. While overall average PLA probe intensity varied more between the vehicle and Dex-treated probe-positive cell populations (165.4 and 202.5, respectively) compared to the entire cell population

(123.5 and 124.4, respectively), it was not significantly changed by Dex in the probe-positive cell population (**Figure 25D**).

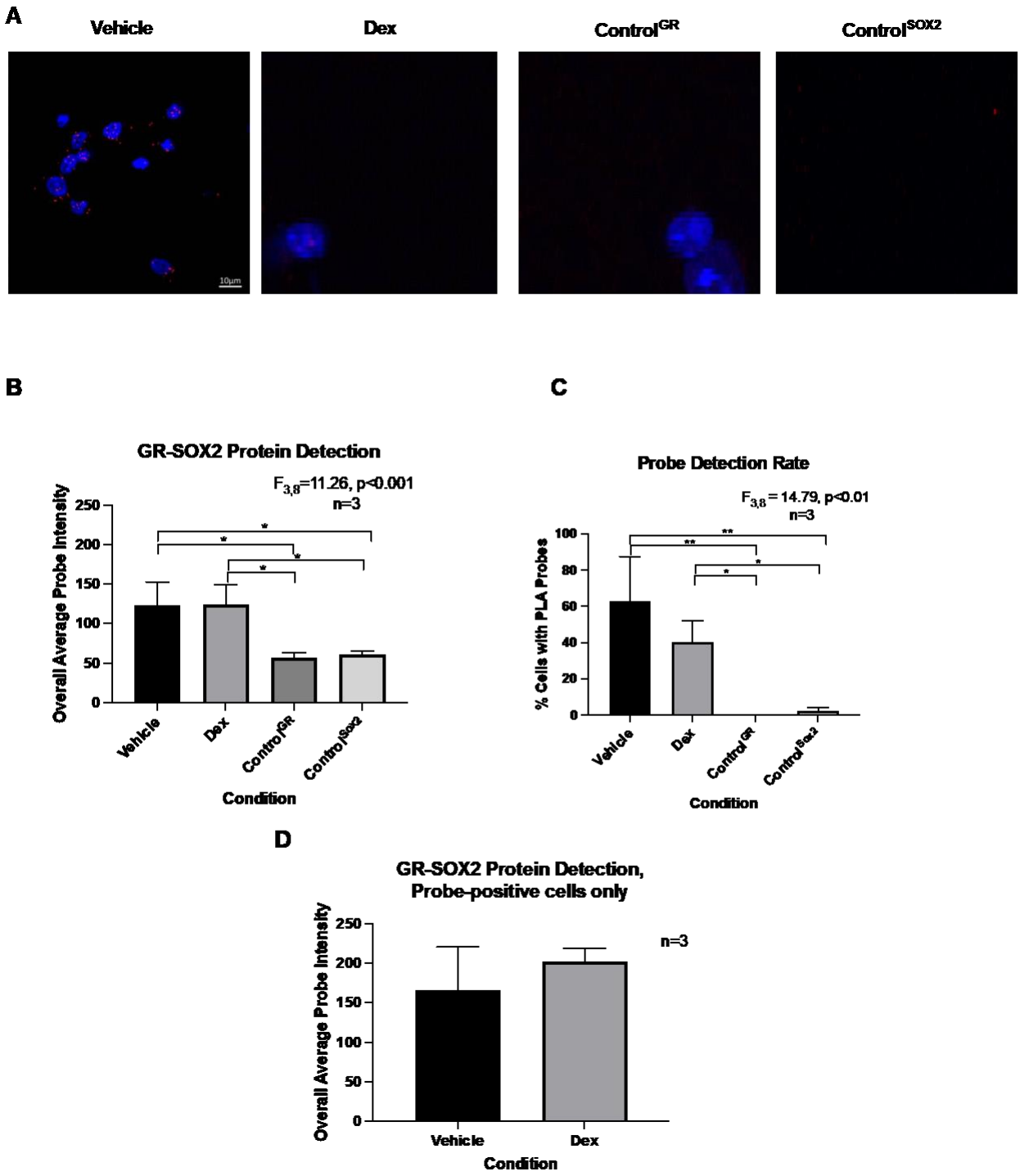

Figure 22. GR-SOX2 nuclear proximity in cultured NSPCs (E14.5)

F25 Legend: A) Detection of GR and SOX2 proximity *in-vitro,* using adherent, proliferating NSPCs treated with either vehicle or Dex for 4h. Blue; Dapi staining of nuclei. Red; PLA probes indicating GR-SOX2 proximity (<40nm). Negative control groups for antibody-specific PLA-probe activity (Control^{GR} and

Control^{SOX2}) had minimal fluorescence of PLA probes. Images shown at 60X magnification contain a 10μm scale bar. Pseudo-color increased post-processing for visual enhancement of publication images. Asterisk indicates the cell shown on the magnified inset, upper right corner. B) Overall average PLA probe intensity per cell per image per embryo in vehicle- (n=1,178 cells, 24 images) or Dex-treated (n=1,256 cells, 24 images) NSPCs (n=3 biological replicates), with all cells per image included. Control groups; Control^{GR} and Control^{SOX2}. One-way ANOVA test reveals a significant difference among group means ($p<0.001$). The single asterisk and bar indicate a significant difference between two groups ($p<0.05$) ($F_{3,8}$ = degrees of freedom for the numerator (DFn=3) or denominator (DFd=8) of the F ratio (F=11.26). C) Average percentage of vehicle-treated (n=726) or Dex-treated (n=529) NSPCs with PLA probes (probe intensity per cell >100) (n=3). Control groups; Control^{GR} and Control^{SOX2}. One-way ANOVA test reveals a significant difference among group means ($p<0.01$). The single or double asterisks and bar indicate a significant difference between two groups ($p<0.05$ or $p<0.01$) ($F_{3,8}$ = degrees of freedom for the numerator (DFn=3) or denominator (DFd=8) of the F ratio (F=14.79). D) Overall average PLA probe intensity per cell per image per embryo, only in probe-positive (probe intensity per cell >100, Fig. 25C) NPSCs treated with vehicle (n=726 cells) or Dex (n=529 cells) for 4h (n=3). Control groups; Control^{GR} and Control^{SOX2}. Unpaired two-tailed t-test does not reveal significance ($p>0.05$).

4.3.2 Genome-wide profiling of the Dex transcriptome in wild-type vs SOX2 KO NSPCs *in-vitro* (P0)

To investigate the functional role of SOX2 in determining transcriptional output following GR activation by Dex, we performed unbiased genome-wide measurements of gene expression by microarray in vehicle or Dex-treated (4h) WT NSPCs derived from the developing mouse telencephalon at postnatal day (P0)(n=6), or NSPCs (P0) derived from the same region of conditionally (at E11.5) SOX2-ablated mice (SOX2 knock out; KO)(n=7). SOX2 ablation did not change MR expression (encoded by *NR3C2;* data not shown*)* or GR expression (encoded by *NR3C1),* suggesting that the transgene does not greatly affect their function (**Figure 23**). For the

microarray technology used in this study signals ≤4 are considered background noise (**Figure 24).** Dex alters the expression of 429 genes ($p<0.05$) in WT NSPCs and 901 genes in SOX2 KO NSPCs at 4h, with some genes classified as robustly Dex-upregulated (fold change; FC ≥ 1.5) or robustly Dex-downregulated (FC ≤ 1.5) (**Figure 25**).

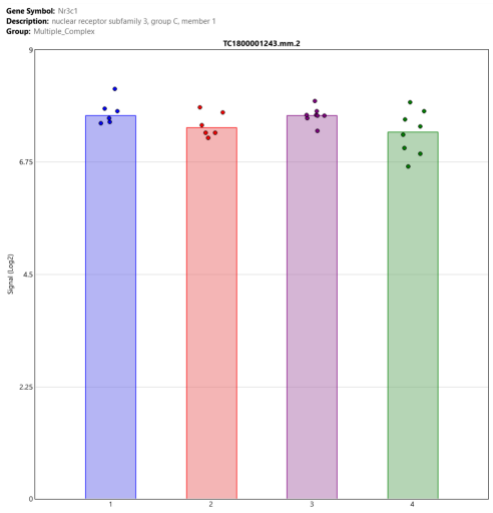

Figure 23. NR3C1 expression determined by microarray.

F26 Legend: mRNA expression of GR, encoded by *Nr3c1*, determined by microarray gene expression measurements in vehicle-treated wildtype NSPCs (P0) (group 1; n=6), Dex-treated wildtype NSPCs (group 2; n=6), vehicle-treated *Sox2*-ablated NSPCs (P0) (group 3; n=7), and Dex-treated *Sox2*-ablated NSPCs (P0) (group 4; n=7). x-axis; treatment group. y-axis; Log2 expression of *Nr3c1* microarray probe(s). Log2 signal values less than ~4 is background noise.

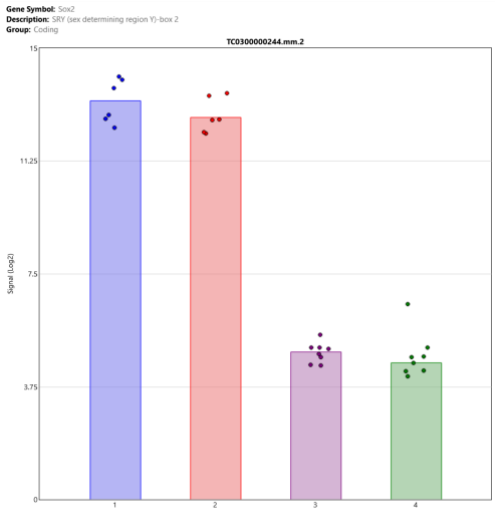

Figure 24. Sox2 expression determined by microarray.

F27 Legend: mRNA expression of *Sox2* determined by microarray gene expression measurements in vehicle-treated wildtype NSPCs (P0) (group 1; n=6), Dex-treated wildtype NSPCs (group 2; n=6), vehicle-treated *Sox2*-ablated NSPCs (P0) (group 3; n=7), and Dex-treated *Sox2*-ablated NSPCs (P0) (group 4; n=7). x-axis; treatment group. y-axis; Log2 expression of *sox2* microarray probe(s). Log2 signal values less than ~4 is background noise.

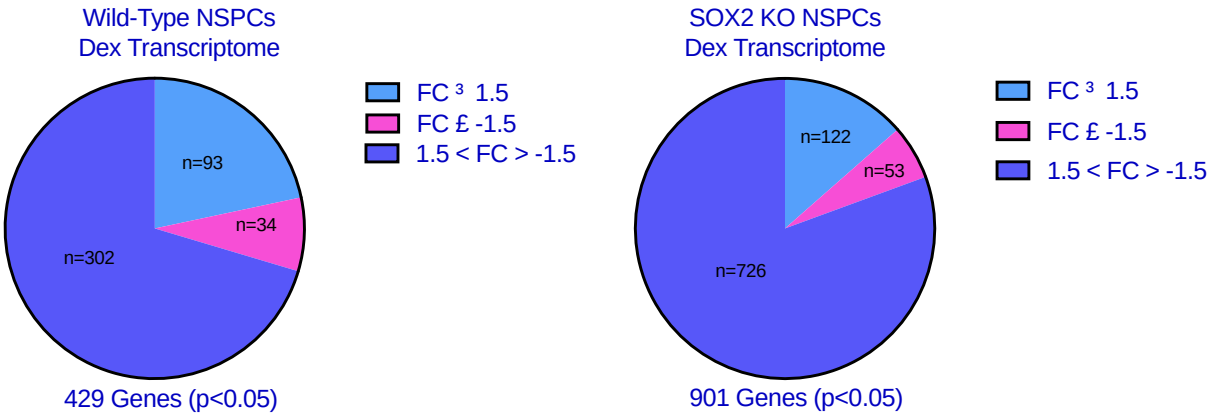

Figure 25. Whole-transcriptome measurements in wild-type vs SOX2-ablated NSPCs (P0).

F28 Legend: Quantification of genes which were robustly upregulated (p<0.05; FC ≥ 1.5), robustly downregulated (p<0.05; FC ≤ -1.5), or moderately regulated (p<0.05; 1.5 < FC > -1.5) following 4h Dex

treatment in WT NSPCs (P0; n=7) or SOX2 KO NSPCs (P0; n=7). FC; fold change of average expression value. Total n of significantly regulated genes (p<0.05) per group is displayed at the bottom of each chart.

4.3.3 Microarray gene expression analyses reveals SOX2-dependent effects of Dex on NSPC gene Expression

Within the groups of robustly Dex-regulated genes, a subset of gene induction or repression occurs in both WT and SOX2 KO NSPCs (i.e., *Hif3a* is Dex-upregulated in both WT and SOX2 KO NSPCs), suggesting that a subset of GR action occurs independently of SOX2 (**Figure 29**; 'Shared')(**Table 4-5**). In contrast, another subset of robustly Dex-regulated genes occurs uniquely in WT NSPCS (n=59) compared to SOX2 NSPCs (i.e. *Cspg4* is Dex-upregulated in WT NSPCs but unaffected in SOX2 KO NSPCS (**Figure 26**; 'WT Unique')(Error! Reference source not found.**-7**). This differential gene response in WT vs SOX2 KO NSPCs suggests that the glucocorticoid response of a subset of GR target genes is SOX2-dependent, because SOX2 is required for the Dex-induced transcriptional outcome. Interestingly, 'Shared' or SOX2-independent genes, which had similar responses to Dex in both WT and SOX2 KO NSPCs, were more likely to have a GR binding site within +/- 10kb of the TSS, while SOX2-dependent genes (i.e. WT-Unique) were less likely to have a GR binding site +/- 10kb relative to their promoters (**Table 10;** determined by overlap analyses of microarray gene ID position and GR ChIP-seq peaks). These data suggest SOX2 acts at distal enhancers to regulate a subset of GR transcriptional output in NSPCs. A final subset of Dex-responsive genes was detected only in SOX2 KO NSPCs but showed no significant Dex response in WT NSPCs. These SOX2 KO unique transcriptional outputs are likely due to major alterations in chromatin connectivity, previously shown to occur following SOX2 ablation (**Figure 26**; 'KO Unique')(Error! Reference source not found.**-9**)[269].

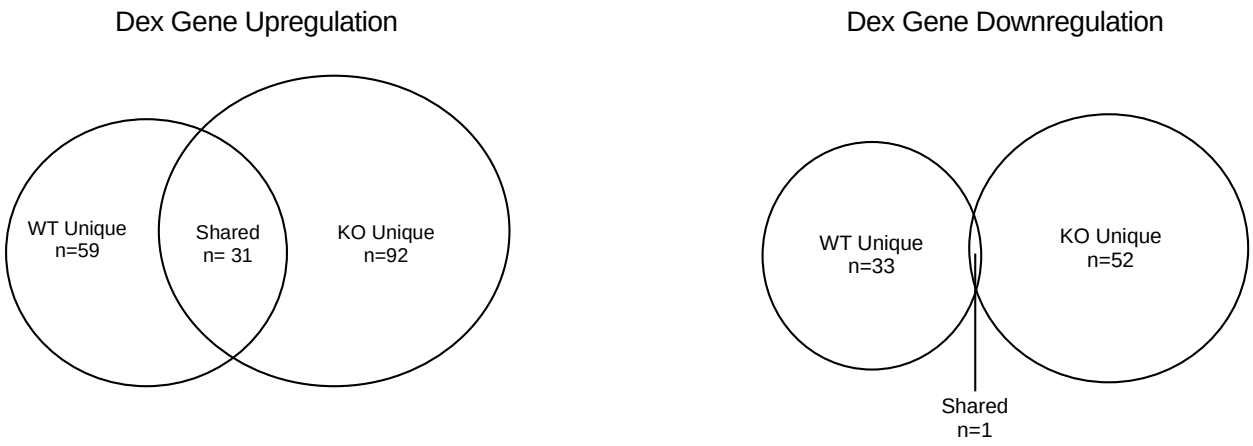

Figure 26. 'Shared' and 'unique' gene responses to Dex in wild-type vs. SOX2 KO NSPCs (P0)

F29 Legend: Quantification of genes which were Dex-upregulated ($p<0.05$)(left) or Dex-downregulated ($p<0.05$)(right) in (i) WT NSPCs only when compared to SOX2 KO NSPCs (WT Unique), (ii) both WT and SOX2 KO NSPCs (Shared), or (iii) SOX2 KO NSPCs only when compared to WT NSPCs (KO Unique).

Table 4. 'Shared' Dex-upregulated genes. (FC≥1.5; $p<0.05$) in both WT (n=6) and SOX2 KO (n=7) NSPCs. 31 genes in total.

Gene Symbol	Affymetrix ID	WT Fold Change	WT P-value	SOX2 KO Fold Change	SOX2 KO P-value
Fam107a	TC1400001439.mm.2	51.43	0.0009	23.69	0.0000
Hif3a	TC0700002445.mm.2	2.68	0.0071	7.84	0.0000
Cftr	TC0600000145.mm.2	3.26	0.0028	6.56	0.0000
Fkbp5	TC1700001757.mm.2	2.76	0.0015	4.60	0.0000
Klf9	TC1900000373.mm.2	3.70	0.0006	4.36	0.0000
Mt2	TC0800001094.mm.2	1.98	0.0153	4.33	0.0000
Kcnn2	TC1800000468.mm.2	6.10	0.0002	4.03	0.0000
Per1	TC1100000900.mm.2	4.85	0.0005	3.53	0.0000
Mgll	TC0600001035.mm.2	1.79	0.0298	3.46	0.0000
Map7d2	TC0X00001619.mm.2	2.48	0.0019	3.31	0.0000
Thrsp	TC0700003764.mm.2	3.65	0.0168	3.13	0.0004
Adamts9	TC0600002756.mm.2	1.63	0.0091	2.88	0.0000
Mfsd2a	TC0400003475.mm.2	1.98	0.0390	2.81	0.0000
Tprn	TC0200000405.mm.2	1.90	0.0151	2.75	0.0000
Lcn2	TC0200003303.mm.2	2.36	0.0253	2.70	0.0000
Nedd9	TC1300001861.mm.2	2.76	0.0001	2.67	0.0000
Per2	TC0100002801.mm.2	2.26	0.0114	2.45	0.0000
Bcat1	TC0600003412.mm.2	2.01	0.0199	2.43	0.0005
Tsc22d3	TC0X00003075.mm.2	2.51	0.0042	2.30	0.0006
Sesn1	TC1000000372.mm.2	2.17	0.0023	2.19	0.0000
Bcl2l1	TC0200004913.mm.2	1.85	0.0280	2.18	0.0098
Ptprj	TC0200004090.mm.2	1.65	0.0127	1.99	0.0000
Dgkz	TC0200004130.mm.2	1.67	0.0118	1.94	0.0002
Cebpd	TC1600000192.mm.2	2.08	0.0314	1.94	0.0066
Plcb4	TC0200002067.mm.2	1.55	0.0345	1.93	0.0051
Pknox2	TC0900002040.mm.2	1.88	0.0267	1.90	0.0094
Lfng	TC0500001695.mm.2	1.58	0.0166	1.84	0.0001
Lgalsl	TC1100002314.mm.2	1.85	0.0140	1.69	0.0014
Klf13	TC0700003406.mm.2	1.72	0.0196	1.68	0.0029
Peg3	TC0700002217.mm.2	2.30	0.0103	1.61	0.0030
Trim36	TC1800001289.mm.2	1.51	0.0241	1.53	0.0068

Table 5. 'Shared' Dex-downregualted genes. (FC≤ 1.5; p<0.05) in both WT (n=6) and SOX2 KO (n=7) NSPCs. 1 gene in total.

Gene Symbol	Affymetrix ID	WT Fold Change	WT P-value	SOX2 KO Fold Change	SOX2 KO P-value
Cntnap4	TC0800001349.mm.2	-1.81	0.0194	-1.81	0.0004

Table 6. 'Unique' Dex-upregulated genes. (FC>1.5; p<0.05) in WT (n=6) NSPCs. 59 genes in total.

Gene Symbol	Affymetrix ID	WT Fold Change	WT P-value
Sprr2j-ps	TC0300000830.mm.2	2.24	0.0047
Slc24a4	TC1200001010.mm.2	2.17	0.036
Aldh3b3	TC1900000020.mm.2	2.07	0.0165
Ptk2b	TC1400002267.mm.2	2.02	0.0021
Brdt	TC0500001073.mm.2	1.91	0.0101
Mt4	TC0800001092.mm.2	1.87	0.0037
Scgn	TC1300001653.mm.2	1.86	0.0078
Sult1e1	TC0500002700.mm.2	1.85	0.0039
Colec11	TC1200001567.mm.2	1.84	0.0033
Fer1l4	TC0200004980.mm.2	1.83	0.0302
Gm19549	TC0700003095.mm.2	1.8	0.0323
Vmn2r105	TC1700001534.mm.2	1.78	0.0072
Gm12789	TC0400001045.mm.2	1.78	0.0197
Ceacam11	TC0700000261.mm.2	1.78	0.0246
Ccdc15	TC0900002047.mm.2	1.76	0.0468
Dnah14	TC0100001736.mm.2	1.74	0.0036
Syt12	TC1900000923.mm.2	1.73	0.0249
Gm20871	TC0Y00000558.mm.2	1.72	0.0277
Trim12c	TC0700003940.mm.2	1.69	0.0163
Gm29073	TC0Y00000325.mm.2	1.67	0.0025
Ppp1r32	TC1900001102.mm.2	1.66	0.0064
Gm21876	TC0X00001940.mm.2	1.66	0.0182
Olfr1386	TC1100000512.mm.2	1.65	0.0183
Olfr323	TC1100002830.mm.2	1.65	0.0372
Vmn2r60	TC0700000736.mm.2	1.64	0.0053
Olfr1129	TC0200001297.mm.2	1.64	0.0128
S100a8	TC0300000811.mm.2	1.63	0.0369
Cldn9	TC1700001599.mm.2	1.61	0.0395
Mmp12	TC0900000046.mm.2	1.6	0.0187
Gsta3	TC0100000135.mm.2	1.59	0.0122
Gm6121	TC0X00001987.mm.2	1.58	0.0378
LOC636187	TC0400002382.mm.2	1.57	0.0239
Il12a	TC0300000567.mm.2	1.57	0.0253
Cspg4	TC0900000686.mm.2	1.57	0.0304
Klra2	TC0600003264.mm.2	1.57	0.0402
Plek	TC1100002249.mm.2	1.56	0.0269
Hebp2	TC1000001807.mm.2	1.56	0.0441
LOC100042443	TC0Y00000149.mm.2	1.55	0.0388
LOC100042279	TC0Y00000174.mm.2	1.55	0.0388
Zfp429	TC1300002246.mm.2	1.54	0.0192
Wfdc1	TC0800001425.mm.2	1.54	0.0322
LOC102639117	TC1900000177.mm.2	1.53	0.0125
Akr1b7	TC0600000327.mm.2	1.53	0.0178
Cd48	TC0100001597.mm.2	1.53	0.0477
Dhrs2	TC1400000776.mm.2	1.52	0.0032
Gm20809	TC0Y00000070.mm.2	1.52	0.013
Ramp3	TC1100000106.mm.2	1.52	0.0134
Wfdc6a	TC0200005120.mm.2	1.52	0.0229
Olfr32	TC0200004081.mm.2	1.51	0.0197
Hbp1	TC1200001601.mm.2	1.51	0.0348
Pramef25	TC0400003932.mm.2	1.51	0.0418
Zfpm1	TC0800001481.mm.2	1.5	0.0093
Gm11545	TC1100003573.mm.2	1.5	0.0177
Gm14685; DXBay18	TC0X00000674.mm.2	1.5	0.0251
DXBay18	TC0X00002420.mm.2	1.5	0.0251
Qprt	TC0700004312.mm.2	1.5	0.0293
Vip	TC1000000036.mm.2	1.5	0.0404
Gsto2	TC1900000728.mm.2	1.5	0.0439
Lpin1	TC1200001460.mm.2	1.5	0.0448

Table 7. 'Unique' Dex-downregulated genes (FC≤ 1.5; p<0.05) in WT (n=6) NSPCs. 33 genes in total.

Gene Symbol	Affymetrix ID	WT Fold Change	WT P-value
Olfr1496	TC1900000284.mm.2	-1.97	0.015
AI182371	TC0200003359.mm.2	-1.93	0.0011
Gm7697	TC0800002364.mm.2	-1.81	0.0175
Olfr1314	TC0200004342.mm.2	-1.81	0.0217
Krt83; Krt81; 5430421N21Rik; Krt85	TC1500002259.mm.2	-1.8	0.0182
Gm21961	TC1500001642.mm.2	-1.8	0.0433
Gm11037	TC0200002006.mm.2	-1.72	0.0442
Gm21955	TC0400000416.mm.2	-1.68	0.0279
Vmn2r11	TC0500002962.mm.2	-1.66	0.0308
Ccdc85c	TC1200002346.mm.2	-1.65	0.0082
Arntl2	TC0600001738.mm.2	-1.64	0.0237
Gm9495	TC0800002362.mm.2	-1.64	0.0413
Amer2	TC1400000846.mm.2	-1.63	0.0035
Shisa5	TC0900001431.mm.2	-1.63	0.0052
Mycn	TC1200001432.mm.2	-1.62	0.0011
Efna2	TC1000000845.mm.2	-1.62	0.0282
Gm8159	TC1400000029.mm.2	-1.61	0.0043
Casp4	TC0900000032.mm.2	-1.6	0.0039
Gnal	TC1800000694.mm.2	-1.59	0.0302
Ero1lb	TC1300000072.mm.2	-1.58	0.0318
Hsd3b6	TC0300002561.mm.2	-1.57	0.0034
Gm3047	TC1400000027.mm.2	-1.57	0.0061
Olfr1311	TC0200004339.mm.2	-1.57	0.0129
Dnmt3b	TC0200002318.mm.2	-1.55	0.0115
Gbp2	TC0300001447.mm.2	-1.55	0.0295
Fam188a	TC0200002974.mm.2	-1.55	0.0465
Serpini2	TC0300002166.mm.2	-1.54	0.0253
Fbxw25	TC0900003092.mm.2	-1.54	0.0383
Vmn1r222	TC1300001618.mm.2	-1.52	0.0182
Creb5; 9430076C15Rik	TC0600000637.mm.2	-1.52	0.0228
Lctl	TC0900000809.mm.2	-1.52	0.0283
Fbxw15	TC0900003089.mm.2	-1.52	0.0361
Kansl1	TC1100003890.mm.2	-1.5	0.0047

Table 8. 'Unique' Dex-upregulated genes (FC>1.5; p<0.05) in SOX2 KO (n=7) NSPCs. 92 genes in total.

Gene Symbol	Affymetrix ID	SOX2 KO Fold Change	SOX2 KO P-value
Zbtb16	TC0900002241.mm.2	4.98	0.0000
Mertk	TC0200001935.mm.2	3.52	0.0014
Plagl1	TC1000000093.mm.2	3.31	0.0000
Chst2	TC0900002862.mm.2	2.77	0.0044
Nfkbia	TC1200001768.mm.2	2.73	0.0000
Kcnt1	TC0200000438.mm.2	2.45	0.0022
Rcan2	TC1700000839.mm.2	2.36	0.0188
Zhx3	TC0200005514.mm.2	2.35	0.0000
Nfkbiz	TC1600001742.mm.2	2.28	0.0049
Arhgap29	TC0300001240.mm.2	2.27	0.0085
Fkbp14	TC0600002315.mm.2	2.15	0.0000
Gabra4	TC0500002563.mm.2	2.09	0.0015
Usp2	TC0900000497.mm.2	2.07	0.0001
Adm	TC0700001630.mm.2	2.06	0.0071
Pmp22	TC1100000822.mm.2	2.05	0.0045
Jade2	TC1100002702.mm.2	2.02	0.0003
Shisa6	TC1100002995.mm.2	1.96	0.0000
Paqr8	TC0100000129.mm.2	1.95	0.0021
Spsb1	TC0400004055.mm.2	1.95	0.0063
Chrm4	TC0200001392.mm.2	1.93	0.0000
Adrb2	TC1800001437.mm.2	1.93	0.0048
Smox	TC0200002018.mm.2	1.88	0.0004
Htr1b	TC0900002751.mm.2	1.88	0.0011
Pip4k2a	TC0200003051.mm.2	1.87	0.0000
Rapgef2	TC0300002188.mm.2	1.87	0.0001
Bcl6	TC1600001400.mm.2	1.87	0.0001
Csrnp1	TC0900003250.mm.2	1.81	0.0015
Timp4	TC0600002948.mm.2	1.79	0.0012
Usp54	TC1400001544.mm.2	1.78	0.0000
Trim9	TC1200001886.mm.2	1.76	0.0000
L3mbtl3	TC1000001913.mm.2	1.76	0.0002
Scgb3a2	TC1800000446.mm.2	1.75	0.0062
Actr3b	TC0500000238.mm.2	1.74	0.0001
Lyzl6	TC1100003877.mm.2	1.74	0.0011
Zim1	TC0700002216.mm.2	1.72	0.0150
Rb1	TC1400002382.mm.2	1.71	0.0084
9330159F19Rik	TC1000000264.mm.2	1.71	0.0255
Tnni3k	TC0300003181.mm.2	1.69	0.0029
Cdh20	TC0100000999.mm.2	1.68	0.0010
Nmnat2	TC0100001373.mm.2	1.68	0.0021
Lacc1	TC1400002454.mm.2	1.67	0.0013
Hs3st1	TC0500002297.mm.2	1.67	0.0124
Klf15	TC0600001074.mm.2	1.66	0.0008
Synpo2l	TC1400001546.mm.2	1.66	0.0037

Table 8 continued.

Gene Symbol	Affymetrix ID	SOX2 KO Fold Change	SOX2 KO P-value
Gm13547	TC0200000509.mm.2	1.66	0.0050
Olfm2	TC0900001845.mm.2	1.65	0.0012
Ftcd	TC1000000746.mm.2	1.64	0.0012
Jdp2	TC1200000837.mm.2	1.64	0.0099
Hbb-bh1	TC0700003912.mm.2	1.64	0.0411
Ezr	TC1700001390.mm.2	1.64	0.0469
Olfr870	TC0900001829.mm.2	1.63	0.0049
Gm20939	TC1700001345.mm.2	1.63	0.0159
Lnpep	TC1700001516.mm.2	1.62	0.0008
Olfr1437	TC1900001162.mm.2	1.62	0.0242
Sik1	TC1700001827.mm.2	1.61	0.0049
Lrrc8a	TC0200005466.mm.2	1.60	0.0091
Agmo	TC1200000334.mm.2	1.60	0.0129
Poln; Haus3	TC0500002229.mm.2	1.60	0.0145
Rhoj	TC1200000664.mm.2	1.60	0.0257
Mxd4	TC0500002231.mm.2	1.59	0.0000
Mt1	TC0800001095.mm.2	1.59	0.0004
Zfp189	TC0400000552.mm.2	1.59	0.0008
Olfr191	TC1600001789.mm.2	1.59	0.0013
Ccdc79	TC0800002803.mm.2	1.59	0.0051
Unc5a	TC1300000643.mm.2	1.59	0.0133
Mrgprx1	TC0700003061.mm.2	1.58	0.0009
Prr16	TC1800000516.mm.2	1.58	0.0031
Pik3r1	TC1300002553.mm.2	1.56	0.0021
Tnpo1	TC1300002510.mm.2	1.56	0.0036
Dlg5	TC1400001573.mm.2	1.56	0.0230
Plekhf2	TC0400002198.mm.2	1.55	0.0014
Camsap2	TC0100003146.mm.2	1.55	0.0061
Fzd1	TC0500001896.mm.2	1.55	0.0317
Sap30	TC0800002252.mm.2	1.54	0.0007
Ip6k2	TC0900001422.mm.2	1.54	0.0012
Kcnh2	TC0500002073.mm.2	1.54	0.0019
Aym1	TC0500001202.mm.2	1.54	0.0154
Baiap2	TC1100002015.mm.2	1.54	0.0216
4921511C20Rik	TC0X00001246.mm.2	1.54	0.0316
Nxpe3	TC1600001743.mm.2	1.53	0.0005
Tmbim7	TC0500000017.mm.2	1.53	0.0021
Hspb1	TC0500001590.mm.2	1.53	0.0164
Ctgf	TC1000000215.mm.2	1.52	0.0208
Tnfrsf21	TC1700000829.mm.2	1.52	0.0246
Ak3	TC1900001336.mm.2	1.51	0.0058
Endod1	TC0900001768.mm.2	1.51	0.0068
Prh1	TC0600001557.mm.2	1.51	0.0162
Nanog	TC0600001391.mm.2	1.51	0.0191
1110007C09Rik	TC1300001954.mm.2	1.51	0.0469
Sycp3	TC1000001081.mm.2	1.50	0.0025
Phyhd1	TC0200005467.mm.2	1.23	0.0150

Table 9. 'Unique' Dex-downregulated genes (FC≤ 1.5; p<0.05) in SOX2 KO (n=7) NSPCs. 52 genes in total.

Gene Symbol	Affymetrix ID	SOX2 KO Fold Change	SOX2 KO P-value
TC1300000607.mm.3	TC1300000607.mm.2	-1.83	0.0068
Lgi2	TC0500002411.mm.2	-1.8	0.0054
Prrx1	TC0100003409.mm.2	-1.79	0.0006
Gm4988	TC0X00000563.mm.2	-1.79	0.0219
Slc6a9	TC0400004192.mm.2	-1.78	0.0083
Stard9	TC0200001798.mm.2	-1.78	0.0295
Deptor	TC1500000392.mm.2	-1.74	0.0043
Ccnjl	TC1100000428.mm.2	-1.72	0.0335
Dmrta1	TC0400000918.mm.2	-1.71	0.0042
Pde1b	TC1500001133.mm.2	-1.69	0.0022
Skint1	TC0400001194.mm.2	-1.67	0.0227
Bend3	TC1000000399.mm.2	-1.66	0.0140
BC035044	TC0600003216.mm.2	-1.65	0.0008
Sod3	TC0500000527.mm.2	-1.64	0.0346
Slitrk2	TC0X00000596.mm.2	-1.62	0.0093
Prrg4	TC0200004251.mm.2	-1.62	0.0396
Npas4	TC1900000944.mm.2	-1.61	0.0219
Gdf9	TC1100000604.mm.2	-1.61	0.0413
Fhl3	TC0400001419.mm.2	-1.59	0.0022
Triml2	TC0800000501.mm.2	-1.59	0.0147
Dgki	TC0600002084.mm.2	-1.59	0.0270
Lpar1	TC0400002737.mm.2	-1.58	0.0314
Dact1	TC1200000608.mm.2	-1.57	0.0080
Cpne8	TC1500002067.mm.2	-1.57	0.0112
Stk26	TC0X00000454.mm.2	-1.57	0.0246
Myh8	TC1100000856.mm.2	-1.57	0.0350
Muc13	TC1600000479.mm.2	-1.56	0.0025
Cd36	TC0500001992.mm.2	-1.56	0.0033
Sema6a	TC1800001312.mm.2	-1.56	0.0238
Vmn1r163; Vmn1r135	TC0700000333.mm.2	-1.55	0.0009
Vmn1r135; Vmn1r163	TC0700000346.mm.2	-1.55	0.0009
Olfr1286	TC0200004322.mm.2	-1.55	0.0265
Cgref1	TC0500002168.mm.2	-1.54	0.0055
Rpusd2	TC0200001756.mm.2	-1.54	0.0219
Phlda1	TC1000001301.mm.2	-1.54	0.0233
St6galnac5	TC0300003150.mm.2	-1.54	0.0274
Irf2bpl	TC1200002110.mm.2	-1.53	0.0061
Esrrg	TC0100001806.mm.2	-1.53	0.0183
Olfr596	TC0700001488.mm.2	-1.52	0.0206
Has2	TC1500001548.mm.2	-1.52	0.0237
Pccb	TC0900002942.mm.2	-1.52	0.0350
Tmeff2	TC0100000364.mm.2	-1.52	0.0435
Slco1a6	TC0600003369.mm.2	-1.52	0.0446
Gm2916	TC1400000015.mm.2	-1.51	0.0042
Xrcc6bp1	TC1000003090.mm.2	-1.51	0.0063
R3hdm4	TC1000002485.mm.2	-1.5	0.0057
Akr1c19	TC1300000020.mm.2	-1.5	0.0080
1700020N01Rik	TC1000000169.mm.2	-1.5	0.0083
Nat8l	TC0500000366.mm.2	-1.5	0.0140
Efnb1	TC0X00000934.mm.2	-1.5	0.0146
Irak4	TC1500000932.mm.2	-1.5	0.0237
Cnih3	TC0100001734.mm.2	-1.5	0.0493

Table 10. WT/KO 'Shared' Dex-response genes or 'WT Unique' Dex-response genes (p<0.05) with a GR binding site located proximally (+/- 10kb) near the gene TSS

Gene Group	Total Genes	# GR Binding Site(s) Proximal to Gene(s)
WT Unique Upregulated	59	5
WT Unique Downregulated	33	1
Shared Upregulated	31	32
Shared Downregulated	1	0

4.3.4 SOX2 is critically involved in canonical GC-responsive signaling pathways

A comparison of gene expression patterns in WT vs SOX2 KO NSPCs highlights alterations in the Dex-responsive trending gene responses, determined by fold change of average expression, involved in canonical glucocorticoid signaling pathways (**Figure 30**). Similar trends are seen in canonical FGF signaling pathways (**Figure 28**). Both of these pathways are critical regulators of NSPC pluripotency and neuronal maturation during neurodevelopment[7,10,358].

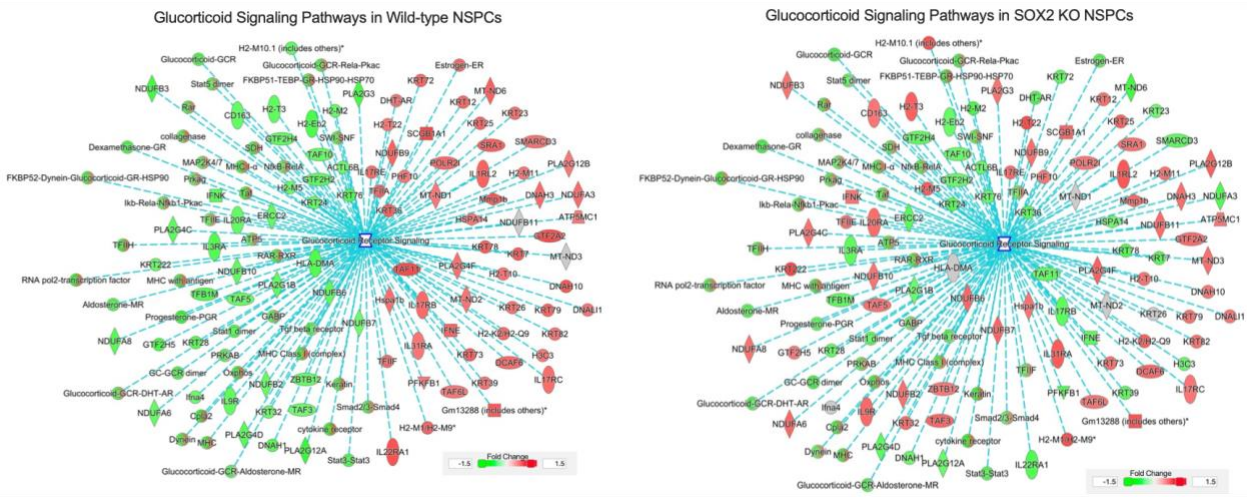

Figure 27. Ingenituy Pathway Analysis (IPA) software predits cannonical GC signaling pathway activation or repression by Dex

F30 Legend: Genes involved in canonical glucocorticoid signaling pathways which are upregulated (Red; FC > 0) or downregulated (Green; FC < 0) by Dex at 4h in WT NSPCs (left) or SOX2 KO NSPCs (right).

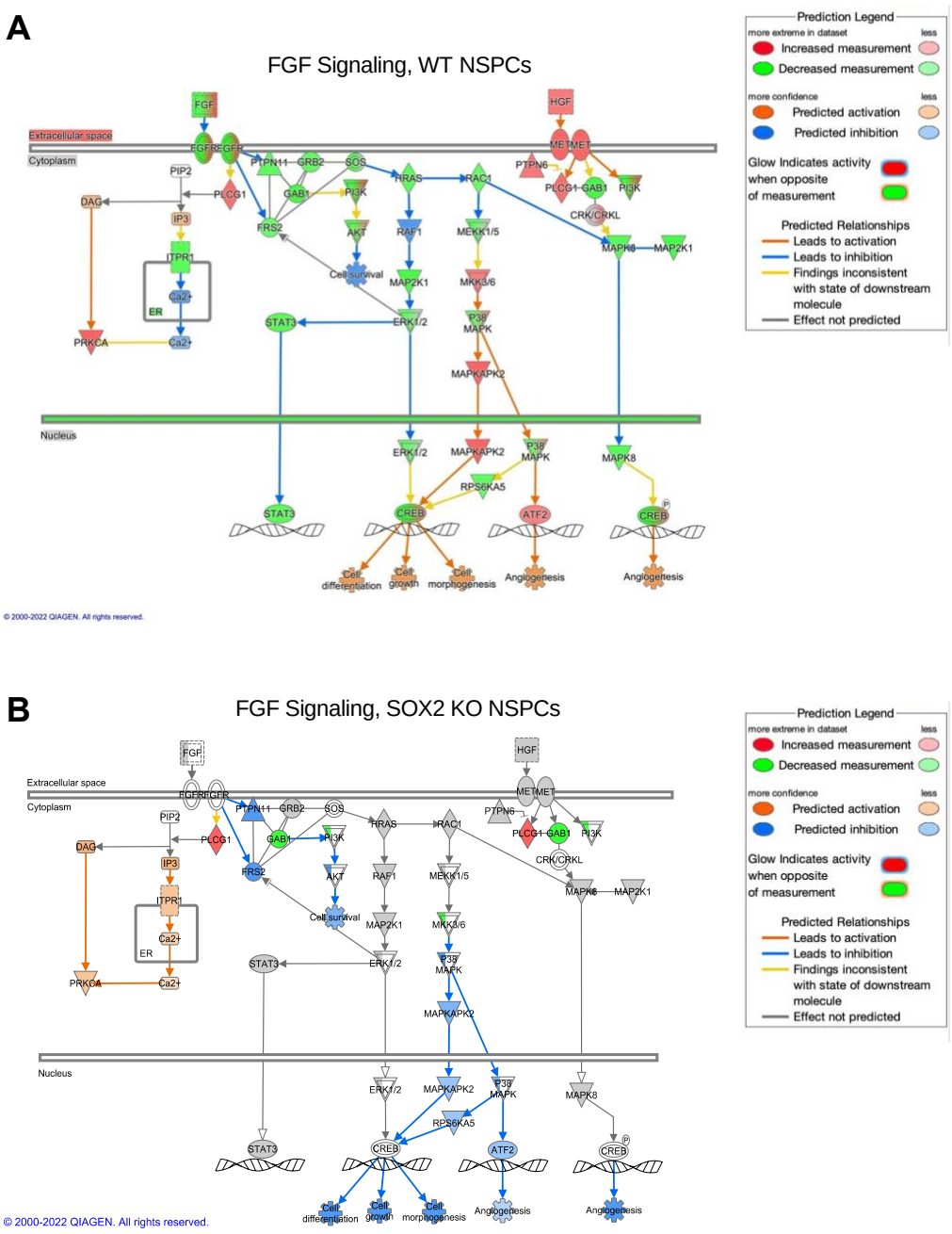

Figure 28. Ingenituy Pathway Analysis (IPA) software predits cannonical FGF signaling pathway activation or repression by Dex

Figure 31 Legend: Canonical FGF signaling pathways in (A) Dex-treated wild-type (WT) NSPCs (n=6) or (B) Dex-treated SOX2 KO NSPCs (n=7). Node color indicates the Dex-responsive gene responses, (see prediction legend) determined by fold change of average expression and/or predicted change by Qiagen IPA software.

4.3.5 Dex-responsive canonical signaling pathways predicted to be differentially activated in WT vs SOX2 KO NSPCs

Using the unfiltered list of genes in vehicle- or Dex-treated WT and SOX2 KO NSPCs (P0) identified by microarray, we utilized IPA software to perform canonical pathway analyses to predict clusters of biological functions that increase or decrease in response to Dex (**Figure 32**). While all listed biological functions do not occur in the brain-derived cell types, those which are prevalent in the CNS may be biologically relevant. For example, SOX2 may be critically involved in restricting activation of endocannabinoid neural synapse formation and dendritic cell maturation, since SOX2 ablation results in Dex-mediated activations of these pathways. As essential regulators of fetal brain development, both SOX2 and endocannabinoids[359] (i.e. anandamide (AEA) and 2-arachidonoylglycerol (2-AG)) influence GR action[24] to direct key neurodevelopmental processes, posing the question of whether interplay exists between all three factors during specific developmental time periods.

Figure 29. Canonical Pathway Analysis of Dex-regulated genes in WT vs SOX2 KO

Figure 32 Legend: Biological functions in various types. Predicted Dex-responsive pathway activation (z-score; indicated by color index) for each biological function is shown on the heat map. WT; left column. SOX2 KO; right column.

4.4 Discussion

PLA data obtained in **Aim 3** support the bioinformatic-informed prediction, based upon data collected in **Aim 2**, of GR and SOX2 interacting within NSPC nuclei to coordinate genomic responses to GR activation. Microarray gene expression data support this possibility because a subset of GC-regulated genes had differential transcriptional outcomes dependant upon the presence of SOX2 (i.e. WT Unique genes; **Figure 26**). It is important to note that all gene expression measurements are relative due to variability in technical factors such as probe hybridization rates, input DNA volume, and the application process[360]. Taking this into consideration, a gene was only considered as 'Shared' or 'Unique' Dex-regulated ($p<0.05$) if the

fold change value was drastic (FC ≥1.5 or FC≤ 1.5). Because the SOX2 cistrome shifts from pluripotency enhancers to neural enhancers during differentiation[344], these genes may vary in NSPCs derived from the P0 vs E14.5 mouse brains. Nonetheless, this approach allows an assessment of whether SOX2 plays a role in determining the selectivity of GR action in NSPCs.

The fact that the number of Dex-regulated genes in NSPCs is dramatically increased upon SOX2 ablation (**Figure 25**) suggests that the presence of SOX2 is required to restrict GR access to a subset of developmentally relevant genes perhaps through the regulation of long-range chromatin looping by SOX2[269]. Another possible explanation is that SOX2 directly antagonizes GR action, and SOX2 loss results in a de-repression of GR responsiveness. Genes with a 'shared' Dex response were not impacted by the global loss of chromatin connectivity resulting from SOX2 ablation, or by the removal of SOX2 as a GR cofactor, pointing to a smaller subset of GR action that occurs independently of SOX2 (**Figure 26**). A limitation of this study is that we cannot discriminate between SOX2 acting as a GR cofactor from SOX2 acting as a mediator of enhancer-promoter connectivity at GR target genes. Future experiments that combine ChIP-seq with ChiA-PET technology to characterize 3D chromatin connectivity in response to Dex in wild-type and SOX2 KO NSPCs may better define a mechanism by which SOX2 modulates select GR-responsive genes in NSPCs. These data will also determine if SOX2 differentially regulates GC activation vs repression of target genes via chromatin loop restructuring. Alternatively, genome wide ChIP-seq profiling of histone acetyltransferases (HATs) and histone deacetylases (HDACs) in wild-type and SOX2 KO animals can profile site-specific, SOX-initiated recruitment of transcriptional co-activators (e.g., HATs) or corepressors (e.g., HDACs) to GR-bound transcriptional enhancers.

A remaining question is whether the SOX2-dependent GC transcriptome controls NSPC cell fate and laminar specification. Knowledge of chromatin connectivity and the SOX2 cistrome could allow the identification of neural-determinant genes whose expression is downregulated following *Sox2* ablation (i.e., *Fos*, *Jun*, *Socs3)* that are co-occupied by GR and SOX2 at connected distal enhancers[269,361]. In this case, excess sGC exposure may have the potential to influence cell fate by modifying enhancer-driven transcription of these critical neural-determinant genes. This may occur in the GR/SOX2 co-expressing neural cell types of the developing telencephalon. These include radial glial cells with potential to self-replicate or generate neural and/or glial progeny (primarily localized to the VZ), and neural progenitor populations with neurogenic potential (primarily localized to the SVZ and the hippocampus dentate gyrus) [213,320,329,362].

4.5 Summary

(i) GR and SOX2 co-localize (<40nm) in nuclear space.

(ii) A subset of GR transcriptional action occurs independently of SOX2, although a larger proportion of the GC transcriptome is dependent upon SOX2 presence.

(iii) Future experiments that profile the 3D chromatin landscape will inform our interpretations of GR/SOX2 modalities at distal enhancer regions in NSPCs.

5.0 General Discussion

5.1 Summary of Findings

One of the major challenges in neurodevelopmental biology is to understand how gene regulatory networks are influenced by intrinsic and exogenous factors during critical cell state transitions and determine the mechanisms for transitions that dictate brain morphology and function. In this study, we generated genome-wide transcriptomic, chromatin accessibility, and DNA-protein binding data to build a comprehensive profile of the gene regulatory processes underlying the brain-specific response to antenatal sGC exposure. We found that the GC transcriptome is controlled by both cis-regulatory and distal-regulatory elements in fetal mouse telencephalon-derived NSPCs. GR binds preferentially to predetermined regions of accessible chromatin to influence gene programming and cell fate decisions[7]. In addition, we identify SOX2 as a TF that impacts the genomic response of select GR target genes in NSPCs to Dex, the fetal brain-accessible sGC widely used in pregnant women in preterm labor or at risk for preterm delivery.

5.2 Investigating GR and SOX2 Crosstalk

5.2.1 In the Central Nervous System

The impact of GR and SOX2 interactions on neurodevelopment could extend beyond the potential role of SOX2 as a transcriptional cofactor or pioneering factor for nuclear GR. For example, neuronal population size in the developing mouse cortex is increased by antenatal Dex *in vivo* (E17.5), accompanied by decreases in SOX2 expression in the proliferative zones (SVZ and VZ) as NSPCs progress towards a committed lineage[7,363]. This developmental stage-specific antagonism of SOX2 may have long-term consequences in NSPCs, because adult rats exposed to Dex *in-utero* display upregulated GR expression, attenuated SOX2 expression, and disordered NSPC function in the hippocampus, accompanied by increased depression susceptibility[364]. Considering that SOX2 deficiency or dysregulation has been associated with neurodevelopmental disorders, these models underscore the importance of understanding how fluctuating GC levels collide with spatiotemporally regulated SOX TF expression to direct NSPC function in embryos and adults [321,352].

Additional long-term consequences of antenatal sGC exposure are present in the PVN of the hypothalamus, the brain region containing neuroendocrine neurons. Specifically, BBB vascular density in the PVN is decreased in prepubertal mice[365] and the size of non-neuronal cell populations surrounding PVN vasculature is attenuated (i.e. decreased total number of astrocytes in adult females or decreased total number of pericytes in adult males)[366]. These studies also report depressive-like behavior in sGC-exposed offspring and suggest disruption in BBB components or neurovasculature may interfere with neural signaling of endocrine neurons in the PVN responsible for controlling HPA-axis responsiveness and stress reactivity[44]. Interestingly, SOX2 regulates

astrocytic and vascular development in the CNS[367] and is capable of reprogramming glial cells to neural progenitors in the adult brain[368,369]. Future initiatives may ask whether sGCs influence SOX2 action in neurovascular-related cell types in the PVN, leading to increased secretion of endogenous GCs and atypical developmental programming of HPA-axis responsivity.

While direct links between antenatal sGCs and long-term neurologic, cognitive or behavioral outcomes in humans remain unresolved, retrospective human population studies associate antenatal sGC therapy with higher rates of cerebral palsy in infants[370] , and neurosensory abnormalities and behavioral disorders in children, [131,132,149], whereas behavioral alterations, cognitive deficits, and risk for neuropsychiatric disorder are observed in adults exposed to sGCs during fetal development[167]. Strikingly, dysregulation of the HPA-axis is a primary long-term consequence of early sGC exposure or conditional *Sox2* ablation in animals, and is also a core pathophysiology of stress-related mental disorders such as depression, anxiety, anorexia nervosa, post-traumatic stress disorder, and schizophrenia in humans[371-377]. Similar health outcomes are observed in the offspring of prenatally stressed human mothers, independent of postnatal effects, identifying the prenatal period as highly sensitive to perturbations in GC signaling[378]. The role of SOX2 in directing GC action in humans remains to be elucidated.

Lastly, functional genetic variants that change the GC transcriptome are highly predictive of co-heritable CNS diseases[379]. It is unknown if genetic variants in SOX2 alter its dynamics at genomic loci that are anchors for enhancer-promoter chromatin loops controlling gene expression. Ambitious experimental endeavors may determine if distinct SOX2 polymorphisms result in altered GC transcriptional responses due to shifts in SOX2-mediated chromatin connectivity. Considering that corticosteroid therapy is at times recommend for persons with a CNS disease associated with SOX2 genetic polymorphisms or mutation (i.e. astrocytoma[380], high myopia[381],

visual system malformations, sensineuronal hearing loss[382-385]), these data may inform the health risks associated with corticosteroid therapy in persons with a distinct SOX2 polymorphism.

5.2.2 In Cancer Pathology

Beyond the scope of neurodevelopment and the HPA-axis, clues exist for SOX2 and GR crosstalk in cancer pathology. In human patient-derived glioblastoma multiforme (GBM) stem cells, SOX2 is a key mediator of cancer cell stemness[386] and is enriched at super enhancers[387]. In addition, higher SOX2 levels in tumor cells correlate with poorer outcomes[386]. Dex is used clinically to reduce tumor-associated edema, a neurological complication of GBM that compromises BBB integrity resulting in inflammation and neurologic symptoms[388]. Dex is also used as a chemosensitizer and an anti-proliferative agent[389]. However, a 2021 systematic review and meta-analysis of clinical data determined that the risk of death for GBM patients with tumor-associated edema increased by 48% if they were treated with Dex[390]. While some researchers suggest this is because Dex impairs the patient's anti-cancer immunity[388], another factor to examine is whether Dex accelerates cancer cell proliferation by modifying SOX2 TF activity in GBM stem cells. Thus, more recent attempts to develop therapeutic targets for GBM that focus on novel mediators of SOX2 signaling may be aided by an understanding of how non-genomic signaling molecules downstream of GR but upstream of SOX2 (e.g., ERK, PI3K/AKT/mTOR)[386,391] impact SOX2's ability to maintain the undifferentiated GBM stem cell identity. The discovery of select GR ligands that impact its potential nuclear interaction with SOX2 while limiting immunosuppressive and metabolic side effects may also prove therapeutic.

Studies in U2OS cells, a human bone osteosarcoma epithelial cell line, show ectopic expression of SOX2 prevents proper formation of GR nuclear condensates and modulates GR's

ability to bind DNA, resulting in altered transcriptional responses. These effects occurred independent of direct GR-SOX2 interactions, suggesting an indirect mechanism by which SOX2 controls GR function (e.g., other intermediate co-factors)[392]. However, the experimental paradigm used to assess GR nuclear localization and function in these studies (i.e., overexpressed or transiently expressed SOX2) may not reflect the nature of endogenous GR/SOX2 crosstalk in osteosarcoma leaving open the possibility that our results obtained with endogenous GR and SOX2 function in primary NSPC cultures may have relevance for the stem cell properties of tumors in humans.

5.3 Concluding Remarks

In summary, excess sGCs have the potential to alter GR transcriptional responses by acting upon a developmentally regulated chromatin landscape to influence the fate of NSPC populations and, ultimately, may contribute to a cascade of biological changes leading to adverse neurologic outcomes[373]. Our genomic data may advise human longitudinal follow-up studies to monitor the development of psychiatric diseases with a SOX2-related etiology such as depression and anxiety[364,393], intellectual disability[394,395], epilepsy[330], schizophrenia and bipolar disorder[270], or motor deficits in children and adults exposed to sGCs *in-utero*[333]. The continuation of this work could ultimately inform safe clinical applications of sGCs, a life preserving therapeutic for preterm infants, which are administered to pregnant women prior to delivery.

Bibliography

1 ACOG committee opnion: antenatal corticosteroid therapy for fetal maturation. *Obstetrics and gynecology* **99**, 871-873 (2002).

2 Liggins, G. C. & Howie, R. N. A controlled trial of antepartum glucocorticoid treatment for prevention of the respiratory distress syndrome in premature infants. *Pediatrics* **50**, 515-525 (1972).

3 Antonow-Schlorke, I. *et al.* Adverse effects of antenatal glucocorticoids on cerebral myelination in sheep. *Obstetrics and gynecology* **113**, 142-151, doi:10.1097/AOG.0b013e3181924d3b (2009).

4 Cheong, J. L. *et al.* Association Between Moderate and Late Preterm Birth and Neurodevelopment and Social-Emotional Development at Age 2 Years. *JAMA pediatrics* **171**, e164805, doi:10.1001/jamapediatrics.2016.4805 (2017).

5 Franca, M. S. *et al.* Neonatal neuronal apoptosis after betamethasone administration in pregnant Wistar rats. *The journal of maternal-fetal & neonatal medicine : the official journal of the European Association of Perinatal Medicine, the Federation of Asia and Oceania Perinatal Societies, the International Society of Perinatal Obstet* **29**, 1089-1093, doi:10.3109/14767058.2015.1035639 (2016).

6 Tijsseling, D. *et al.* Effects of antenatal glucocorticoid therapy on hippocampal histology of preterm infants. *PloS one* **7**, e33369, doi:10.1371/journal.pone.0033369 (2012).

7 Tsiarli, M. A. *et al.* Antenatal dexamethasone exposure differentially affects distinct cortical neural progenitor cells and triggers long-term changes in murine cerebral architecture and behavior. *Translational psychiatry* **7**, e1153, doi:10.1038/tp.2017.65 (2017).

8 Uno, H. *et al.* Brain damage induced by prenatal exposure to dexamethasone in fetal rhesus macaques. I. Hippocampus. *Brain Res Dev Brain Res* **53**, 157-167, doi:10.1016/0165-3806(90)90002-g (1990).

9 Damsted, S. K., Born, A. P., Paulson, O. B. & Uldall, P. Exogenous glucocorticoids and adverse cerebral effects in children. *Eur J Paediatr Neurol* **15**, 465-477, doi:10.1016/j.ejpn.2011.05.002 (2011).

10 Frahm, K. A. *et al.* A comparison of the sexually dimorphic dexamethasone transcriptome in mouse cerebral cortical and hypothalamic embryonic neural stem cells. *Mol Cell Endocrinol* **471**, 42-50, doi:10.1016/j.mce.2017.05.026 (2018).

11 Forrest, M. P. *et al.* Open Chromatin Profiling in hiPSC-Derived Neurons Prioritizes Functional Noncoding Psychiatric Risk Variants and Highlights Neurodevelopmental Loci. *Cell Stem Cell* **21**, 305-318 e308, doi:10.1016/j.stem.2017.07.008 (2017).

12 Larrigan, S., Shah, S., Fernandes, A. & Mattar, P. Chromatin Remodeling in the Brain-a NuRDevelopmental Odyssey. *Int J Mol Sci* **22**, doi:10.3390/ijms22094768 (2021).

13 Markenscoff-Papadimitriou, E. *et al.* A Chromatin Accessibility Atlas of the Developing Human Telencephalon. *Cell* **182**, 754-769 e718, doi:10.1016/j.cell.2020.06.002 (2020).

14 Trevino, A. E. *et al.* Chromatin accessibility dynamics in a model of human forebrain development. *Science* **367**, doi:10.1126/science.aay1645 (2020).

15 Kempfer, R. & Pombo, A. Methods for mapping 3D chromosome architecture. *Nat Rev Genet* **21**, 207-226, doi:10.1038/s41576-019-0195-2 (2020).

16 Weikum, E. R., Knuesel, M. T., Ortlund, E. A. & Yamamoto, K. R. Glucocorticoid receptor control of transcription: precision and plasticity via allostery. *Nat Rev Mol Cell Biol* **18**, 159-174, doi:10.1038/nrm.2016.152 (2017).

17 John, S. *et al.* Chromatin accessibility pre-determines glucocorticoid receptor binding patterns. *Nat Genet* **43**, 264-268, doi:10.1038/ng.759 (2011).

18 McDowell, I. C. *et al.* Glucocorticoid receptor recruits to enhancers and drives activation by motif-directed binding. *Genome Res* **28**, 1272-1284, doi:10.1101/gr.233346.117 (2018).

19 Podobinska, M. *et al.* Epigenetic Modulation of Stem Cells in Neurodevelopment: The Role of Methylation and Acetylation. *Front Cell Neurosci* **11**, 23, doi:10.3389/fncel.2017.00023 (2017).

20 Johnson, T. A. *et al.* Conventional and pioneer modes of glucocorticoid receptor interaction with enhancer chromatin in vivo. *Nucleic Acids Res* **46**, 203-214, doi:10.1093/nar/gkx1044 (2018).

21 Johnson, T. A., Paakinaho, V., Kim, S., Hager, G. L. & Presman, D. M. Genome-wide binding potential and regulatory activity of the glucocorticoid receptor's monomeric and dimeric forms. *Nat Commun* **12**, 1987, doi:10.1038/s41467-021-22234-9 (2021).

22 Oakley, R. H. & Cidlowski, J. A. The biology of the glucocorticoid receptor: new signaling mechanisms in health and disease. *J Allergy Clin Immunol* **132**, 1033-1044, doi:10.1016/j.jaci.2013.09.007 (2013).

23 Sacta, M. A., Chinenov, Y. & Rogatsky, I. Glucocorticoid Signaling: An Update from a Genomic Perspective. *Annu Rev Physiol* **78**, 155-180, doi:10.1146/annurev-physiol-021115-105323 (2016).

24 Franks, A. L., Berry, K. J. & DeFranco, D. B. Prenatal drug exposure and neurodevelopmental programming of glucocorticoid signalling. *J Neuroendocrinol* **32**, e12786, doi:10.1111/jne.12786 (2020).

25 McCormick, S. D. & Bradshaw, D. Hormonal control of salt and water balance in vertebrates. *Gen Comp Endocrinol* **147**, 3-8, doi:10.1016/j.ygcen.2005.12.009 (2006).

26 Yang, S. & Zhang, L. Glucocorticoids and vascular reactivity. *Curr Vasc Pharmacol* **2**, 1-12, doi:10.2174/1570161043476483 (2004).

27 Son, G. H., Cha, H. K., Chung, S. & Kim, K. Multimodal Regulation of Circadian Glucocorticoid Rhythm by Central and Adrenal Clocks. *J Endocr Soc* **2**, 444-459, doi:10.1210/js.2018-00021 (2018).

28 Ramamoorthy, S. & Cidlowski, J. A. Corticosteroids: Mechanisms of Action in Health and Disease. *Rheum Dis Clin North Am* **42**, 15-31, vii, doi:10.1016/j.rdc.2015.08.002 (2016).

29 Pariante, C. M. & Lightman, S. L. The HPA axis in major depression: classical theories and new developments. *Trends in neurosciences* **31**, 464-468, doi:10.1016/j.tins.2008.06.006 (2008).

30 Herman, J. P., McKlveen, J. M., Solomon, M. B., Carvalho-Netto, E. & Myers, B. Neural regulation of the stress response: glucocorticoid feedback mechanisms. *Brazilian journal of medical and biological research = Revista brasileira de pesquisas medicas e biologicas* **45**, 292-298 (2012).

31 Crowley, S. K. & Girdler, S. S. Neurosteroid, GABAergic and hypothalamic pituitary adrenal (HPA) axis regulation: what is the current state of knowledge in humans? *Psychopharmacology* **231**, 3619-3634, doi:10.1007/s00213-014-3572-8 (2014).

32 de Kloet, E. R., Joels, M. & Holsboer, F. Stress and the brain: from adaptation to disease. *Nat Rev Neurosci* **6**, 463-475, doi:10.1038/nrn1683 (2005).

33 Lupien, S. J., McEwen, B. S., Gunnar, M. R. & Heim, C. Effects of stress throughout the lifespan on the brain, behaviour and cognition. *Nat Rev Neurosci* **10**, 434-445, doi:10.1038/nrn2639 (2009).

34 Ulrich-Lai, Y. M. & Herman, J. P. Neural regulation of endocrine and autonomic stress responses. *Nature reviews. Neuroscience* **10**, 397-409, doi:10.1038/nrn2647 (2009).

35 Spiga, F., Walker, J. J., Terry, J. R. & Lightman, S. L. HPA axis-rhythms. *Comprehensive Physiology* **4**, 1273-1298, doi:10.1002/cphy.c140003 (2014).

36 Silverman, M. N. & Sternberg, E. M. Glucocorticoid regulation of inflammation and its functional correlates: from HPA axis to glucocorticoid receptor dysfunction. *Ann N Y Acad Sci* **1261**, 55-63, doi:10.1111/j.1749-6632.2012.06633.x (2012).

37 Reul, J. M. *et al.* Glucocorticoids, epigenetic control and stress resilience. *Neurobiol Stress* **1**, 44-59, doi:10.1016/j.ynstr.2014.10.001 (2015).

38 Morsi, A., DeFranco, D. & Witchel, S. F. The Hypothalamic-Pituitary-Adrenal Axis and the Fetus. *Horm Res Paediatr* **89**, 380-387, doi:10.1159/000488106 (2018).

39 Michael, A. E., Thurston, L. M. & Rae, M. T. Glucocorticoid metabolism and reproduction: a tale of two enzymes. *Reproduction* **126**, 425-441, doi:10.1530/rep.0.1260425 (2003).

40 Murphy, B. E. Human fetal serum cortisol levels related to gestational age: evidence of a midgestational fall and a steep late gestational rise, independent of sex or mode of delivery. *Am J Obstet Gynecol* **144**, 276-282, doi:10.1016/0002-9378(82)90579-8 (1982).

41 Ishimoto, H. & Jaffe, R. B. Development and function of the human fetal adrenal cortex: a key component in the feto-placental unit. *Endocr Rev* **32**, 317-355, doi:10.1210/er.2010-0001 (2011).

42 Togher, K. L. *et al.* Epigenetic regulation of the placental HSD11B2 barrier and its role as a critical regulator of fetal development. *Epigenetics* **9**, 816-822, doi:10.4161/epi.28703 (2014).

43 Carson, R., Monaghan-Nichols, A. P., DeFranco, D. B. & Rudine, A. C. Effects of antenatal glucocorticoids on the developing brain. *Steroids* **114**, 25-32, doi:10.1016/j.steroids.2016.05.012 (2016).

44 Moisiadis, V. G. & Matthews, S. G. Glucocorticoids and fetal programming part 2: Mechanisms. *Nat Rev Endocrinol* **10**, 403-411, doi:10.1038/nrendo.2014.74 (2014).

45 Hamada, H. & Matthews, S. G. Prenatal programming of stress responsiveness and behaviours: Progress and perspectives. *J Neuroendocrinol* **31**, e12674, doi:10.1111/jne.12674 (2019).

46 Klengel, T. & Binder, E. B. Epigenetics of Stress-Related Psychiatric Disorders and Gene x Environment Interactions. *Neuron* **86**, 1343-1357, doi:10.1016/j.neuron.2015.05.036 (2015).

47 Moisiadis, V. G. & Matthews, S. G. Glucocorticoids and fetal programming part 1: Outcomes. *Nat Rev Endocrinol* **10**, 391-402, doi:10.1038/nrendo.2014.73 (2014).

48 Rainey, W. E., Rehman, K. S. & Carr, B. R. The human fetal adrenal: making adrenal androgens for placental estrogens. *Semin Reprod Med* **22**, 327-336, doi:10.1055/s-2004-861549 (2004).

49 Johnston, Z. C. *et al.* The human fetal adrenal produces cortisol but no detectable aldosterone throughout the second trimester. *BMC Med* **16**, 23, doi:10.1186/s12916-018-1009-7 (2018).

50 Xu, E. H. & Lambert, M. H. Structural insights into regulation of nuclear receptors by ligands. *Nucl Recept Signal* **1**, e004, doi:10.1621/nrs.01004 (2003).

51 Weikum, E. R., Liu, X. & Ortlund, E. A. The nuclear receptor superfamily: A structural perspective. *Protein Sci* **27**, 1876-1892, doi:10.1002/pro.3496 (2018).

52 Vettorazzi, S., Nalbantoglu, D., Gebhardt, J. C. M. & Tuckermann, J. A guide to changing paradigms of glucocorticoid receptor function-a model system for genome regulation and physiology. *FEBS J* **289**, 5718-5743, doi:10.1111/febs.16100 (2022).

53 Joels, M., Sarabdjitsingh, R. A. & Karst, H. Unraveling the time domains of corticosteroid hormone influences on brain activity: rapid, slow, and chronic modes. *Pharmacological reviews* **64**, 901-938, doi:10.1124/pr.112.005892 (2012).

54 Groeneweg, F. L., Karst, H., de Kloet, E. R. & Joels, M. Mineralocorticoid and glucocorticoid receptors at the neuronal membrane, regulators of nongenomic corticosteroid signalling. *Mol Cell Endocrinol* **350**, 299-309, doi:10.1016/j.mce.2011.06.020 (2012).

55 Samarasinghe, R. A., Witchell, S. F. & DeFranco, D. B. Cooperativity and complementarity: synergies in non-classical and classical glucocorticoid signaling. *Cell Cycle* **11**, 2819-2827, doi:10.4161/cc.21018 (2012).

56 Dahiya, V. & Bagchi, G. Non-canonical androgen signaling pathways and implications in prostate cancer. *Biochim Biophys Acta Mol Cell Res* **1869**, 119357, doi:10.1016/j.bbamcr.2022.119357 (2022).

57 Zamagni, A., Cortesi, M., Zanoni, M. & Tesei, A. Non-nuclear AR Signaling in Prostate Cancer. *Front Chem* **7**, 651, doi:10.3389/fchem.2019.00651 (2019).

58 Bonaccorsi, L. *et al.* Prostate cancer: a model of integration of genomic and non-genomic effects of the androgen receptor in cell lines model. *Steroids* **73**, 1030-1037, doi:10.1016/j.steroids.2008.01.028 (2008).

59 Garg, D., Ng, S. S. M., Baig, K. M., Driggers, P. & Segars, J. Progesterone-Mediated Non-Classical Signaling. *Trends Endocrinol Metab* **28**, 656-668, doi:10.1016/j.tem.2017.05.006 (2017).

60 Bridgham, J. T. *et al.* Protein evolution by molecular tinkering: diversification of the nuclear receptor superfamily from a ligand-dependent ancestor. *PLoS biology* **8**, doi:10.1371/journal.pbio.1000497 (2010).

61 Lavery, D. N. & McEwan, I. J. Structure and function of steroid receptor AF1 transactivation domains: induction of active conformations. *Biochem J* **391**, 449-464, doi:10.1042/BJ20050872 (2005).

62 Trevino, L. S. & Weigel, N. L. Phosphorylation: a fundamental regulator of steroid receptor action. *Trends Endocrinol Metab* **24**, 515-524, doi:10.1016/j.tem.2013.05.008 (2013).

63 Kino, T. GR-regulating Serine/Threonine Kinases: New Physiologic and Pathologic Implications. *Trends Endocrinol Metab* **29**, 260-270, doi:10.1016/j.tem.2018.01.010 (2018).

64 Davies, T. H., Ning, Y. M. & Sanchez, E. R. A new first step in activation of steroid receptors: hormone-induced switching of FKBP51 and FKBP52 immunophilins. *J Biol Chem* **277**, 4597-4600, doi:10.1074/jbc.C100531200 (2002).

65 Picard, D. *et al.* Reduced levels of hsp90 compromise steroid receptor action in vivo. *Nature* **348**, 166-168, doi:10.1038/348166a0 (1990).

66 Mazaira, G. I., Echeverria, P. C. & Galigniana, M. D. Nucleocytoplasmic shuttling of the glucocorticoid receptor is influenced by tetratricopeptide repeat-containing proteins. *J Cell Sci* **133**, doi:10.1242/jcs.238873 (2020).

67 Aranda, A. & Pascual, A. Nuclear hormone receptors and gene expression. *Physiol Rev* **81**, 1269-1304, doi:10.1152/physrev.2001.81.3.1269 (2001).

68 Diamond, M. I., Miner, J. N., Yoshinaga, S. K. & Yamamoto, K. R. Transcription factor interactions: selectors of positive or negative regulation from a single DNA element. *Science* **249**, 1266-1272, doi:10.1126/science.2119054 (1990).

69 Cole, T. J. *et al.* Targeted disruption of the glucocorticoid receptor gene blocks adrenergic chromaffin cell development and severely retards lung maturation. *Genes Dev* **9**, 1608-1621, doi:10.1101/gad.9.13.1608 (1995).

70 Reichardt, H. M. *et al.* DNA binding of the glucocorticoid receptor is not essential for survival. *Cell* **93**, 531-541, doi:10.1016/s0092-8674(00)81183-6 (1998).

71 Kassel, O. *et al.* A nuclear isoform of the focal adhesion LIM-domain protein Trip6 integrates activating and repressing signals at AP-1- and NF-kappaB-regulated promoters. *Genes Dev* **18**, 2518-2528, doi:10.1101/gad.322404 (2004).

72 Newton, R., Leigh, R. & Giembycz, M. A. Pharmacological strategies for improving the efficacy and therapeutic ratio of glucocorticoids in inflammatory lung diseases. *Pharmacol Ther* **125**, 286-327, doi:10.1016/j.pharmthera.2009.11.003 (2010).

73 Uhlenhaut, N. H. *et al.* Insights into negative regulation by the glucocorticoid receptor from genome-wide profiling of inflammatory cistromes. *Mol Cell* **49**, 158-171, doi:10.1016/j.molcel.2012.10.013 (2013).

74 Datson, N. A. *et al.* Specific regulatory motifs predict glucocorticoid responsiveness of hippocampal gene expression. *Endocrinology* **152**, 3749-3757, doi:10.1210/en.2011-0287 (2011).

75 Ratman, D. *et al.* How glucocorticoid receptors modulate the activity of other transcription factors: a scope beyond tethering. *Mol Cell Endocrinol* **380**, 41-54, doi:10.1016/j.mce.2012.12.014 (2013).

76 Rosenfeld, M. G. & Glass, C. K. Coregulator codes of transcriptional regulation by nuclear receptors. *J Biol Chem* **276**, 36865-36868, doi:10.1074/jbc.R100041200 (2001).

77 Lim, H. W. *et al.* Genomic redistribution of GR monomers and dimers mediates transcriptional response to exogenous glucocorticoid in vivo. *Genome Res* **25**, 836-844, doi:10.1101/gr.188581.114 (2015).

78 Schiller, B. J., Chodankar, R., Watson, L. C., Stallcup, M. R. & Yamamoto, K. R. Glucocorticoid receptor binds half sites as a monomer and regulates specific target genes. *Genome Biol* **15**, 418, doi:10.1186/s13059-014-0418-y (2014).

79 Hudson, W. H. *et al.* Distal substitutions drive divergent DNA specificity among paralogous transcription factors through subdivision of conformational space. *Proc Natl Acad Sci U S A* **113**, 326-331, doi:10.1073/pnas.1518960113 (2016).

80 Sacta, M. A. *et al.* Gene-specific mechanisms direct glucocorticoid-receptor-driven repression of inflammatory response genes in macrophages. *Elife* **7**, doi:10.7554/eLife.34864 (2018).

81 Zhou, K., Gaullier, G. & Luger, K. Nucleosome structure and dynamics are coming of age. *Nat Struct Mol Biol* **26**, 3-13, doi:10.1038/s41594-018-0166-x (2019).

82 Babokhov, M., Hibino, K., Itoh, Y. & Maeshima, K. Local Chromatin Motion and Transcription. *J Mol Biol* **432**, 694-700, doi:10.1016/j.jmb.2019.10.018 (2020).

83 Shvedunova, M. & Akhtar, A. Modulation of cellular processes by histone and non-histone protein acetylation. *Nat Rev Mol Cell Biol* **23**, 329-349, doi:10.1038/s41580-021-00441-y (2022).

84 Love, M. I. *et al.* Role of the chromatin landscape and sequence in determining cell type-specific genomic glucocorticoid receptor binding and gene regulation. *Nucleic Acids Res* **45**, 1805-1819, doi:10.1093/nar/gkw1163 (2017).

85 D'Ippolito, A. M. *et al.* Pre-established Chromatin Interactions Mediate the Genomic Response to Glucocorticoids. *Cell Syst* **7**, 146-160 e147, doi:10.1016/j.cels.2018.06.007 (2018).

86 Natarajan, A., Yardimci, G. G., Sheffield, N. C., Crawford, G. E. & Ohler, U. Predicting cell-type-specific gene expression from regions of open chromatin. *Genome Res* **22**, 1711-1722, doi:10.1101/gr.135129.111 (2012).

87 Song, L. *et al.* Open chromatin defined by DNaseI and FAIRE identifies regulatory elements that shape cell-type identity. *Genome Res* **21**, 1757-1767, doi:10.1101/gr.121541.111 (2011).

88 Hoffman, J. A., Trotter, K. W., Ward, J. M. & Archer, T. K. BRG1 governs glucocorticoid receptor interactions with chromatin and pioneer factors across the genome. *Elife* **7**, doi:10.7554/eLife.35073 (2018).

89 Langlais, D., Couture, C., Balsalobre, A. & Drouin, J. The Stat3/GR interaction code: predictive value of direct/indirect DNA recruitment for transcription outcome. *Mol Cell* **47**, 38-49, doi:10.1016/j.molcel.2012.04.021 (2012).

90 Wiench, M. *et al.* DNA methylation status predicts cell type-specific enhancer activity. *EMBO J* **30**, 3028-3039, doi:10.1038/emboj.2011.210 (2011).

91 Burd, C. J. & Archer, T. K. Chromatin architecture defines the glucocorticoid response. *Mol Cell Endocrinol* **380**, 25-31, doi:10.1016/j.mce.2013.03.020 (2013).

92 Biddie, S. C. *et al.* Transcription factor AP1 potentiates chromatin accessibility and glucocorticoid receptor binding. *Mol Cell* **43**, 145-155, doi:10.1016/j.molcel.2011.06.016 (2011).

93 Carroll, J. S. *et al.* Chromosome-wide mapping of estrogen receptor binding reveals long-range regulation requiring the forkhead protein FoxA1. *Cell* **122**, 33-43, doi:10.1016/j.cell.2005.05.008 (2005).

94 Devine, J. H., Hewetson, A., Lee, V. H. & Chilton, B. S. After chromatin is SWItched-on can it be RUSHed? *Mol Cell Endocrinol* **151**, 49-56, doi:10.1016/s0303-7207(99)00013-1 (1999).

95 De Bosscher, K. *et al.* Glucocorticoids repress NF-kappaB-driven genes by disturbing the interaction of p65 with the basal transcription machinery, irrespective of coactivator levels in the cell. *Proc Natl Acad Sci U S A* **97**, 3919-3924, doi:10.1073/pnas.97.8.3919 (2000).

96 Rogatsky, I., Luecke, H. F., Leitman, D. C. & Yamamoto, K. R. Alternate surfaces of transcriptional coregulator GRIP1 function in different glucocorticoid receptor activation and repression contexts. *Proc Natl Acad Sci U S A* **99**, 16701-16706, doi:10.1073/pnas.262671599 (2002).

97 Luecke, H. F. & Yamamoto, K. R. The glucocorticoid receptor blocks P-TEFb recruitment by NFkappaB to effect promoter-specific transcriptional repression. *Genes Dev* **19**, 1116-1127, doi:10.1101/gad.1297105 (2005).

98 Nissen, R. M. & Yamamoto, K. R. The glucocorticoid receptor inhibits NFkappaB by interfering with serine-2 phosphorylation of the RNA polymerase II carboxy-terminal domain. *Genes Dev* **14**, 2314-2329, doi:10.1101/gad.827900 (2000).

99 McEwan, I. J. *et al.* The glucocorticoid receptor functions at multiple steps during transcription initiation by RNA polymerase II. *J Biol Chem* **269**, 25629-25636 (1994).

100 Chodankar, R., Wu, D. Y., Schiller, B. J., Yamamoto, K. R. & Stallcup, M. R. Hic-5 is a transcription coregulator that acts before and/or after glucocorticoid receptor genome occupancy in a gene-selective manner. *Proc Natl Acad Sci U S A* **111**, 4007-4012, doi:10.1073/pnas.1400522111 (2014).

101 Bernardo, G. M. & Keri, R. A. FOXA1: a transcription factor with parallel functions in development and cancer. *Biosci Rep* **32**, 113-130, doi:10.1042/BSR20110046 (2012).

102 He, H. H. *et al.* Differential DNase I hypersensitivity reveals factor-dependent chromatin dynamics. *Genome Res* **22**, 1015-1025, doi:10.1101/gr.133280.111 (2012).

103 Coutinho, A. E. & Chapman, K. E. The anti-inflammatory and immunosuppressive effects of glucocorticoids, recent developments and mechanistic insights. *Mol Cell Endocrinol* **335**, 2-13, doi:10.1016/j.mce.2010.04.005 (2011).

104 Ashwell, J. D., Lu, F. W. & Vacchio, M. S. Glucocorticoids in T cell development and function*. *Annu Rev Immunol* **18**, 309-345, doi:10.1146/annurev.immunol.18.1.309 (2000).

105 Lim, H. Y., Muller, N., Herold, M. J., van den Brandt, J. & Reichardt, H. M. Glucocorticoids exert opposing effects on macrophage function dependent on their concentration. *Immunology* **122**, 47-53, doi:10.1111/j.1365-2567.2007.02611.x (2007).

106 Stellato, C. Post-transcriptional and nongenomic effects of glucocorticoids. *Proc Am Thorac Soc* **1**, 255-263, doi:10.1513/pats.200402-015MS (2004).

107 Gold, P. W. The organization of the stress system and its dysregulation in depressive illness. *Mol Psychiatry* **20**, 32-47, doi:10.1038/mp.2014.163 (2015).

108 Sholter, D. E. & Armstrong, P. W. Adverse effects of corticosteroids on the cardiovascular system. *Can J Cardiol* **16**, 505-511 (2000).

109 Buchman, A. L. Side effects of corticosteroid therapy. *J Clin Gastroenterol* **33**, 289-294, doi:10.1097/00004836-200110000-00006 (2001).

110 Aljebab, F., Choonara, I. & Conroy, S. Systematic Review of the Toxicity of Long-Course Oral Corticosteroids in Children. *PloS one* **12**, e0170259, doi:10.1371/journal.pone.0170259 (2017).

111 Hains, A. B. & Arnsten, A. F. Molecular mechanisms of stress-induced prefrontal cortical impairment: implications for mental illness. *Learn Mem* **15**, 551-564, doi:10.1101/lm.921708 (2008).

112 Arnsten, A. F. Stress signalling pathways that impair prefrontal cortex structure and function. *Nat Rev Neurosci* **10**, 410-422, doi:10.1038/nrn2648 (2009).

113 Arnsten, A. F. Stress weakens prefrontal networks: molecular insults to higher cognition. *Nat Neurosci* **18**, 1376-1385, doi:10.1038/nn.4087 (2015).

114 Brown, E. S. & Chandler, P. A. Mood and Cognitive Changes During Systemic Corticosteroid Therapy. *Prim Care Companion J Clin Psychiatry* **3**, 17-21, doi:10.4088/pcc.v03n0104 (2001).

115 Yasir, M., Goyal, A. & Sonthalia, S. in *StatPearls* (2022).

116 Paragliola, R. M., Papi, G., Pontecorvi, A. & Corsello, S. M. Treatment with Synthetic Glucocorticoids and the Hypothalamus-Pituitary-Adrenal Axis. *International journal of molecular sciences* **18**, doi:10.3390/ijms18102201 (2017).

117 Aulakh, R. & Singh, S. Strategies for minimizing corticosteroid toxicity: a review. *Indian J Pediatr* **75**, 1067-1073, doi:10.1007/s12098-008-0211-6 (2008).

118 Sarabdjitsingh, R. A. *et al.* Disrupted corticosterone pulsatile patterns attenuate responsiveness to glucocorticoid signaling in rat brain. *Endocrinology* **151**, 1177-1186, doi:10.1210/en.2009-1119 (2010).

119 Ly, K. I. & Wen, P. Y. Clinical Relevance of Steroid Use in Neuro-Oncology. *Curr Neurol Neurosci Rep* **17**, 5, doi:10.1007/s11910-017-0713-6 (2017).

120 Dietrich, J., Rao, K., Pastorino, S. & Kesari, S. Corticosteroids in brain cancer patients: benefits and pitfalls. *Expert Rev Clin Pharmacol* **4**, 233-242, doi:10.1586/ecp.11.1 (2011).

121 Huang, J. *et al.* Immune Checkpoint in Glioblastoma: Promising and Challenging. *Front Pharmacol* **8**, 242, doi:10.3389/fphar.2017.00242 (2017).

122 *Preterm Birth*, <https://www.cdc.gov/reproductivehealth/maternalinfanthealth/pretermbirth.htm> (2018).

123 *Infant Mortality*, <https://www.cdc.gov/reproductivehealth/maternalinfanthealth/infantmortality.htm> (2019).

124 Jobe, A. H. & Soll, R. F. Choice and dose of corticosteroid for antenatal treatments. *Am J Obstet Gynecol* **190**, 878-881, doi:10.1016/j.ajog.2004.01.044 (2004).

125 Audette, M. C., Challis, J. R., Jones, R. L., Sibley, C. P. & Matthews, S. G. Synthetic glucocorticoid reduces human placental system a transport in women treated with antenatal therapy. *J Clin Endocrinol Metab* **99**, E2226-2233, doi:10.1210/jc.2014-2157 (2014).

126 Morhart, P. *et al.* Influence of Timing of Antenatal Corticosteroid Administration on Morbidity of Preterm Neonates. *In Vivo* **36**, 1777-1784, doi:10.21873/invivo.12891 (2022).

127 Kapoor, A., Petropoulos, S. & Matthews, S. G. Fetal programming of hypothalamic-pituitary-adrenal (HPA) axis function and behavior by synthetic glucocorticoids. *Brain Res Rev* **57**, 586-595, doi:10.1016/j.brainresrev.2007.06.013 (2008).

128 Krozowski, Z. S. & Funder, J. W. Renal mineralocorticoid receptors and hippocampal corticosterone-binding species have identical intrinsic steroid specificity. *Proc Natl Acad Sci U S A* **80**, 6056-6060, doi:10.1073/pnas.80.19.6056 (1983).

129 Andrews, M. H. & Matthews, S. G. Regulation of glucocorticoid receptor mRNA and heat shock protein 70 mRNA in the developing sheep brain. *Brain Res* **878**, 174-182, doi:10.1016/s0006-8993(00)02735-9 (2000).

130 French, N. P., Hagan, R., Evans, S. F., Mullan, A. & Newnham, J. P. Repeated antenatal corticosteroids: effects on cerebral palsy and childhood behavior. *Am J Obstet Gynecol* **190**, 588-595, doi:10.1016/j.ajog.2003.12.016 (2004).

131 Raikkonen, K., Gissler, M. & Kajantie, E. Associations Between Maternal Antenatal Corticosteroid Treatment and Mental and Behavioral Disorders in Children. *JAMA* **323**, 1924-1933, doi:10.1001/jama.2020.3937 (2020).

132 Melamed, N. *et al.* Neurodevelopmental disorders among term infants exposed to antenatal corticosteroids during pregnancy: a population-based study. *BMJ Open* **9**, e031197, doi:10.1136/bmjopen-2019-031197 (2019).

133 Sotiriadis, A. *et al.* Neurodevelopmental Outcome After a Single Course of Antenatal Steroids in Children Born Preterm: A Systematic Review and Meta-analysis. *Obstetrics and gynecology* **125**, 1385-1396, doi:10.1097/AOG.0000000000000748 (2015).

134 Eriksson, L., Haglund, B., Ewald, U., Odlind, V. & Kieler, H. Short and long-term effects of antenatal corticosteroids assessed in a cohort of 7,827 children born preterm. *Acta Obstet Gynecol Scand* **88**, 933-938, doi:10.1080/00016340903111542 (2009).

135 Ishikawa, H. *et al.* The Effects of Antenatal Corticosteroids on Short- and Long-Term Outcomes in Small-for-Gestational-Age Infants. *Int J Med Sci* **12**, 295-300, doi:10.7150/ijms.11523 (2015).

136 Kuk, J. Y. *et al.* Optimal time interval between a single course of antenatal corticosteroids and delivery for reduction of respiratory distress syndrome in preterm twins. *Am J Obstet Gynecol* **209**, 256 e251-257, doi:10.1016/j.ajog.2013.06.020 (2013).

137 Haas, D. M., Sischy, A. C., McCullough, W. & Simsiman, A. J. Maternal ethnicity influences on neonatal respiratory outcomes after antenatal corticosteroid use for anticipated preterm delivery. *The journal of maternal-fetal & neonatal medicine : the official journal of the European Association of Perinatal Medicine, the Federation of Asia and Oceania Perinatal Societies, the International Society of Perinatal Obstet* **24**, 516-520, doi:10.3109/14767058.2010.506228 (2011).

138 Roberge, S. *et al.* Role of fetal sex in the outcome of antenatal glucocorticoid treatment to prevent respiratory distress syndrome: systematic review and meta-analysis. *J Obstet Gynaecol Can* **33**, 216-226, doi:10.1016/s1701-2163(16)34822-8 (2011).

139 Borowski, K. S. *et al.* Neonatal Genetic Variation in Steroid Metabolism and Key Respiratory Function Genes and Perinatal Outcomes in Single and Multiple Courses of Corticosteroids. *Am J Perinatol* **32**, 1126-1132, doi:10.1055/s-0035-1549217 (2015).

140 Spinillo, A. *et al.* Two-year infant neurodevelopmental outcome after single or multiple antenatal courses of corticosteroids to prevent complications of prematurity. *Am J Obstet Gynecol* **191**, 217-224, doi:10.1016/j.ajog.2003.12.023 (2004).

141 Jarjour, I. T. Neurodevelopmental outcome after extreme prematurity: a review of the literature. *Pediatric neurology* **52**, 143-152, doi:10.1016/j.pediatrneurol.2014.10.027 (2015).

142 Davis, E. P. *et al.* Effect of prenatal glucocorticoid treatment on size at birth among infants born at term gestation. *J Perinatol* **29**, 731-737, doi:10.1038/jp.2009.85 (2009).

143 Edelmann, M. N., Sandman, C. A., Glynn, L. M., Wing, D. A. & Davis, E. P. Antenatal glucocorticoid treatment is associated with diurnal cortisol regulation in term-born children. *Psychoneuroendocrinology* **72**, 106-112, doi:10.1016/j.psyneuen.2016.06.012 (2016).

144 Sarid, E. B., Stoopler, M. L., Morency, A. M. & Garfinkle, J. Neurological implications of antenatal corticosteroids on late preterm and term infants: a scoping review. *Pediatr Res*, doi:10.1038/s41390-022-02135-3 (2022).

145 Tao, S. *et al.* Associations between antenatal corticosteroid exposure and neurodevelopment in infants. *Am J Obstet Gynecol*, doi:10.1016/j.ajog.2022.05.060 (2022).

146 Battarbee, A. N. *et al.* Optimal timing of antenatal corticosteroid administration and preterm neonatal and early childhood outcomes. *Am J Obstet Gynecol MFM* **2**, 100077, doi:10.1016/j.ajogmf.2019.100077 (2020).

147 Modi, N. *et al.* The effects of repeated antenatal glucocorticoid therapy on the developing brain. *Pediatric research* **50**, 581-585, doi:10.1203/00006450-200111000-00008 (2001).

148 Ninan, K., Liyanage, S. K., Murphy, K. E., Asztalos, E. V. & McDonald, S. D. Evaluation of Long-term Outcomes Associated With Preterm Exposure to Antenatal Corticosteroids: A Systematic Review and Meta-analysis. *JAMA pediatrics* **176**, e220483, doi:10.1001/jamapediatrics.2022.0483 (2022).

149 Davis, E. P., Sandman, C. A., Buss, C., Wing, D. A. & Head, K. Fetal glucocorticoid exposure is associated with preadolescent brain development. *Biological psychiatry* **74**, 647-655, doi:10.1016/j.biopsych.2013.03.009 (2013).

150 Crowther, C. A. *et al.* Mid-Childhood Outcomes of Repeat Antenatal Corticosteroids: A Randomized Controlled Trial. *Pediatrics* **138**, doi:10.1542/peds.2016-0947 (2016).

151 Cartwright, R. D. *et al.* Association of Fetal Growth Restriction With Neurocognitive Function After Repeated Antenatal Betamethasone Treatment vs Placebo: Secondary Analysis of the ACTORDS Randomized Clinical Trial. *JAMA Netw Open* **2**, e187636, doi:10.1001/jamanetworkopen.2018.7636 (2019).

152 Miracle, X. *et al.* Guideline for the use of antenatal corticosteroids for fetal maturation. *J Perinat Med* **36**, 191-196, doi:10.1515/JPM.2008.032 (2008).

153 Asztalos, E. *et al.* Association between gestational age at birth, antenatal corticosteroids, and outcomes at 5 years: multiple courses of antenatal corticosteroids for preterm birth study at 5 years of age (MACS-5). *BMC Pregnancy Childbirth* **14**, 272, doi:10.1186/1471-2393-14-272 (2014).

154 Barker, D. J. & Thornburg, K. L. Placental programming of chronic diseases, cancer and lifespan: a review. *Placenta* **34**, 841-845, doi:10.1016/j.placenta.2013.07.063 (2013).

155 Ballard, P. L., Gluckman, P. D., Liggins, G. C., Kaplan, S. L. & Grumbach, M. M. Steroid and growth hormone levels in premature infants after prenatal betamethasone therapy to prevent respiratory distress syndrome. *Pediatr Res* **14**, 122-127, doi:10.1203/00006450-198002000-00011 (1980).

156 Parker, C. R., Jr., Atkinson, M. W., Owen, J. & Andrews, W. W. Dynamics of the fetal adrenal, cholesterol, and apolipoprotein B responses to antenatal betamethasone therapy. *Am J Obstet Gynecol* **174**, 562-565, doi:10.1016/s0002-9378(96)70428-3 (1996).

157 Ballard, P. L., Granberg, P. & Ballard, R. A. Glucocorticoid levels in maternal and cord serum after prenatal betamethasone therapy to prevent respiratory distress syndrome. *J Clin Invest* **56**, 1548-1554, doi:10.1172/JCI108236 (1975).

158 Davis, E. P. *et al.* Effects of prenatal betamethasone exposure on regulation of stress physiology in healthy premature infants. *Psychoneuroendocrinology* **29**, 1028-1036, doi:10.1016/j.psyneuen.2003.10.005 (2004).

159 Davis, E. P. *et al.* Antenatal betamethasone treatment has a persisting influence on infant HPA axis regulation. *J Perinatol* **26**, 147-153, doi:10.1038/sj.jp.7211447 (2006).

160 Schaffer, L., Luzi, F., Burkhardt, T., Rauh, M. & Beinder, E. Antenatal betamethasone administration alters stress physiology in healthy neonates. *Obstetrics and gynecology* **113**, 1082-1088, doi:10.1097/AOG.0b013e3181a1f0e6 (2009).

161 Ashwood, P. J. *et al.* Neonatal adrenal function after repeat dose prenatal corticosteroids: a randomized controlled trial. *Am J Obstet Gynecol* **194**, 861-867, doi:10.1016/j.ajog.2005.08.063 (2006).

162 Davis, E. P., Waffarn, F. & Sandman, C. A. Prenatal treatment with glucocorticoids sensitizes the hpa axis response to stress among full-term infants. *Dev Psychobiol* **53**, 175-183, doi:10.1002/dev.20510 (2011).

163 Grunau, R. E. *et al.* Neonatal procedural pain exposure predicts lower cortisol and behavioral reactivity in preterm infants in the NICU. *Pain* **113**, 293-300, doi:10.1016/j.pain.2004.10.020 (2005).

164 Grunau, R. E. *et al.* Neonatal pain, parenting stress and interaction, in relation to cognitive and motor development at 8 and 18 months in preterm infants. *Pain* **143**, 138-146, doi:10.1016/j.pain.2009.02.014 (2009).

165 Alexander, N. *et al.* Impact of antenatal synthetic glucocorticoid exposure on endocrine stress reactivity in term-born children. *J Clin Endocrinol Metab* **97**, 3538-3544, doi:10.1210/jc.2012-1970 (2012).

166 Alexander, N. *et al.* Impact of Antenatal Glucocorticoid Therapy and Risk of Preterm Delivery on Intelligence in Term-Born Children. *J Clin Endocrinol Metab* **101**, 581-589, doi:10.1210/jc.2015-2453 (2016).

167 Waffarn, F. & Davis, E. P. Effects of antenatal corticosteroids on the hypothalamic-pituitary-adrenocortical axis of the fetus and newborn: experimental findings and clinical considerations. *Am J Obstet Gynecol* **207**, 446-454, doi:10.1016/j.ajog.2012.06.012 (2012).

168 Doyle, L. W. Antenatal corticosteroids and outcomes into adulthood. *Paediatr Perinat Epidemiol* **36**, 640-642, doi:10.1111/ppe.12919 (2022).

169 Koutmani, Y. & Karalis, K. P. Neural stem cells respond to stress hormones: distinguishing beneficial from detrimental stress. *Front Physiol* **6**, 77, doi:10.3389/fphys.2015.00077 (2015).

170 Hauser, J. *et al.* Effects of prenatal dexamethasone treatment on postnatal physical, endocrine, and social development in the common marmoset monkey. *Endocrinology* **148**, 1813-1822, doi:10.1210/en.2006-1306 (2007).

171 Rodriguez, J. S. *et al.* Prenatal betamethasone exposure has sex specific effects in reversal learning and attention in juvenile baboons. *Am J Obstet Gynecol* **204**, 545 e541-510, doi:10.1016/j.ajog.2011.01.063 (2011).

172 Noorlander, C. W., Visser, G. H., Ramakers, G. M., Nikkels, P. G. & de Graan, P. N. Prenatal corticosteroid exposure affects hippocampal plasticity and reduces lifespan. *Dev Neurobiol* **68**, 237-246, doi:10.1002/dneu.20583 (2008).

173 Borges, S. *et al.* Dopaminergic modulation of affective and social deficits induced by prenatal glucocorticoid exposure. *Neuropsychopharmacology* **38**, 2068-2079, doi:10.1038/npp.2013.108 (2013).

174 Uno, H. *et al.* Neurotoxicity of glucocorticoids in the primate brain. *Horm Behav* **28**, 336-348, doi:10.1006/hbeh.1994.1030 (1994).

175 Sloboda, D. M., Moss, T. J., Gurrin, L. C., Newnham, J. P. & Challis, J. R. The effect of prenatal betamethasone administration on postnatal ovine hypothalamic-pituitary-adrenal function. *J Endocrinol* **172**, 71-81, doi:10.1677/joe.0.1720071 (2002).

176 de Vries, A. *et al.* Prenatal dexamethasone exposure induces changes in nonhuman primate offspring cardiometabolic and hypothalamic-pituitary-adrenal axis function. *J Clin Invest* **117**, 1058-1067, doi:10.1172/JCI30982 (2007).

177 Levitt, N. S., Lindsay, R. S., Holmes, M. C. & Seckl, J. R. Dexamethasone in the last week of pregnancy attenuates hippocampal glucocorticoid receptor gene expression and elevates blood pressure in the adult offspring in the rat. *Neuroendocrinology* **64**, 412-418, doi:10.1159/000127146 (1996).

178 Hauser, J., Feldon, J. & Pryce, C. R. Direct and dam-mediated effects of prenatal dexamethasone on emotionality, cognition and HPA axis in adult Wistar rats. *Horm Behav* **56**, 364-375, doi:10.1016/j.yhbeh.2009.07.003 (2009).

179 Braun, T. *et al.* Effects of maternal dexamethasone treatment in early pregnancy on pituitary-adrenal axis in fetal sheep. *Endocrinology* **150**, 5466-5477, doi:10.1210/en.2009-0086 (2009).

180 Sloboda, D. M. *et al.* Prenatal betamethasone exposure results in pituitary-adrenal hyporesponsiveness in adult sheep. *Am J Physiol Endocrinol Metab* **292**, E61-70, doi:10.1152/ajpendo.00270.2006 (2007).

181 Coe, C. L. & Lubach, G. R. Developmental consequences of antenatal dexamethasone treatment in nonhuman primates. *Neurosci Biobehav Rev* **29**, 227-235, doi:10.1016/j.neubiorev.2004.10.003 (2005).

182 Banjanin, S., Kapoor, A. & Matthews, S. G. Prenatal glucocorticoid exposure alters hypothalamic-pituitary-adrenal function and blood pressure in mature male guinea pigs. *J Physiol* **558**, 305-318, doi:10.1113/jphysiol.2004.063669 (2004).

183 Dunn, E., Kapoor, A., Leen, J. & Matthews, S. G. Prenatal synthetic glucocorticoid exposure alters hypothalamic-pituitary-adrenal regulation and pregnancy outcomes in mature female guinea pigs. *J Physiol* **588**, 887-899, doi:10.1113/jphysiol.2009.182139 (2010).

184 van der Merwe, J. L., Sacco, A., Toelen, J. & Deprest, J. Long-term neuropathological and/or neurobehavioral effects of antenatal corticosteroid therapy in animal models: a systematic review. *Pediatr Res* **87**, 1157-1170, doi:10.1038/s41390-019-0712-1 (2020).

185 Rodrigues, A. J. *et al.* Mechanisms of initiation and reversal of drug-seeking behavior induced by prenatal exposure to glucocorticoids. *Mol Psychiatry* **17**, 1295-1305, doi:10.1038/mp.2011.126 (2012).

186 Hiroi, R., Carbone, D. L., Zuloaga, D. G., Bimonte-Nelson, H. A. & Handa, R. J. Sex-dependent programming effects of prenatal glucocorticoid treatment on the developing serotonin system and stress-related behaviors in adulthood. *Neuroscience* **320**, 43-56, doi:10.1016/j.neuroscience.2016.01.055 (2016).

187 Muneoka, K. *et al.* Prenatal dexamethasone exposure alters brain monoamine metabolism and adrenocortical response in rat offspring. *Am J Physiol* **273**, R1669-1675, doi:10.1152/ajpregu.1997.273.5.R1669 (1997).

188 Oliveira, M. *et al.* Programming effects of antenatal corticosteroids exposure in male sexual behavior. *J Sex Med* **8**, 1965-1974, doi:10.1111/j.1743-6109.2010.02170.x (2011).

189 Hosp, J. A. & Luft, A. R. Dopaminergic meso-cortical projections to m1: role in motor learning and motor cortex plasticity. *Front Neurol* **4**, 145, doi:10.3389/fneur.2013.00145 (2013).

190 Holson, R. R., Gough, B., Sullivan, P., Badger, T. & Sheehan, D. M. Prenatal dexamethasone or stress but not ACTH or corticosterone alter sexual behavior in male rats. *Neurotoxicol Teratol* **17**, 393-401, doi:10.1016/0892-0362(94)00074-n (1995).

191 Welberg, L. A., Seckl, J. R. & Holmes, M. C. Prenatal glucocorticoid programming of brain corticosteroid receptors and corticotrophin-releasing hormone: possible implications for behaviour. *Neuroscience* **104**, 71-79, doi:10.1016/s0306-4522(01)00065-3 (2001).

192 Oliveira, M. *et al.* Induction of a hyperanxious state by antenatal dexamethasone: a case for less detrimental natural corticosteroids. *Biol Psychiatry* **59**, 844-852, doi:10.1016/j.biopsych.2005.08.020 (2006).

193 Nagano, M., Liu, M., Inagaki, H., Kawada, T. & Suzuki, H. Early intervention with fluoxetine reverses abnormalities in the serotonergic system and behavior of rats exposed prenatally to dexamethasone. *Neuropharmacology* **63**, 292-300, doi:10.1016/j.neuropharm.2012.03.027 (2012).

194 Diaz Heijtz, R., Fuchs, E., Feldon, J., Pryce, C. R. & Forssberg, H. Effects of antenatal dexamethasone treatment on glucocorticoid receptor and calcyon gene expression in the prefrontal cortex of neonatal and adult common marmoset monkeys. *Behav Brain Funct* **6**, 18, doi:10.1186/1744-9081-6-18 (2010).

195 Vinukonda, G. *et al.* Effect of prenatal glucocorticoids on cerebral vasculature of the developing brain. *Stroke* **41**, 1766-1773, doi:10.1161/STROKEAHA.110.588400 (2010).

196 Sundberg, M., Savola, S., Hienola, A., Korhonen, L. & Lindholm, D. Glucocorticoid hormones decrease proliferation of embryonic neural stem cells through ubiquitin-mediated degradation of cyclin D1. *J Neurosci* **26**, 5402-5410, doi:10.1523/JNEUROSCI.4906-05.2006 (2006).

197 Yu, S. *et al.* Depletion of the neural precursor cell pool by glucocorticoids. *Ann Neurol* **67**, 21-30, doi:10.1002/ana.21812 (2010).

198 Ichinohashi, Y. *et al.* Dexamethasone administration to the neonatal rat results in neurological dysfunction at the juvenile stage even at low doses. *Early Hum Dev* **89**, 283-288, doi:10.1016/j.earlhumdev.2012.10.007 (2013).

199 Bose, R. *et al.* Glucocorticoids induce long-lasting effects in neural stem cells resulting in senescence-related alterations. *Cell Death Dis* **1**, e92, doi:10.1038/cddis.2010.60 (2010).

200 Sippel, M. *et al.* Dexamethasone regulates expression of BRUCE/Apollon and the proliferation of neural progenitor cells. *FEBS Lett* **583**, 2213-2217, doi:10.1016/j.febslet.2009.06.018 (2009).

201 Rogatsky, I., Trowbridge, J. M. & Garabedian, M. J. Glucocorticoid receptor-mediated cell cycle arrest is achieved through distinct cell-specific transcriptional regulatory mechanisms. *Mol Cell Biol* **17**, 3181-3193, doi:10.1128/MCB.17.6.3181 (1997).

202 Ninomiya, E. *et al.* Glucocorticoids promote neural progenitor cell proliferation derived from human induced pluripotent stem cells. *Springerplus* **3**, 527, doi:10.1186/2193-1801-3-527 (2014).

203 Peffer, M. E. *et al.* Minireview: the impact of antenatal therapeutic synthetic glucocorticoids on the developing fetal brain. *Mol Endocrinol* **29**, 658-666, doi:10.1210/me.2015-1042 (2015).

204 Samarasinghe, R. A. *et al.* Nongenomic glucocorticoid receptor action regulates gap junction intercellular communication and neural progenitor cell proliferation. *Proc Natl Acad Sci U S A* **108**, 16657-16662, doi:10.1073/pnas.1102821108 (2011).

205 Uhlen, P., Fritz, N., Smedler, E., Malmersjo, S. & Kanatani, S. Calcium signaling in neocortical development. *Dev Neurobiol* **75**, 360-368, doi:10.1002/dneu.22273 (2015).

206 Cheng, A. *et al.* Gap junctional communication is required to maintain mouse cortical neural progenitor cells in a proliferative state. *Dev Biol* **272**, 203-216, doi:10.1016/j.ydbio.2004.04.031 (2004).

207 Weissman, T. A., Riquelme, P. A., Ivic, L., Flint, A. C. & Kriegstein, A. R. Calcium waves propagate through radial glial cells and modulate proliferation in the developing neocortex. *Neuron* **43**, 647-661, doi:10.1016/j.neuron.2004.08.015 (2004).

208 Lin, J. H. *et al.* Purinergic signaling regulates neural progenitor cell expansion and neurogenesis. *Dev Biol* **302**, 356-366, doi:10.1016/j.ydbio.2006.09.017 (2007).

209 Peffer, M. E. *et al.* Caveolin-1 regulates genomic action of the glucocorticoid receptor in neural stem cells. *Mol Cell Biol* **34**, 2611-2623, doi:10.1128/MCB.01121-13 (2014).

210 Anacker, C. *et al.* Role for the kinase SGK1 in stress, depression, and glucocorticoid effects on hippocampal neurogenesis. *Proc Natl Acad Sci U S A* **110**, 8708-8713, doi:10.1073/pnas.1300886110 (2013).

211 Reynolds, B. A. & Weiss, S. Generation of neurons and astrocytes from isolated cells of the adult mammalian central nervous system. *Science* **255**, 1707-1710, doi:10.1126/science.1553558 (1992).

212 Azari, H., Sharififar, S., Rahman, M., Ansari, S. & Reynolds, B. A. Establishing embryonic mouse neural stem cell culture using the neurosphere assay. *J Vis Exp*, doi:10.3791/2457 (2011).

213 Tsiarli, M. A., Paula Monaghan, A. & Defranco, D. B. Differential subcellular localization of the glucocorticoid receptor in distinct neural stem and progenitor populations of the mouse telencephalon in vivo. *Brain Res* **1523**, 10-27, doi:10.1016/j.brainres.2013.06.001 (2013).

214 Takahashi, T., Goto, T., Miyama, S., Nowakowski, R. S. & Caviness, V. S., Jr. Sequence of neuron origin and neocortical laminar fate: relation to cell cycle of origin in the developing murine cerebral wall. *J Neurosci* **19**, 10357-10371 (1999).

215 Murphy, B. E., Sebenick, M. & Patchell, M. E. Cortisol production and metabolism in the human fetus and its reflection in the maternal urine. *J Steroid Biochem* **12**, 37-45, doi:10.1016/0022-4731(80)90248-4 (1980).

216 Venihaki, M., Carrigan, A., Dikkes, P. & Majzoub, J. A. Circadian rise in maternal glucocorticoid prevents pulmonary dysplasia in fetal mice with adrenal insufficiency. *Proc Natl Acad Sci U S A* **97**, 7336-7341, doi:10.1073/pnas.97.13.7336 (2000).

217 Matabosch, X. *et al.* Steroid production and excretion by the pregnant mouse, particularly in relation to pregnancies with fetuses deficient in Delta7-sterol reductase (Dhcr7), the enzyme associated with Smith-Lemli-Opitz syndrome. *J Steroid Biochem Mol Biol* **116**, 61-70, doi:10.1016/j.jsbmb.2009.04.011 (2009).

218 Pulvers, J. N. & Huttner, W. B. Brca1 is required for embryonic development of the mouse cerebral cortex to normal size by preventing apoptosis of early neural progenitors. *Development* **136**, 1859-1868, doi:10.1242/dev.033498 (2009).

219 Frahm, K. A. *et al.* Research Resource: The Dexamethasone Transcriptome in Hypothalamic Embryonic Neural Stem Cells. *Mol Endocrinol* **30**, 144-154, doi:10.1210/me.2015-1258 (2016).

220 Meijer, O. C. *et al.* Penetration of dexamethasone into brain glucocorticoid targets is enhanced in mdr1A P-glycoprotein knockout mice. *Endocrinology* **139**, 1789-1793, doi:10.1210/endo.139.4.5917 (1998).

221 Qian, X. *et al.* Timing of CNS cell generation: a programmed sequence of neuron and glial cell production from isolated murine cortical stem cells. *Neuron* **28**, 69-80, doi:10.1016/s0896-6273(00)00086-6 (2000).

222 Shen, Q. *et al.* The timing of cortical neurogenesis is encoded within lineages of individual progenitor cells. *Nat Neurosci* **9**, 743-751, doi:10.1038/nn1694 (2006).

223 Gao, P. *et al.* Deterministic progenitor behavior and unitary production of neurons in the neocortex. *Cell* **159**, 775-788, doi:10.1016/j.cell.2014.10.027 (2014).

224 Toma, K. & Hanashima, C. Switching modes in corticogenesis: mechanisms of neuronal subtype transitions and integration in the cerebral cortex. *Front Neurosci* **9**, 274, doi:10.3389/fnins.2015.00274 (2015).

225 Kageyama, R. & Nakajima, K. Timing and shaping mechanisms of neural development. *Neurosci Res* **138**, 1-2, doi:10.1016/j.neures.2018.12.003 (2019).

226 Tamura, S., Suzuki, Y., Kikuchi, K. & Tsuiki, S. Identification and characterization of Mg2+-dependent phosphotyrosyl protein phosphatase from rat liver cytosol. *Biochem Biophys Res Commun* **140**, 212-218, doi:10.1016/0006-291x(86)91078-8 (1986).

227 Buenrostro, J. D., Wu, B., Chang, H. Y. & Greenleaf, W. J. ATAC-seq: A Method for Assaying Chromatin Accessibility Genome-Wide. *Curr Protoc Mol Biol* **109**, 21 29 21-21 29 29, doi:10.1002/0471142727.mb2129s109 (2015).

228 Kanton, S. *et al.* Organoid single-cell genomic atlas uncovers human-specific features of brain development. *Nature* **574**, 418-422, doi:10.1038/s41586-019-1654-9 (2019).

229 Rhodes, C. T. *et al.* An epigenome atlas of neural progenitors within the embryonic mouse forebrain. *Nat Commun* **13**, 4196, doi:10.1038/s41467-022-31793-4 (2022).

230 Yao, H. *et al.* CHD7 promotes neural progenitor differentiation in embryonic stem cells via altered chromatin accessibility and nascent gene expression. *Sci Rep* **10**, 17445, doi:10.1038/s41598-020-74537-4 (2020).

231 Berg, D. A. *et al.* A Common Embryonic Origin of Stem Cells Drives Developmental and Adult Neurogenesis. *Cell* **177**, 654-668 e615, doi:10.1016/j.cell.2019.02.010 (2019).

232 Thurman, R. E. *et al.* The accessible chromatin landscape of the human genome. *Nature* **489**, 75-82, doi:10.1038/nature11232 (2012).

233 John, S. *et al.* Interaction of the glucocorticoid receptor with the chromatin landscape. *Mol Cell* **29**, 611-624, doi:10.1016/j.molcel.2008.02.010 (2008).

234 Frank, C. L. *et al.* Regulation of chromatin accessibility and Zic binding at enhancers in the developing cerebellum. *Nat Neurosci* **18**, 647-656, doi:10.1038/nn.3995 (2015).

235 Wang, Y. *et al.* N(6)-methyladenosine RNA modification regulates embryonic neural stem cell self-renewal through histone modifications. *Nat Neurosci* **21**, 195-206, doi:10.1038/s41593-017-0057-1 (2018).

236 Creyghton, M. P. *et al.* Histone H3K27ac separates active from poised enhancers and predicts developmental state. *Proc Natl Acad Sci U S A* **107**, 21931-21936, doi:10.1073/pnas.1016071107 (2010).

237 Rada-Iglesias, A. *et al.* A unique chromatin signature uncovers early developmental enhancers in humans. *Nature* **470**, 279-283, doi:10.1038/nature09692 (2011).

238 Bartova, E., Krejci, J., Harnicarova, A., Galiova, G. & Kozubek, S. Histone modifications and nuclear architecture: a review. *J Histochem Cytochem* **56**, 711-721, doi:10.1369/jhc.2008.951251 (2008).

239 Bonn, S. *et al.* Tissue-specific analysis of chromatin state identifies temporal signatures of enhancer activity during embryonic development. *Nat Genet* **44**, 148-156, doi:10.1038/ng.1064 (2012).

240 Shlyueva, D., Stampfel, G. & Stark, A. Transcriptional enhancers: from properties to genome-wide predictions. *Nat Rev Genet* **15**, 272-286, doi:10.1038/nrg3682 (2014).

241 Catarino, R. R. & Stark, A. Assessing sufficiency and necessity of enhancer activities for gene expression and the mechanisms of transcription activation. *Genes Dev* **32**, 202-223, doi:10.1101/gad.310367.117 (2018).

242 Jin, F. *et al.* A high-resolution map of the three-dimensional chromatin interactome in human cells. *Nature* **503**, 290-294, doi:10.1038/nature12644 (2013).

243 Lam, M. T., Li, W., Rosenfeld, M. G. & Glass, C. K. Enhancer RNAs and regulated transcriptional programs. *Trends Biochem Sci* **39**, 170-182, doi:10.1016/j.tibs.2014.02.007 (2014).

244 Li, W., Notani, D. & Rosenfeld, M. G. Enhancers as non-coding RNA transcription units: recent insights and future perspectives. *Nat Rev Genet* **17**, 207-223, doi:10.1038/nrg.2016.4 (2016).

245 Peng, Y. & Zhang, Y. Enhancer and super-enhancer: Positive regulators in gene transcription. *Animal Model Exp Med* **1**, 169-179, doi:10.1002/ame2.12032 (2018).

246 Mansisidor, A. R. & Risca, V. I. Chromatin accessibility: methods, mechanisms, and biological insights. *Nucleus* **13**, 236-276, doi:10.1080/19491034.2022.2143106 (2022).

247 Hota, S. K. & Bruneau, B. G. ATP-dependent chromatin remodeling during mammalian development. *Development* **143**, 2882-2897, doi:10.1242/dev.128892 (2016).

248 Wu, J. N. *et al.* Functionally distinct patterns of nucleosome remodeling at enhancers in glucocorticoid-treated acute lymphoblastic leukemia. *Epigenetics Chromatin* **8**, 53, doi:10.1186/s13072-015-0046-0 (2015).

249 Borczyk, M., Zieba, M., Korostynski, M. & Piechota, M. Role of Non-Coding Regulatory Elements in the Control of GR-Dependent Gene Expression. *Int J Mol Sci* **22**, doi:10.3390/ijms22084258 (2021).

250 Siersbaek, R. *et al.* Extensive chromatin remodelling and establishment of transcription factor 'hotspots' during early adipogenesis. *EMBO J* **30**, 1459-1472, doi:10.1038/emboj.2011.65 (2011).

251 Fletcher, T. M. *et al.* ATP-dependent mobilization of the glucocorticoid receptor during chromatin remodeling. *Mol Cell Biol* **22**, 3255-3263, doi:10.1128/MCB.22.10.3255-3263.2002 (2002).

252 King, H. A., Trotter, K. W. & Archer, T. K. Chromatin remodeling during glucocorticoid receptor regulated transactivation. *Biochim Biophys Acta* **1819**, 716-726, doi:10.1016/j.bbagrm.2012.02.019 (2012).

253 Stortz, M., Pecci, A., Presman, D. M. & Levi, V. Unraveling the molecular interactions involved in phase separation of glucocorticoid receptor. *BMC Biol* **18**, 59, doi:10.1186/s12915-020-00788-2 (2020).

254 Stortz, M., Presman, D. M., Pecci, A. & Levi, V. Phasing the intranuclear organization of steroid hormone receptors. *Biochem J* **478**, 443-461, doi:10.1042/BCJ20200883 (2021).

255 Crudo, A. *et al.* Prenatal synthetic glucocorticoid treatment changes DNA methylation states in male organ systems: multigenerational effects. *Endocrinology* **153**, 3269-3283, doi:10.1210/en.2011-2160 (2012).

256 Sears, D. W., Osman, N., Tate, B., McKenzie, I. F. & Hogarth, P. M. Molecular cloning and expression of the mouse high affinity Fc receptor for IgG. *J Immunol* **144**, 371-378 (1990).

257 Corces, M. R. *et al.* An improved ATAC-seq protocol reduces background and enables interrogation of frozen tissues. *Nat Methods* **14**, 959-962, doi:10.1038/nmeth.4396 (2017).

258 Stark R, B. G. DiffBind: differential binding analysis of ChIP-Seq peak data. (2011). <http://bioconductor.org/packages/release/bioc/vignettes/DiffBind/inst/doc/DiffBind.pdf >.

259 Klemm, S. L., Shipony, Z. & Greenleaf, W. J. Chromatin accessibility and the regulatory epigenome. *Nat Rev Genet* **20**, 207-220, doi:10.1038/s41576-018-0089-8 (2019).

260 Gaborit, V. *et al.* Chromatin accessibility combined with enhancer clusters activation mediates heterogeneous response to dexamethasone in myeloma cells. *bioRxiv*, 2021.2009.2006.459068, doi:10.1101/2021.09.06.459068 (2021).

261 Hoffman, J. A. *et al.* Multimodal regulatory elements within a hormone-specific super enhancer control a heterogeneous transcriptional response. *Mol Cell* **82**, 803-815 e805, doi:10.1016/j.molcel.2021.12.035 (2022).

262 Sun, H. *et al.* Genome-wide mapping of RNA Pol-II promoter usage in mouse tissues by ChIP-seq. *Nucleic Acids Res* **39**, 190-201, doi:10.1093/nar/gkq775 (2011).

263 Cottrell, E. C. & Seckl, J. R. Prenatal stress, glucocorticoids and the programming of adult disease. *Front Behav Neurosci* **3**, 19, doi:10.3389/neuro.08.019.2009 (2009).

264 Harabula, I. & Pombo, A. The dynamics of chromatin architecture in brain development and function. *Curr Opin Genet Dev* **67**, 84-93, doi:10.1016/j.gde.2020.12.008 (2021).

265 de la Torre-Ubieta, L. *et al.* The Dynamic Landscape of Open Chromatin during Human Cortical Neurogenesis. *Cell* **172**, 289-304 e218, doi:10.1016/j.cell.2017.12.014 (2018).

266 Won, H. *et al.* Chromosome conformation elucidates regulatory relationships in developing human brain. *Nature* **538**, 523-527, doi:10.1038/nature19847 (2016).

267 Lafontaine, D. L., Yang, L., Dekker, J. & Gibcus, J. H. Hi-C 3.0: Improved Protocol for Genome-Wide Chromosome Conformation Capture. *Curr Protoc* **1**, e198, doi:10.1002/cpz1.198 (2021).

268 Kubo, N. *et al.* Promoter-proximal CTCF binding promotes distal enhancer-dependent gene activation. *Nat Struct Mol Biol* **28**, 152-161, doi:10.1038/s41594-020-00539-5 (2021).

269 Bertolini, J. A. *et al.* Mapping the Global Chromatin Connectivity Network for Sox2 Function in Neural Stem Cell Maintenance. *Cell Stem Cell* **24**, 462-476 e466, doi:10.1016/j.stem.2019.02.004 (2019).

270 D'Aurizio, R. *et al.* Bridging between Mouse and Human Enhancer-Promoter Long-Range Interactions in Neural Stem Cells, to Understand Enhancer Function in Neurodevelopmental Disease. *Int J Mol Sci* **23**, doi:10.3390/ijms23147964 (2022).

271 Cisse, II *et al.* Real-time dynamics of RNA polymerase II clustering in live human cells. *Science* **341**, 664-667, doi:10.1126/science.1239053 (2013).

272 Feigin, M. E. & Malbon, C. C. RGS19 regulates Wnt-beta-catenin signaling through inactivation of Galpha(o). *J Cell Sci* **120**, 3404-3414, doi:10.1242/jcs.011254 (2007).

273 Nasu, M., Esumi, S., Hatakeyama, J., Tamamaki, N. & Shimamura, K. Two-Phase Lineage Specification of Telencephalon Progenitors Generated From Mouse Embryonic Stem Cells. *Front Cell Dev Biol* **9**, 632381, doi:10.3389/fcell.2021.632381 (2021).

274 Ohta, S. *et al.* Sox6 up-regulation by macrophage migration inhibitory factor promotes survival and maintenance of mouse neural stem/progenitor cells. *PloS one* **8**, e74315, doi:10.1371/journal.pone.0074315 (2013).

275 Panman, L. *et al.* Sox6 and Otx2 control the specification of substantia nigra and ventral tegmental area dopamine neurons. *Cell Rep* **8**, 1018-1025, doi:10.1016/j.celrep.2014.07.016 (2014).

276 Hoffmann, A. & Spengler, D. Chromatin Remodeling Complex NuRD in Neurodevelopment and Neurodevelopmental Disorders. *Front Genet* **10**, 682, doi:10.3389/fgene.2019.00682 (2019).

277 Mullegama, S. V. *et al.* Transcriptome analysis of MBD5-associated neurodevelopmental disorder (MAND) neural progenitor cells reveals dysregulation of autism-associated genes. *Sci Rep* **11**, 11295, doi:10.1038/s41598-021-90798-z (2021).

278 Rajarajan, P. *et al.* Neuron-specific signatures in the chromosomal connectome associated with schizophrenia risk. *Science* **362**, doi:10.1126/science.aat4311 (2018).

279 Polman, J. A. *et al.* A genome-wide signature of glucocorticoid receptor binding in neuronal PC12 cells. *BMC Neurosci* **13**, 118, doi:10.1186/1471-2202-13-118 (2012).

280 Diaz-Gallardo, M. Y., Cote-Velez, A., Charli, J. L. & Joseph-Bravo, P. A rapid interference between glucocorticoids and cAMP-activated signalling in hypothalamic neurones prevents binding of phosphorylated cAMP response element binding protein and glucocorticoid receptor at the CRE-Like and composite GRE sites of thyrotrophin-releasing hormone gene promoter. *J Neuroendocrinol* **22**, 282-293, doi:10.1111/j.1365-2826.2010.01966.x (2010).

281 Paakinaho, V., Johnson, T. A., Presman, D. M. & Hager, G. L. Glucocorticoid receptor quaternary structure drives chromatin occupancy and transcriptional outcome. *Genome Res* **29**, 1223-1234, doi:10.1101/gr.244814.118 (2019).

282 Boeva, V. Analysis of Genomic Sequence Motifs for Deciphering Transcription Factor Binding and Transcriptional Regulation in Eukaryotic Cells. *Front Genet* **7**, 24, doi:10.3389/fgene.2016.00024 (2016).

283 Bonifer, C. & Cockerill, P. N. Chromatin priming of genes in development: Concepts, mechanisms and consequences. *Exp Hematol* **49**, 1-8, doi:10.1016/j.exphem.2017.01.003 (2017).

284 Feldmann, A. *et al.* Transcription factor occupancy can mediate active turnover of DNA methylation at regulatory regions. *PLoS Genet* **9**, e1003994, doi:10.1371/journal.pgen.1003994 (2013).

285 Ichiyama, K. *et al.* The methylcytosine dioxygenase Tet2 promotes DNA demethylation and activation of cytokine gene expression in T cells. *Immunity* **42**, 613-626, doi:10.1016/j.immuni.2015.03.005 (2015).

286 Banerjee, S. *et al.* Identifying Transcriptional Regulatory Modules Among Different Chromatin States in Mouse Neural Stem Cells. *Front Genet* **9**, 731, doi:10.3389/fgene.2018.00731 (2018).

287 Matsuda, T. *et al.* Pioneer Factor NeuroD1 Rearranges Transcriptional and Epigenetic Profiles to Execute Microglia-Neuron Conversion. *Neuron* **101**, 472-485 e477, doi:10.1016/j.neuron.2018.12.010 (2019).

288 Larson, E. D. *et al.* Cell-type-specific chromatin occupancy by the pioneer factor Zelda drives key developmental transitions in Drosophila. *Nat Commun* **12**, 7153, doi:10.1038/s41467-021-27506-y (2021).

289 Braun, S. M. G. *et al.* BAF subunit switching regulates chromatin accessibility to control cell cycle exit in the developing mammalian cortex. *Genes Dev* **35**, 335-353, doi:10.1101/gad.342345.120 (2021).

290 Rollins, D. A. & Rogatsky, I. Dual Cross-Linking Chromatin Immunoprecipitation Protocol for Next-Generation Sequencing (ChIPseq) in Macrophages. *Methods Mol Biol* **1951**, 87-98, doi:10.1007/978-1-4939-9130-3_7 (2019).

291 Wang, C. *et al.* Extensive epigenomic integration of the glucocorticoid response in primary human monocytes and in vitro derived macrophages. *Sci Rep* **9**, 2772, doi:10.1038/s41598-019-39395-9 (2019).

292 Pooley, J. R. *et al.* Genome-Wide Identification of Basic Helix-Loop-Helix and NF-1 Motifs Underlying GR Binding Sites in Male Rat Hippocampus. *Endocrinology* **158**, 1486-1501, doi:10.1210/en.2016-1929 (2017).

293 Astrand, C., Belikov, S. & Wrange, O. Histone acetylation characterizes chromatin presetting by NF1 and Oct1 and enhances glucocorticoid receptor binding to the MMTV promoter. *Exp Cell Res* **315**, 2604-2615, doi:10.1016/j.yexcr.2009.05.012 (2009).

294 Meijsing, S. H. *et al.* DNA binding site sequence directs glucocorticoid receptor structure and activity. *Science* **324**, 407-410, doi:10.1126/science.1164265 (2009).

295 Watson, L. C. *et al.* The glucocorticoid receptor dimer interface allosterically transmits sequence-specific DNA signals. *Nat Struct Mol Biol* **20**, 876-883, doi:10.1038/nsmb.2595 (2013).

296 Sarkar, A. & Hochedlinger, K. The sox family of transcription factors: versatile regulators of stem and progenitor cell fate. *Cell Stem Cell* **12**, 15-30, doi:10.1016/j.stem.2012.12.007 (2013).

297 Wegner, M. All purpose Sox: The many roles of Sox proteins in gene expression. *Int J Biochem Cell Biol* **42**, 381-390, doi:10.1016/j.biocel.2009.07.006 (2010).

298 Bergsland, M. *et al.* Sequentially acting Sox transcription factors in neural lineage development. *Genes Dev* **25**, 2453-2464, doi:10.1101/gad.176008.111 (2011).

299 Reddy, T. E. *et al.* Genomic determination of the glucocorticoid response reveals unexpected mechanisms of gene regulation. *Genome Res* **19**, 2163-2171, doi:10.1101/gr.097022.109 (2009).

300 Yu, C. Y. *et al.* Genome-wide analysis of glucocorticoid receptor binding regions in adipocytes reveal gene network involved in triglyceride homeostasis. *PloS one* **5**, e15188, doi:10.1371/journal.pone.0015188 (2010).

301 Stavreva, D. A. *et al.* Dynamics of chromatin accessibility and long-range interactions in response to glucocorticoid pulsing. *Genome Res* **25**, 845-857, doi:10.1101/gr.184168.114 (2015).

302 Stavreva, D. A. *et al.* Ultradian hormone stimulation induces glucocorticoid receptor-mediated pulses of gene transcription. *Nat Cell Biol* **11**, 1093-1102, doi:10.1038/ncb1922 (2009).

303 Paakinaho, V. *et al.* Single-molecule analysis of steroid receptor and cofactor action in living cells. *Nat Commun* **8**, 15896, doi:10.1038/ncomms15896 (2017).

304 Desvergne, B. & Heligon, C. Steroid hormone pulsing drives cyclic gene expression. *Nat Cell Biol* **11**, 1051-1053, doi:10.1038/ncb0909-1051 (2009).

305 Hess, P. & Payvar, F. Hormone withdrawal triggers a premature and sustained gene activation from delayed secondary glucocorticoid response elements. *J Biol Chem* **267**, 3490-3497 (1992).

306 Cohen, D. M. & Steger, D. J. Nuclear Receptor Function through Genomics: Lessons from the Glucocorticoid Receptor. *Trends Endocrinol Metab* **28**, 531-540, doi:10.1016/j.tem.2017.04.001 (2017).

307 Silverman, M. N. *et al.* Glucocorticoid receptor dimerization is required for proper recovery of LPS-induced inflammation, sickness behavior and metabolism in mice. *Mol Psychiatry* **18**, 1006-1017, doi:10.1038/mp.2012.131 (2013).

308 Presman, D. M. *et al.* DNA binding triggers tetramerization of the glucocorticoid receptor in live cells. *Proc Natl Acad Sci U S A* **113**, 8236-8241, doi:10.1073/pnas.1606774113 (2016).

309 Zenz, R. *et al.* Activator protein 1 (Fos/Jun) functions in inflammatory bone and skin disease. *Arthritis Res Ther* **10**, 201, doi:10.1186/ar2338 (2008).

310 Rao, K. V. & Fox, C. F. Epidermal growth factor stimulates tyrosine phosphorylation of human glucocorticoid receptor in cultured cells. *Biochem Biophys Res Commun* **144**, 512-519, doi:10.1016/s0006-291x(87)80539-9 (1987).

311 Saad, S. *et al.* High glucose transactivates the EGF receptor and up-regulates serum glucocorticoid kinase in the proximal tubule. *Kidney Int* **68**, 985-997, doi:10.1111/j.1523-1755.2005.00492.x (2005).

312 Wu, J. & Bresnick, E. H. Glucocorticoid and growth factor synergism requirement for Notch4 chromatin domain activation. *Mol Cell Biol* **27**, 2411-2422, doi:10.1128/MCB.02152-06 (2007).

313 Chalepakis, G., Schauer, M., Cao, X. A. & Beato, M. Efficient binding of glucocorticoid receptor to its responsive element requires a dimer and DNA flanking sequences. *DNA Cell Biol* **9**, 355-368, doi:10.1089/dna.1990.9.355 (1990).

314 Timmermans, S., Vandewalle, J. & Libert, C. Dimerization of the Glucocorticoid Receptor and Its Importance in (Patho)physiology: A Primer. *Cells* **11**, doi:10.3390/cells11040683 (2022).

315 Schone, S. *et al.* Sequences flanking the core-binding site modulate glucocorticoid receptor structure and activity. *Nat Commun* **7**, 12621, doi:10.1038/ncomms12621 (2016).

316 Meijsing, S. H., Elbi, C., Luecke, H. F., Hager, G. L. & Yamamoto, K. R. The ligand binding domain controls glucocorticoid receptor dynamics independent of ligand release. *Mol Cell Biol* **27**, 2442-2451, doi:10.1128/MCB.01570-06 (2007).

317 Zhang, Y. *et al.* Chromatin connectivity maps reveal dynamic promoter-enhancer long-range associations. *Nature* **504**, 306-310, doi:10.1038/nature12716 (2013).

318 Oh, K. S. *et al.* Anti-Inflammatory Chromatinscape Suggests Alternative Mechanisms of Glucocorticoid Receptor Action. *Immunity* **47**, 298-309 e295, doi:10.1016/j.immuni.2017.07.012 (2017).

319 Wang, H. *et al.* Glucocorticoid receptor wields chromatin interactions to tune transcription for cytoskeleton stabilization in podocytes. *Commun Biol* **4**, 675, doi:10.1038/s42003-021-02209-8 (2021).

320 Hutton, S. R. & Pevny, L. H. SOX2 expression levels distinguish between neural progenitor populations of the developing dorsal telencephalon. *Dev Biol* **352**, 40-47, doi:10.1016/j.ydbio.2011.01.015 (2011).

321 Mercurio, S., Serra, L. & Nicolis, S. K. More than just Stem Cells: Functional Roles of the Transcription Factor Sox2 in Differentiated Glia and Neurons. *Int J Mol Sci* **20**, doi:10.3390/ijms20184540 (2019).

322 Takahashi, K. & Yamanaka, S. Induction of pluripotent stem cells from mouse embryonic and adult fibroblast cultures by defined factors. *Cell* **126**, 663-676, doi:10.1016/j.cell.2006.07.024 (2006).

323 Takahashi, K. & Yamanaka, S. A decade of transcription factor-mediated reprogramming to pluripotency. *Nat Rev Mol Cell Biol* **17**, 183-193, doi:10.1038/nrm.2016.8 (2016).

324 Bernard, P. & Harley, V. R. Acquisition of SOX transcription factor specificity through protein-protein interaction, modulation of Wnt signalling and post-translational modification. *Int J Biochem Cell Biol* **42**, 400-410, doi:10.1016/j.biocel.2009.10.017 (2010).

325 Favaro, R. *et al.* Hippocampal development and neural stem cell maintenance require Sox2-dependent regulation of Shh. *Nat Neurosci* **12**, 1248-1256, doi:10.1038/nn.2397 (2009).

326 Tang, M. *et al.* Interactions of Wnt/beta-catenin signaling and sonic hedgehog regulate the neurogenesis of ventral midbrain dopamine neurons. *J Neurosci* **30**, 9280-9291, doi:10.1523/JNEUROSCI.0860-10.2010 (2010).

327 Kormish, J. D., Sinner, D. & Zorn, A. M. Interactions between SOX factors and Wnt/beta-catenin signaling in development and disease. *Dev Dyn* **239**, 56-68, doi:10.1002/dvdy.22046 (2010).

328 Mercurio, S. *et al.* Sox2 Acts in Thalamic Neurons to Control the Development of Retina-Thalamus-Cortex Connectivity. *iScience* **15**, 257-273, doi:10.1016/j.isci.2019.04.030 (2019).

329 Mercurio, S. *et al.* An early Sox2-dependent gene expression programme required for hippocampal dentate gyrus development. *Open Biol* **11**, 200339, doi:10.1098/rsob.200339 (2021).

330 Sisodiya, S. M. *et al.* Role of SOX2 mutations in human hippocampal malformations and epilepsy. *Epilepsia* **47**, 534-542, doi:10.1111/j.1528-1167.2006.00464.x (2006).

331 Ferri, A. *et al.* Sox2 is required for embryonic development of the ventral telencephalon through the activation of the ventral determinants Nkx2.1 and Shh. *Development* **140**, 1250-1261, doi:10.1242/dev.073411 (2013).

332 Ragge, N. K. *et al.* SOX2 anophthalmia syndrome. *Am J Med Genet A* **135**, 1-7; discussion 8, doi:10.1002/ajmg.a.30642 (2005).

333 Mercurio, S., Serra, L., Pagin, M. & Nicolis, S. K. Deconstructing Sox2 Function in Brain Development and Disease. *Cells* **11**, doi:10.3390/cells11101604 (2022).

334 Episkopou, V. SOX2 functions in adult neural stem cells. *Trends Neurosci* **28**, 219-221, doi:10.1016/j.tins.2005.03.003 (2005).

335 Ribeiro, F. F. & Xapelli, S. An Overview of Adult Neurogenesis. *Adv Exp Med Biol* **1331**, 77-94, doi:10.1007/978-3-030-74046-7_7 (2021).

336 Arnold, K. *et al.* Sox2(+) adult stem and progenitor cells are important for tissue regeneration and survival of mice. *Cell Stem Cell* **9**, 317-329, doi:10.1016/j.stem.2011.09.001 (2011).

337 Stevanovic, M. *et al.* SOX Transcription Factors as Important Regulators of Neuronal and Glial Differentiation During Nervous System Development and Adult Neurogenesis. *Front Mol Neurosci* **14**, 654031, doi:10.3389/fnmol.2021.654031 (2021).

338 Sudbeck, P. & Scherer, G. Two independent nuclear localization signals are present in the DNA-binding high-mobility group domains of SRY and SOX9. *J Biol Chem* **272**, 27848-27852, doi:10.1074/jbc.272.44.27848 (1997).

339 Yasuhara, N. *et al.* Triggering neural differentiation of ES cells by subtype switching of importin-alpha. *Nat Cell Biol* **9**, 72-79, doi:10.1038/ncb1521 (2007).

340 Jagga, B. *et al.* Structural basis for nuclear import selectivity of pioneer transcription factor SOX2. *Nat Commun* **12**, 28, doi:10.1038/s41467-020-20194-0 (2021).

341 Kamachi, Y., Uchikawa, M. & Kondoh, H. Pairing SOX off: with partners in the regulation of embryonic development. *Trends Genet* **16**, 182-187, doi:10.1016/s0168-9525(99)01955-1 (2000).

342 Cavaleri, F. & Scholer, H. R. Nanog: a new recruit to the embryonic stem cell orchestra. *Cell* **113**, 551-552, doi:10.1016/s0092-8674(03)00394-5 (2003).

343 Mateo, J. L. *et al.* Characterization of the neural stem cell gene regulatory network identifies OLIG2 as a multifunctional regulator of self-renewal. *Genome Res* **25**, 41-56, doi:10.1101/gr.173435.114 (2015).

344 Bunina, D. *et al.* Genomic Rewiring of SOX2 Chromatin Interaction Network during Differentiation of ESCs to Postmitotic Neurons. *Cell Syst* **10**, 480-494 e488, doi:10.1016/j.cels.2020.05.003 (2020).

345 Wegner, M. From head to toes: the multiple facets of Sox proteins. *Nucleic Acids Res* **27**, 1409-1420, doi:10.1093/nar/27.6.1409 (1999).

346 Wegner, M. Secrets to a healthy Sox life: lessons for melanocytes. *Pigment Cell Res* **18**, 74-85, doi:10.1111/j.1600-0749.2005.00218.x (2005).

347 Amador-Arjona, A. *et al.* SOX2 primes the epigenetic landscape in neural precursors enabling proper gene activation during hippocampal neurogenesis. *Proc Natl Acad Sci U S A* **112**, E1936-1945, doi:10.1073/pnas.1421480112 (2015).

348 Puligilla, C., Dabdoub, A., Brenowitz, S. D. & Kelley, M. W. Sox2 induces neuronal formation in the developing mammalian cochlea. *J Neurosci* **30**, 714-722, doi:10.1523/JNEUROSCI.3852-09.2010 (2010).

349 Malaga Gadea, F. C. & Nikolova, E. N. Structural Plasticity of Pioneer Factor Sox2 and DNA Bendability Modulate Nucleosome Engagement and Sox2-Oct4 Synergism. *J Mol Biol* **435**, 167916, doi:10.1016/j.jmb.2022.167916 (2023).

350 Hovland, A. S. *et al.* Pluripotency factors are repurposed to shape the epigenomic landscape of neural crest cells. *Dev Cell* **57**, 2257-2272 e2255, doi:10.1016/j.devcel.2022.09.006 (2022).

351 McDowell, T. L. *et al.* Localization of a putative transcriptional regulator (ATRX) at pericentromeric heterochromatin and the short arms of acrocentric chromosomes. *Proc Natl Acad Sci U S A* **96**, 13983-13988, doi:10.1073/pnas.96.24.13983 (1999).

352 Wei, C. L., Nicolis, S. K., Zhu, Y. & Pagin, M. Sox2-Dependent 3D Chromatin Interactomes in Transcription, Neural Stem Cell Proliferation and Neurodevelopmental Diseases. *J Exp Neurosci* **13**, 1179069519868224, doi:10.1177/1179069519868224 (2019).

353 Ellis, P. *et al.* SOX2, a persistent marker for multipotential neural stem cells derived from embryonic stem cells, the embryo or the adult. *Dev Neurosci* **26**, 148-165, doi:10.1159/000082134 (2004).

354 Medina, D. L. *et al.* TrkB regulates neocortex formation through the Shc/PLCgamma-mediated control of neuronal migration. *EMBO J* **23**, 3803-3814, doi:10.1038/sj.emboj.7600399 (2004).

355 Kempermann, G., Jessberger, S., Steiner, B. & Kronenberg, G. Milestones of neuronal development in the adult hippocampus. *Trends Neurosci* **27**, 447-452, doi:10.1016/j.tins.2004.05.013 (2004).

356 Romer, J. T. *et al.* Suppression of the Shh pathway using a small molecule inhibitor eliminates medulloblastoma in Ptc1(+/-)p53(-/-) mice. *Cancer Cell* **6**, 229-240, doi:10.1016/j.ccr.2004.08.019 (2004).

357 Alam, M. S. Proximity Ligation Assay (PLA). *Curr Protoc Immunol* **123**, e58, doi:10.1002/cpim.58 (2018).

358 Mossahebi-Mohammadi, M., Quan, M., Zhang, J. S. & Li, X. FGF Signaling Pathway: A Key Regulator of Stem Cell Pluripotency. *Front Cell Dev Biol* **8**, 79, doi:10.3389/fcell.2020.00079 (2020).

359 Ruiz-Contreras, H. A. *et al.* Modulatory Activity of the Endocannabinoid System in the Development and Proliferation of Cells in the CNS. *Neurotox Res* **40**, 1690-1706, doi:10.1007/s12640-022-00592-6 (2022).

360 Jaksik, R., Iwanaszko, M., Rzeszowska-Wolny, J. & Kimmel, M. Microarray experiments and factors which affect their reliability. *Biol Direct* **10**, 46, doi:10.1186/s13062-015-0077-2 (2015).

361 Pagin, M. *et al.* FOS Rescues Neuronal Differentiation of Sox2-Deleted Neural Stem Cells by Genome-Wide Regulation of Common SOX2 and AP1(FOS-JUN) Target Genes. *Cells* **10**, doi:10.3390/cells10071757 (2021).

362 Bani-Yaghoub, M. *et al.* Role of Sox2 in the development of the mouse neocortex. *Dev Biol* **295**, 52-66, doi:10.1016/j.ydbio.2006.03.007 (2006).

363 Hagey, D. W. & Muhr, J. Sox2 acts in a dose-dependent fashion to regulate proliferation of cortical progenitors. *Cell Rep* **9**, 1908-1920, doi:10.1016/j.celrep.2014.11.013 (2014).

364 Jiang, T. *et al.* Programming changes of hippocampal miR-134-5p/SOX2 signal mediate the susceptibility to depression in prenatal dexamethasone-exposed female offspring. *Cell Biol Toxicol*, doi:10.1007/s10565-021-09590-4 (2021).

365 Frahm, K. A. & Tobet, S. A. Development of the blood-brain barrier within the paraventricular nucleus of the hypothalamus: influence of fetal glucocorticoid excess. *Brain Struct Funct* **220**, 2225-2234, doi:10.1007/s00429-014-0787-8 (2015).

366 Frahm, K. A., Handa, R. J. & Tobet, S. A. Embryonic Exposure to Dexamethasone Affects Nonneuronal Cells in the Adult Paraventricular Nucleus of the Hypothalamus. *J Endocr Soc* **2**, 140-153, doi:10.1210/js.2017-00439 (2018).

367 Kautzman, A. G. *et al.* Sox2 regulates astrocytic and vascular development in the retina. *Glia* **66**, 623-636, doi:10.1002/glia.23269 (2018).

368 Niu, W. *et al.* SOX2 reprograms resident astrocytes into neural progenitors in the adult brain. *Stem Cell Reports* **4**, 780-794, doi:10.1016/j.stemcr.2015.03.006 (2015).

369 Corti, S. *et al.* Direct reprogramming of human astrocytes into neural stem cells and neurons. *Exp Cell Res* **318**, 1528-1541, doi:10.1016/j.yexcr.2012.02.040 (2012).

370 Wapner, R. J. *et al.* Long-term outcomes after repeat doses of antenatal corticosteroids. *N Engl J Med* **357**, 1190-1198, doi:10.1056/NEJMoa071453 (2007).

371 Bou Khalil, R., Souaiby, L. & Fares, N. The importance of the hypothalamo-pituitary-adrenal axis as a therapeutic target in anorexia nervosa. *Physiol Behav* **171**, 13-20, doi:10.1016/j.physbeh.2016.12.035 (2017).

372 Dunlop, B. W. & Wong, A. The hypothalamic-pituitary-adrenal axis in PTSD: Pathophysiology and treatment interventions. *Prog Neuropsychopharmacol Biol Psychiatry* **89**, 361-379, doi:10.1016/j.pnpbp.2018.10.010 (2019).

373 Juruena, M. F., Eror, F., Cleare, A. J. & Young, A. H. The Role of Early Life Stress in HPA Axis and Anxiety. *Adv Exp Med Biol* **1191**, 141-153, doi:10.1007/978-981-32-9705-0_9 (2020).

374 Leistner, C. & Menke, A. Hypothalamic-pituitary-adrenal axis and stress. *Handb Clin Neurol* **175**, 55-64, doi:10.1016/B978-0-444-64123-6.00004-7 (2020).

375 Menke, A. Is the HPA Axis as Target for Depression Outdated, or Is There a New Hope? *Front Psychiatry* **10**, 101, doi:10.3389/fpsyt.2019.00101 (2019).

376 Zorn, J. V. *et al.* Cortisol stress reactivity across psychiatric disorders: A systematic review and meta-analysis. *Psychoneuroendocrinology* **77**, 25-36, doi:10.1016/j.psyneuen.2016.11.036 (2017).

377 Jayakody, S. A. *et al.* SOX2 regulates the hypothalamic-pituitary axis at multiple levels. *J Clin Invest* **122**, 3635-3646, doi:10.1172/JCI64311 (2012).

378 Talge, N. M. *et al.* Antenatal maternal stress and long-term effects on child neurodevelopment: how and why? *J Child Psychol Psychiatry* **48**, 245-261, doi:10.1111/j.1469-7610.2006.01714.x (2007).

379 Arloth, J. *et al.* Genetic Differences in the Immediate Transcriptome Response to Stress Predict Risk-Related Brain Function and Psychiatric Disorders. *Neuron* **86**, 1189-1202, doi:10.1016/j.neuron.2015.05.034 (2015).

380 Morais de Castro, E. *et al.* Pediatric Astrocytomas and Their Association With Polymorphisms in Embryonic Stem Cell Marker Genes. *J Child Neurol* **37**, 534-540, doi:10.1177/08830738221091043 (2022).

381 Li, L. *et al.* Genetic association study of SOX2 gene polymorphisms with high myopia in a Chinese population. *Eur J Ophthalmol* **31**, 734-739, doi:10.1177/1120672120904666 (2021).

382 Underwood, A. *et al.* Evolutionary Landscape of SOX Genes to Inform Genotype-to-Phenotype Relationships. *Genes (Basel)* **14**, doi:10.3390/genes14010222 (2023).

383 Fantes, J. *et al.* Mutations in SOX2 cause anophthalmia. *Nat Genet* **33**, 461-463, doi:10.1038/ng1120 (2003).

384 Hagstrom, S. A. *et al.* SOX2 mutation causes anophthalmia, hearing loss, and brain anomalies. *Am J Med Genet A* **138A**, 95-98, doi:10.1002/ajmg.a.30803 (2005).

385 Leung, M. A. *et al.* Sudden Sensorineural Hearing Loss: Primary Care Update. *Hawaii J Med Public Health* **75**, 172-174 (2016).

386 Garros-Regulez, L. *et al.* Targeting SOX2 as a Therapeutic Strategy in Glioblastoma. *Front Oncol* **6**, 222, doi:10.3389/fonc.2016.00222 (2016).

387 Mack, S. C. *et al.* Chromatin landscapes reveal developmentally encoded transcriptional states that define human glioblastoma. *J Exp Med* **216**, 1071-1090, doi:10.1084/jem.20190196 (2019).

388 Wong, E. T., Lok, E., Gautam, S. & Swanson, K. D. Dexamethasone exerts profound immunologic interference on treatment efficacy for recurrent glioblastoma. *Br J Cancer* **113**, 232-241, doi:10.1038/bjc.2015.238 (2015).

389 Afshari, A. R. *et al.* Advantages and drawbacks of dexamethasone in glioblastoma multiforme. *Crit Rev Oncol Hematol* **172**, 103625, doi:10.1016/j.critrevonc.2022.103625 (2022).

390 Zhou, L. *et al.* The Prognostic Effect of Dexamethasone on Patients With Glioblastoma: A Systematic Review and Meta-Analysis. *Front Pharmacol* **12**, 727707, doi:10.3389/fphar.2021.727707 (2021).

391 Ayroldi, E. *et al.* Mechanisms of the anti-inflammatory effects of glucocorticoids: genomic and nongenomic interference with MAPK signaling pathways. *FASEB J* **26**, 4805-4820, doi:10.1096/fj.12-216382 (2012).

392 Stortz, M. *et al.* SOX2 Modulates the Nuclear Organization and Transcriptional Activity of the Glucocorticoid Receptor. *J Mol Biol* **434**, 167869, doi:10.1016/j.jmb.2022.167869 (2022).

393 Boehler, N. A., Fung, S. W., Hegazi, S., Cheng, A. H. & Cheng, H. M. Sox2 Ablation in the Suprachiasmatic Nucleus Perturbs Anxiety- and Depressive-like Behaviors. *Neurol Int* **13**, 541-554, doi:10.3390/neurolint13040054 (2021).

394 Abrous, D. N. & Wojtowicz, J. M. Interaction between Neurogenesis and Hippocampal Memory System: New Vistas. *Cold Spring Harb Perspect Biol* **7**, doi:10.1101/cshperspect.a018952 (2015).

395 Alam, M. J. *et al.* Adult Neurogenesis Conserves Hippocampal Memory Capacity. *J Neurosci* **38**, 6854-6863, doi:10.1523/JNEUROSCI.2976-17.2018 (2018).